Process for continuous purification of single-chain antibody fragments based on Simulated Moving Bed Chromatography

Dissertation

zur Erlangung des akademischen Grades

Doktoringenieur
(Dr.-Ing.)

von: M.Sc. Carlos Andrés Martínez Cristancho

geboren am: 12. Oktober 1978

in: Bogotá (Kolumbien)

genehmigt durch die Fakultät für Verfahrens- und Systemtechnik der Otto-von-Guericke-Universität Magdeburg

Promotionskommission:
Prof. Dr.-Ing. Udo Reichl
Prof. Dr.-Ing. Andreas Seidel-Morgenstern
Prof. Dr.-Ing. Stephan Scholl
Prof. Dr.-Ing. Malte Kaspereit

eingereicht am: 28. Februar 2013

Promotionskolloquium am 29. Mai 2013

Forschungsberichte aus dem Max-Planck-Institut
für Dynamik komplexer technischer Systeme

Band 42

Carlos Andrés Martínez Cristancho

Process for continuous purification of single-chain antibody fragments based on Simulated Moving Bed Chromatography

Shaker Verlag
Aachen 2013

Bibliographic information published by the Deutsche Nationalbibliothek
The Deutsche Nationalbibliothek lists this publication in the Deutsche Nationalbibliografie; detailed bibliographic data are available in the Internet at http://dnb.d-nb.de.

Zugl.: Magdeburg, Univ., Diss., 2013

Printed in Germany.

ISBN 978-3-8440-2359-6
ISSN 1439-4804

Shaker Verlag GmbH • P.O. BOX 101818 • D-52018 Aachen
Phone: 0049/2407/9596-0 • Telefax: 0049/2407/9596-9
Internet: www.shaker.de • e-mail: info@shaker.de

Acknowledgements

First and foremost, my heartfelt thanks to my "Doktorvater", Prof. Dr.-Ing. habil. Andreas Seidel-Morgenstern, for his ever-patient counsel and tireless guidance during my stay at his group at the Max Planck Institute for Dynamics of Complex Technical Systems in Magdeburg. I will always remember our creative and fruitful discussions in the frame of this extraordinary project. It was simply a pleasure and honor to work with him during the last four years.

I am deeply grateful to Prof. Dr.-Ing. Stephan Scholl and Prof. Dr.-Ing. Malte Kaspereit for reviewing this thesis and accepting to be co-examiners of this work.

I would like to express my profound gratitude to Stefanie Lautsch, Andrea López Carbajal and Christian Südekum, who helped me to shape this work due to the supervision of their master and diplom theses.

The finacial support by the German Research Foundation in the frame of the project SFB578, "From Gene to Product", is gratefully acknowledged.

Every experience in life is accompanied by new friends and discoveries. In this journey, I owe much to my colleagues of the group "Physical and Chemical Foundations of Process Engineering" at Max Planck Institute in Magdeburg. The entire group itself deserves my gratitude for its stimulating and nice atmosphere. Special thanks to Jacqueline Kaufmann, Martin Uxa, Luise Borchert, Matthias Eicke, Kamilla Galan, Gregor Kiedorf, Erik Temmel, Bernhard Kramer, Javier García Palacios, Héctor Rubiera, Leo Alvarado, Jadwiga Nowak, Ana Markovic, Michaela Bratz, Anett Raasch, Ju Weon Lee, Dawid Kiwala, Christof Hamel and Zoltan Horvath. Thanks for giving me advice on different experimental or theoretical topics and for being there when some help was needed. They made the time in Magdeburg a very special and unforgettable one for me.

I would like to thank everyone at the Techniche Universität Braunschweig working in the frame of the project SFB578, in particular Dr. Ezequiel Franco-Lara, Miriam Steinwand, David Frode and Dr. Michael Hust, who worked on the upstream processing of the single-chain antibody fragment.

My special thanks goes to Dr. Florian David, for guiding me through the fascinating world of recombinant proteins. We worked and cooperated together on this project and he gave me always nice suggestions and support.

But most of all, thanks to my mother and syster, Myriam Aurora Cristancho Mayorga and Diana Katherine Martínez Cristancho, for their love and patience throughout the journey as a PhD student far away from home.

And to my girlfriend Daniela, the most generous, wise and faithful counsellor every time.

Frankfurt am Main, February 2013

Carlos Andrés Martínez Cristancho

Zusammenfassung

In den letzten Jahren ist der Markt für rekombinante Antikörperfragmente sehr schnell gewachsen und die Antiköperfragmente stellen im Bereich der Therapeutika eine neue Alternative zu den monoklonalen Antikörpern dar. Die sogenannten single-chain Fragmente (scFv), welche über aktive Antigenbindungsstellen verfügen, sind besonders attraktiv in Forschung, Diagnostik und Therapie. Aufgrund signifikanter Erfolge im Upstream-Verfahren besteht ein starkes Bedürfnis an effizienten kontinuierlichen Aufreinigungsprozessen, die rekombinante Proteine isolieren können, im Vergleich zu den etablierten mehrstufigen diskontinuierlichen chromatographischen Prozessen.

Diese Doktorarbeit beschreibt die theoretische Auslegung und experimentelle Validierung eines Simulated Moving Bed (SMB) Prozesses unter Verwendung der sogenannten Immobilized Metal ion Affinity Chromatography (IMAC) für die Aufreinigung eines single-chain Antikörperfragment. Ziel ist es, das Antikörperfragment aus dem Zellkulturüberstand in möglichst hoher Reinheit zu gewinnen. Zuerst wurde der Zellkulturüberstand mit dem Antikörperfragment mittels einer stufenweisen pH-Gradienten Batch-Chromatographie charakterisiert. Der Einfluss der Zusammensetzung des Lösungsmittels (pH) auf die Adsorptionsisothermen wurde durch pH-Gradienten Batch-Versuche untersucht.

Die vorgeschlagene Auslegung basiert auf der rekursiven Lösung eines Gleichgewichtsstufenmodells, welches einen entsprechenden True Moving Bed (TMB) Prozess beschreibt. Mögliche Betriebsbedingungen wurden theoretisch untersucht und experimentell im Labor-Maßstab SMB-Anlage mit einem methodischen Ansatz realisiert.

Die Ergebnisse des kontinuierlichen SMB Prozesses wurden mit Resultaten für das einfachere Batch-Verfahren hinsichtlich Reinheit, Ausbeute und Produktivität verglichen. Diese Arbeit liefert den experimentellen Nachweis der Machbarkeit dieses neuartigen SMB Prozesses für die kontinuierliche Aufreinigung von Antikörperfragmenten.

Abstract

During the last years the market for recombinant antibody fragments has been growing very fast. Small-sized fragments can offer new alternatives to the full-length monoclonal antibodies (mAb) in the field of antibody-based therapeutics. Among them, the single-chain antibody fragments (scFv) are the smallest antibody fragments that still possess a complete antigen-binding site. Hence, they are ideal for research, diagnostic and therapy, which require good tissue penetration. The high titers obtained with recombinant proteins are imposing a tremendous challenge in the development of more efficient continuous purification processes, which can isolate recombinant proteins in an easier way, compared to the established multi-step discontinuous chromatographic scheme.

This work focuses on the theoretical design and experimental validation of a Simulated Moving Bed (SMB) chromatography process using Immobilized Metal Ion Affinity Chromatography (IMAC) for the purification of a single-chain antibody fragment. First, the cell culture supernatant containing the antibody fragment and originating from Bacillus megaterium was characterized using a stepwise pH-gradient batch chromatography. The influence of solvent composition (pH) on the adsorption isotherm parameters of the antibody fragment and its impurities were determined in single-column runs.

Based on the estimated adsorption isotherm parameters a feasible multicolumn open-loop 3-zone pH-gradient SMB process is suggested, which possesses the potential to isolate continuously the single-chain antibody fragment. The design is based on a recursive solution of an equilibrium stage model of an equivalent True Moving Bed (TMB) process. Possible operating conditions were theoretically proposed using the simulations obtained using the model and experimentally realized in a lab-scale SMB unit using a methodological approach.

The observed performance of the continuous process is compared to the corresponding batch process in terms of purity, yield, productivity, and buffer consumption. The potential of this innovative SMB process is clearly demonstrated.

Nomenclature

Latin Symbols	Definition
A_c	Cross-sectional area of the column
c^k	Concentration of component k
D_{ax}^k	Axial Diffusion coefficient
F	Phase ratio
H^k	Adsorption equilibrium constant of k
k	Capacity factor
k'_0	Retention factor
L	Column lenght
m^k	Mass of component k
m_i	Dimensionless flow rate ratio in zone i
N_{eq}	Number of equilibrium stages
q^k	Loading of component k
$t_{injection}$	Injection time
t_R	Retention time
t_{switch}	Switching time
t_0	Hold-up time
t_{cycle}	Cycle time
u	Linear velocity
$V_{i,dead}$	Extra-column dead volumen in zone i
V_{SP}	Stationary phase volume
V_{MP}	Mobile phase volume

V_c	Column volume
$\dot{V}$	Flow rate
$\dot{V}_i^{SMB}$	Flow rate of zone i in SMB
$\dot{V}_i^{TMB}$	Flow rate of zone i in TMB
$\dot{V}_s$	Flow rate of stationary phase
w	Peak width
Y	Yield
x	Position coordinate

Greek Symbols	Definition
β	Safety factor
χ	Dimensionless factor chi
η	Dimensionless factor eta
γ	Dimensionless factor gamma
ε	Porosity
μ	First and second central moment

Subscripts and superscripts	Definition
D	Desorbent
E	Extract
F	Feed
$fraction$	Refered to collected fraction in batch
k	Component k
$port$	Refered to outlet port in SMB
R	Raffinate

Abbreviations	Definition
AC	Affinity Chromatography
B. megaterium	Bacillus megaterium

CHO	Chinese Hamster Ovary cells
CSS	Cyclic steady state
E. coli	Escherichia coli
ELISA	Enzyme-linked Immunosorbent Assay
Fab	Fragment antigen binding
FDA	US Food and Drug Administration
GMP	Good Manufacturing Practices
HETP	Height Equivalent to a Theoretical Plate
HIC	Hydrophobic Interaction Chromatography
IEC	Ion Exchange Chromatography
IgG	Immunoglobulin Gamma
IMAC	Immobilized Metal Ion Affinity Chromatography
mAbs	Monoclonal Antibodies
MOL	Method of lines
ODE	Ordinary differential equation
PDE	Partial differential equation
PUR	Purity
PRD	Specific productivity
scFv	single-chain antibody fragment
SDC	Specific buffer consumption
SDS-PAGE	Sodium Dodecyl Sulfate Polyacrylamide Gel ele.
SEC	Size Exclusion Chromatography
SMB	Simulated Moving Bed Chromatography
TMB	True Moving Bed Chromatography

List of Tables

List of Figures

Contents

Chapter 1

Introduction

During the last decades liquid chromatography became increasingly important in the development of antibody-based therapeutics [138]. Chromatography based separations are an essential purification technology in the pharmaceutical and biotechnology industries due to the availability of a large arsenal of stationary phases and multiple operating modes applicable at various scales [38, 71].

The biopharmaceutical industries have to meet stringent demands of the health care authorities regarding drug safety and purity (Good Manufacturing Practices (GMP) and the US Food and Drug Administration (FDA)). The methods employed must satisfy the quality and quantity requirements as well as the cost-effectiveness to bring target products to the market as soon as possible [36]. The success of the next generation of antibody-based therapeutics will strongly depend on the development of appropiate, simple and efficient downstream processes [41, 63, 110].

This thesis explores the possibility to reduce the number of consecutive batch chromatographic steps, and thereby to shorten the time and cost of downstream processing, by designing and validating a novel continuous chromatographic purification process based on the simulated moving bed (SMB) principle.

The classical SMB technology was conceived already in 1961 by Broughton and Gerhold and was developed later for separations of petrochemicals and sugars [17, 18]. In the 1990's the SMB process experienced a renaissance after first successful applications for the separation of enantiomers in the pharmaceutical industry [43]. The SMB process is a continuous, high performance, multi-column chromatographic separation process that can be adapted to the current needs in bioseparations, where highly diluted valuable recombinant proteins must be recovered from complex fermentation broths, cell culture supernatants, or animal extracts [6, 51, 75].

Recombinant antibody fragments represent the next generation of antibody-based therapeutics and are an alternative to the full-length monoclonal antibodies in therapeutic and diagnostic applications requiring good tissue penetration [16, 118]. Among them, the single-chain antibody fragment (scFv) is the smallest antibody fragment that still possesses a complete antigen-binding site, which makes this antibody format very attractive for research and development of novel antibody-based drugs [45, 136].

The aim of this work is the design and experimental validation of an innovative open-loop 3-zone simulated moving bed process exploiting a stepwise pH-gradient using immobilized metal ion affinity chromatography (IMAC) for the purification of single-chain antibody fragments.

The broader goal of this work is to offer simple approaches that can be applied to other recombinant proteins as well in order to isolate them efficiently with the desired target purities at low costs.

1.1 Structure of the thesis

This thesis describes at first in chapter 2 the general structure of monoclonal antibodies (MAbs) and antibody fragments. This chapter also provides an overview of the different expression systems available for the production of these biomolecules. Additionally, chapter 2 outlines briefly current applications and sales of therapeutic antibody fragments.

Chapter 3 presents the basic principle of chromatography, and introduces the thermodynamic adsorption equilibria and mathematical models applied in this work. The chapter focuses on gradient elution chromatography and the chromatographic techniques applicable for protein purification. The chapter also covers the background of continuous counter-current chromatography in the field of bioseparations. Finally, performance parameters are introduced to evaluate batch and continuous chromatography.

Chapter 4 highlights recent developments and the state-of-the-art in the discontinuous and continuous purification of high-value biomolecules such as antibodies and antibody fragments. The chapter also describes the chromatographic mechanism applied in this work called immobilized metal ion affinity chromatography.

The materials and analytical methods used in this work are explained in chapter 5. The clarified cell culture supernatant containing the single-chain antibody fragment is described in more detail. Afterwards, the specific stationary phase and the buffers

used as mobile phase are introduced. Then, the analytical techniques applied for assessing either batch or SMB processes are presented. At the end of the chapter, the chromatographic equipment used for the discontinuous and continuous separations is described.

Chapter 6 describes the single-column batch experiments carried out under stepwise pH-gradient elution conditions. The chapter discusses the influence of the pH and sample load on the isolation of the single-chain antibody fragment. A mathematical model based on the equilibrium-dispersive model and an empirical description of the pH in the columns as a function of time and position is proposed. The model predicts the stepwise pH-gradient elution of the relevant components and was used to determine the critical dependence of the adsorption equilibrium constants on pH. Concrete measures to evaluate the performance of conventional batch chromatography are provided.

Chapter 7 presents a theoretical concept that enables the design of a continuous chromatographic purification of the single-chain antibody fragments using the multi-colum SMB technology. The concept is based on steady state concentration profiles predicted by the equivalent true moving bed (TMB) model. An equilibrium stage model was derived to predict the regions of feasible operating parameters and corresponding internal concentration profiles of the open-loop 3-zone pH-gradient SMB configuration, which allow the recovery and purification of the single-chain antibody fragment. A parametric study was carried out for a pseudo-binary mixture whose adsorption behavior is described by linear adsorption equilibria.

Chapter 8 deals with the experimental validation of the previously designed open-loop 3-zone pH-gradient SMB process. After characterizing the individual chromatographic columns, the subsequent experimental investigations quantify the effects of the switching time and the dimensionless flow rate ratios on the performance of the SMB operation. The results of several experimental SMB-runs carried out are discussed in detail.

Finally, chapter 9 summarizes the most important results achieved during the realization of this work and suggests future activities based on the main findings of this thesis.

Chapter 2

Antibodies and antibody fragments

This chapter deals with the structure of monoclonal antibodies and engineered recombinant antibody fragments. Additionally, the most common expression systems applied to produce them are described. Examples of antibody fragments already in the market are mentioned in order to illustrate the broad range of applications and the economic viability of recombinant antibody fragments as biopharmaceuticals.

2.1 Monoclonal antibodies

Monoclonal antibodies (MAbs) are the most representative products of the protein-based therapeutic market [15, 100]. Since the last decade monoclonal antibodies are market leaders in terms of volume sales and also represent the fastest-growing area in biotherapeutics [20, 50].

MAbs are members of a family of molecules called immunoglobulins, which are produced by a type of white blood cells called B-lymphocytes in response to the entry of foreign molecules into the body [76]. These proteins play a vital role in the immune system.

Immunoglobulins consist of two identical heavy chains, H-chains, and two non-glycosylated light chains, L-chains, linked through disulfide bridges in combination with non-covalent bonds [76]. Each heavy chain is composed of 4 domains, three constant, CH1, CH2, CH3 and one variable, VH. Each light chain is composed of 2 domains, one variable, VL, and one constant, CL1, as depicted in Figure 2.1 [48].

The heavy and light variable domains, VH and VL, form the antigen-binding region, where the antigen is recognized by the antibody in a highly specific interaction.

The constant domains constitute the non-antigen-binding part called fragment crystallizable region (Fc) that mediates essential immunological functions such as complement activation or lymphocyte binding [96].

Five different immunoglobulin classes can be distinguished (IgG, IgA, IgM, IgD and IgE), which differ in size, amino acids composition, and carbohydrate composition of the heavy chain. However, all immunoglobulins have the common structure described, independent of their specifity [70].

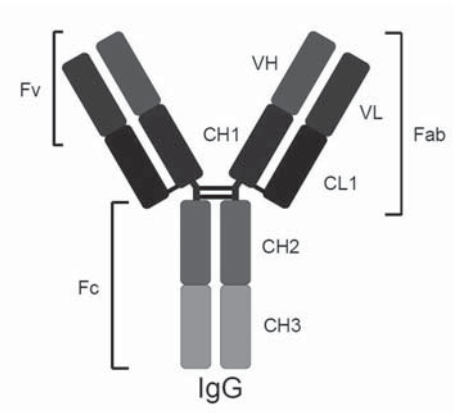

Figure 2.1: Schematic representation of immunoglobulin G (IgG) [115]

2.2 Engineered recombinant antibody fragments

Full-length antibodies are not always the best option for certain applications and small-sized antibody fragments can be sometimes more suitable. Genetically engineered recombinant technology allows the design of novel antibody formats according to special needs for therapy, diagnosis and easy purification without sacrificing the desired antigen recognition site [115].

Compared to low molecular weight drugs, therapeutic antibodies have higher target specificities and exquisite binding capacities, lower systemic toxicities and longer half-life times [118]. As a matter of fact, a significant proportion of future drugs to be licensed and launched in the next decade will be based on engineered recombinant antibody fragment products [83].

2.2.1 Fragment antigen binding

Fragment antigen binding (Fab) formats are non-glycosilated antibodies that consist only of two light chains, VL and CL1, and two truncated heavy chains, VH and CH1 [5]. These chains are covalently linked by a disulfide bridge as depicted in Figure 2.2.

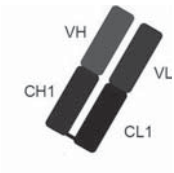

Figure 2.2: Schematic representation of a fragment antigen binding (Fab) [115]

2.2.2 Single-chain fragment variable

The single-chain fragment variable (scFv) format is one of the most popular recombinant antibody formats [89]. It is the smallest fragment that still contains the complete antigen-binding region [136].

Figure 2.3: Schematic representation of a single-chain fragment variable (scFv) [115]

Single-chain antibody fragments possess the same specificities for their antigens as the monoclonal antibodies [14]. This kind of fragment is poorly to moderately stable, but it is easily expressed and could be used as a suitable basis for many other antibody fragments. The variable domains, VH and VL, are artificially linked by a flexible polypeptide linker as depicted in Figure 2.3. Multimer formation is determined by the linker length. Shorter linkers (0-12 amino acids) favor the formation of dimers or trimers [4].

2.3 Expression systems

Appropiate expression systems for the production of antibodies and their fragments are well-known [36]. A main difficulty is represented by complex process streams where the target molecules are released (e.g. fermentation broths, cell culture supernatants, plant and animal extracts) [99]. Therefore, several downstream steps are necessary to achieve certain purity and the costs associated are estimated to be 50-80 % of the total manufacturing costs [63].

Typically, eukaryotic expression systems, such as yeast, plant and mammalian cells, are the means to choose for high-yield expression of monoclonal antibodies. On the other side, prokaryotic expression systems, bacteria, are more suitable for the production of small non-glycosylated antibody fragments [13, 136].

Each expression system is characterized by the activity, concentration and yield of the expressed antibody [22]. Advances in upstream technology affect in different ways downstream processes. The feedstock from which target proteins are extracted specifies to a significant extent the required downstream purification scheme [52].

The most common mammalian host cells used to express monoclonal antibodies are chinese hamster ovary cells (CHO), which possess the glycosylation machinery for the production of full-format antibodies [96].

The principal disadvantages of mammalian cell expression are the high production costs and strict safety precautions required to reduce the risk of pathogenic contamination [5]. One additional drawback is that monoclonal antibodies exhibit limited tissue penetration because of their size (approximately 150 kDa) and have therefore limited ability to reach intracellular targets.

Escherichia coli (*E. coli*) is usually the expression system for small non-glycosylated recombinant antibody fragments [92, 116]. The expression of proteins in these organisms is faster, easier and cheaper than in mammalian cell lines. High yields can be obtained depending on the fragment type [136]. *E.coli* is a gram-negative bacterium. Consequently, the antibody fragments are expressed and retained in the periplasm requiring cell lysis and additional recovery steps [5, 83]. It should also be mentioned, that this type of bacteria may contain endotoxins as components of the cell wall, i.e., substances which can be harmful for humans [20].

Bacillus megaterium (*B. megaterium*) is a gram-positive bacterium and another interesting expression system, which lacks the outer membrane. The secretion of the recombinant proteins takes place directly into the growth medium, which means less recovery steps are required. In addition to that, the specific activity of the antibody fragments is reported in some cases to be higher than of the ones produced

in *E. Coli* [68]. Many different engineered antibody formats and multiple methods for tailoring specificities are currently available [62].

Antibody fragments are produced in simple and high-yield production processes such as bacterial fermentations that lead to relatively low manufacturing costs. These "small-size" antibody fragments present flexible structure, highly specific-binding and enhanced tissue penetration allowing more effective access to disease targets, but lower stability and reduced half-life time [118].

Table 2.1 compares features of the most common expression systems for antibodies and antibody fragments, namely the mamalian cell culture and the bacterial fermentation:

Table 2.1: A comparison between mammalian cell culture and bacterial fermentation (according to Humphreys and Glover [62])

	Mammalian cell culture	Bacterial fermentation (*E.Coli*)
Antibody class	Monoclonal Antibody (IgG)	Antibody Fragments (Fab, scFv)
Production scale	Up to 15 m^3	Up to 100 m^3
Production yield	0.4 to 2 g/L	0.4 to 2 g/L
Capital investment/g product	High	Medium
Cost of goods	High	Low
Glycosylation	Yes	No
Time to first production	12 to 24 months	8 to 10 months
Special regulatory issues	Viral load	High endotoxin load

2.4 Therapeutic applications and sales

Therapeutic applications of recombinant antibody fragments are based on immunotherapy or tumor imaging.

In immunotherapy, the antibody fragments can bind and block the activity of many pathogens [45]. Besides, in radioimmunotherapy (RIT) , an antibody fragment is labeled with a radiation-emitting isotope. If these molecules bind only specifically an antigen associated to a tumor cell, this cell will receive a lethal dose of radiation. The principal advantages compared with other techniques are short treatment time and reduced side effects for most patients [61].

In tumor imaging, the single photon emission computed tomography (SPECT) is used to determine the location and stage of tumors. This technique takes advantage

of isotope-labeled antibody fragments. These biomolecules bind certain antigen, associated with the target sick cell and then these antibody formats are traced in the body using special detection equipment and showing the position and dimension of the tumors [136].

Applications of monoclonal antibodies and antibody fragments are based on the pharmacological properties of the different formats. Some of them are summarized in Table 2.2:

Table 2.2: Pharmacological properties of MAbs, Fab and scFv according to Gottschalk and Mundt in [76]

Parameter	MAb	Fab	scFv
Molecular Weight in kDa	150	50	27
Tumor / tissue penetration	+	++	+++
Equilibrium half-life time	> 1 h	30 min	10 min
Clearance half-life time	1-3 weeks	5-6 h	3-4 h

The market is dominated by monoclonal antibodies derived from the conventional immunoglobulin gamma format (IgG) because they are structurally stable and have a long in vivo half-life time [83, 118]. However, among the antibody-based products three antibody fragments are already in the market and approved by the FDA. The commercial names of these fragments are: Lucentis®, Reopro® and Cimzia® [104].

Ranibizumab (Lucentis®) is a Fab fragment-based drug is used to treat wet age-related macular degeneration and macular edema due to retinal vein occlusion. It is expressed in *E.Coli* and prescribed as an injection into the eye [87].

Abciximab (Reopro®) is also a Fab fragment indicated as an adjunct to percutaneous coronary intervention (PCI) for the prevention of cardiac ischemic complications [109].

Certolizumab (Cimzia®) is a recombinant humanized antibody Fab fragment manufactured in *E. coli* and conjugated later to polyethylene glycol. It presents specificity for human tumor necrosis factor alpha (TNF-α) , neutralizing its performance, and is administered by subcutaneous injection [25].

Approximately 28 monoclonal antibodies have been approved for therapeutic use in the United States in 2009, and over 200 candidates are in the clinical pipeline [99]. Worldwide sales of therapeutic MAbs have risen dramatically in the last years from $4.0 billion in 2001 to over $30 billion in 2008 [83, 86, 104].

Table 2.3 summarizes the data of the sales in million US$ of the mentioned

therapeutic antibody fragments in 2009:

Table 2.3: Sales of therapeutic antibody fragments in 2009 [80]

Product	Target	Company	Indication	Sales
Lucentis®	VEGF	Genentech and Novartis	Wet age-related macular degeneration	2344
Reopro®	GP-R IIb/IIa	Eli Lilly and Centocor	Percutaneous coronary interventions	232
Cimzia®	TNF-α	UCB Pharma	Chron's Disease and Rheumatoid arthritis	95

Chromatographic purification of monoclonal antibodies and antibody fragments will continue to be an essential part and a key process economic driver in the development and production of biopharmaceuticals. The theoretical foundations of chromatography will be explained in the next chapter.

Chapter 3

Theoretical foundations of chromatography and operating principles

This chapter explains the principle and supplies a short theoretical basis of chromatographic processes. First, the basic principles of discontinuous liquid chromatography and adsorption equilibria are covered. Thereby, the operating modes applied in protein chromatography are introduced and the different techniques available are described. Finally, the design of continuous counter-current chromatographic process is addressed and suitable criteria to evaluate process performance are defined.

3.1 Discontinuous single-column chromatography

Classical discontinuous single-column chromatography has been practiced long enough as a powerful and versatile multi-component separation process. Additionally, there are many references describing various batch chromatographic techniques for proteins and biomolecules [20, 36, 69].

In conventional chromatography, a mixture of components fed at the inlet of a column packed with solid porous particles is transported by a fluid phase. Each component interacts to a greater or lesser extent with the solid particles and, thus, leaves the column at a specific time producing a signal at the detector.

The specific affinities of the porous particles to the components of the feed mixture are crucial to accomplish the separation. In such chromatographic processes, the mass transfer between the mobile and stationary phases is typically very efficient. A

large number of theoretical equilibrium stages (in the range of thousands) can be established in columns of modest length. This efficiency is the result of applying typically small porous particle sizes in the low μm-range providing high interfacial areas and low intraparticle diffusional resistances [57].

3.1.1 Thermodynamics of adsorption equilibria

In chromatography, the reversible binding of components via adsorption is strong enough to separate the components of a mixture without affecting their nature [60, 117]. In order to design any chromatographic purification process, the knowledge of the thermodynamic adsorption equilibria is of considerable importance [119].

Adsorption equilibria are mostly determined experimentally at constant temperature [119]. Adsorption isotherms relate the concentrations of a component, k, adsorbed at the stationary phase, q^k, with the corresponding equilibrium concentrations in the mobile phase, c^k, at a specific temperature [111].

The simplest adsorption equilibrium models introduce adsorption equilibrium constants or initial slopes of the adsorption isotherms, H^k, as a thermodynamic parameter to express the equilibrium established for each component, k, between the stationary and the mobile phase at diluted conditions. Equation (3.1) describes the interactions between the components in the mixture to be separated and the stationary phase in a chromatographic column for diluted or linear conditions [57].

$$q^k = H^k \cdot c^k \tag{3.1}$$

This simple and practical relationship will be used in the course of this work to describe the adsorption phenomena observed.

3.1.2 Parameters of chromatographic systems

A chromatogram for the injection of two different components, k_1 and k_2, is shown in Figure 3.1. In the vertical axis the intensity of the signal provided by the detector is represented while in the x-axis the time elapsed or the processed volume can be seen.

Typical parameters obtained from such a chromatogram are the hold-up time, t_0, and for a component, $k = A, B$, the retention time, t_R^k, the width at the base of the peak, w^k, the width at half height of the peak, $w_{1/2}^k$, and the peak height, h^k.

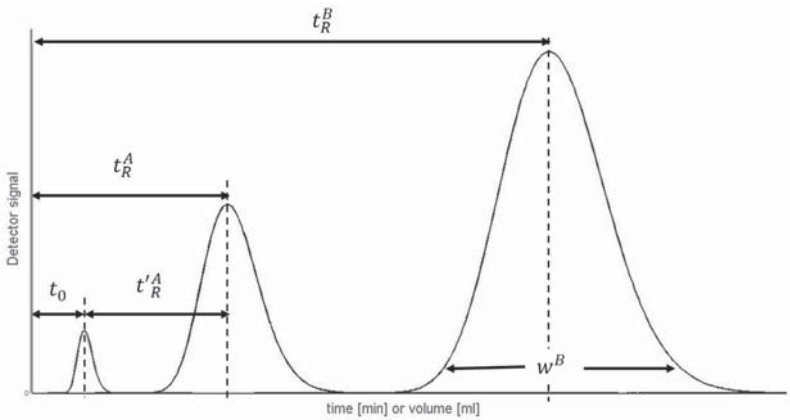

Figure 3.1: Chromatogram for the separation of a mixture containing two components, A, B, and the hold-up time, t_0, of a non-adsorbed component

The components are separated according to their retention times. The retention time is the time lag between the injection of the sample and the maximum of the peak observed for that component.

The hold-up time, t_0, is the time that a non-adsorbed substance needs to pass the column length and reach the detector as illustrated in Figure 3.1. The hold-up time is given by Equation (3.2):

$$t_0 = \frac{V \cdot \varepsilon}{\dot{V}} \tag{3.2}$$

with the column volume, V_c, the total column porosity, ε, and the volumetric flow rate, $\dot{V}$.

Evaluating the retention times, retention factors, $k_0'^k$, can be defined by Equation (3.3):

$$k_0'^k = \frac{t_R^k - t_0}{t_0} \tag{3.3}$$

The column volume can be divided in external volume, V_{ext}, volume of the adsorbent, V_{ads} and internal pore volume, V_{int} [57].

Using these volumes, different types of porosity can be defined using Equation (3.4) for the external porosity, ε_{ext}, Equation (3.5) for the internal porosity, ε_{int}, and Equation (3.6) for the total column porosity, ε:

$$\varepsilon_{ext} = \frac{V_{ext}}{V} \tag{3.4}$$

$$\varepsilon_{int} = \frac{V_{int}}{V_{ads}} = \frac{V_{int}}{(1 - \varepsilon_{ext}) \cdot V} \tag{3.5}$$

$$\varepsilon = \frac{V_{ext} + V_{int}}{V} = \varepsilon_{ext} + (1 - \varepsilon_{ext}) \cdot \varepsilon_{int} \tag{3.6}$$

A phase ratio, F, given by Equation (3.7), is often considered as the ratio between the stationary and the mobile phase:

$$F = \frac{1 - \varepsilon}{\varepsilon} \tag{3.7}$$

The retention time of an adsorbed component, t_R^k, is given under linear conditions by Equation (3.8) using the adsorption equilibrium constant, H^k defined in Equation (3.1):

$$t_R^k = t_0 \cdot (1 + F \cdot H^k) \tag{3.8}$$

Equation (3.8) can be derived based on mass balance considerations provided in the next section.

3.2 Models of chromatography

Discontinuous and continuous chromatography play an important role in downstream processing in the biopharmaceutical industries. For this reason, chromatographic models are of large relevance in order to evaluate and optimize the performance of separation processes. Such models are typically based on the solution of mass

balance equations together with the thermodynamic adsorption equilibria of the components involved in the chromatographic system [42].

Chromatographic columns are typically well packed with relatively small-size particles. Thus, radial gradients are small and chromatographic columns are usually considered spatially as one dimensional in the axial direction, x. The models considered here have two independent variables, time, t, and axial position, x, and two dependent variables, the concentrations of the components in the mobile phase, c^k, and in the stationary phase, q^k.

3.2.1 Stage models

There are basically two versions of stage models. Martin & Synge developed a continuous equilibrium stage model in 1941 [88]. A couple of years later, Craig developed a similar but discrete model based on an apparatus capable to perform liquid-liquid extractions with a large number of physically distinct stages [27]. In practice, both empirical approaches are similar and under certain conditions equivalent [57].

Stage models consider that the chromatographic column is divided in a number of identical equilibrium stages, N_{eq}^k. In each stage of volume, V_{stage}, the equilibrium between mobile and stationary phases is considered to be established instantaneously. The stage model was developed initially for components with linear adsorption isotherms. The predicted elution profiles can then be estimated independently for each component [84].

For each stage, j, a mass balance equation for a component, k, can be written as:

$$\varepsilon \cdot V_{stage} \cdot \frac{dc_j^k}{dt} + (1-\varepsilon) \cdot V_{stage} \cdot \frac{dq_j^k}{dt} = \dot{V} \cdot (c_{j-1}^k - c_j^k) \quad \text{for } j = 1, 2, ..., N_{eq}^k \tag{3.9}$$

Hereby, $\dot{V}$ is the volumetric flow rate of the fluid phase through the stage. In this work, the continuous stage model of Martin and Synge under steady state conditions is applied later for the study of the continuous chromatographic processes. Then, the mass balance of each component k for the stage j is under steady state conditions can be written as:

$$0 = \dot{V} \cdot (c_{j-1}^k - c_j^k) \qquad \text{for } j = 1, 2, ..., N_{eq}^k \tag{3.10}$$

Dividing the column length, L, by the number of equilibrium stages, N_{eq}^k, results in a component specific height equivalent to a theoretical plate, $HETP^k$:

$$HETP^k = \frac{L}{N_{eq}^k} \tag{3.11}$$

The number of equilibrium stages, N_{eq}^k, or the height equivalent to a theoretical plate, $HETP^k$, are used to characterize the efficiency of the stationary phase. A large number of N_{eq}^k indicates a higher efficiency or a smaller $HETP^k$.

Under linear conditions and for large stage numbers, the shapes of chromatographic peaks follow the classical Gauss distribution and the number of equilibrium stages can be estimated using Equation (3.12) [57]:

$$N_{eq}^k = 16 \cdot (\frac{t_R^k}{w^k})^2 \tag{3.12}$$

In reality, the shape and position of the peaks present deformations like sharpened adsorption fronts and dispersed desorption fronts or vice versa. In this case, the number of equilibrium stages can be estimated more precisely applying the method of moments for a component k using Equation (3.13) [131]:

$$N_{eq}^k = \frac{(\mu_1^k)^2}{\mu_2^k} \tag{3.13}$$

The moments represent condensed characteristics of an elution profile. They can be easily measured experimentally [131]. In practice, only the first and second moments of an elution profile, μ_1^k and μ_2^k, are evaluated [57].

The first moment, μ_1^k, characterizes the retention time used to calculate the adsorption equilibrium constant. It can be calculated with Equation (3.14):

$$\mu_1^k = t_R^k = \frac{\int_0^\infty t \cdot c_{N_{eq}^k}^k \cdot dt}{\int_0^\infty c_{N_{eq}^k}^k \cdot dt} \approx \frac{\sum_{i=1}^n t_i \cdot c_{i,N_{eq}^k}^k \cdot \Delta t_i}{\sum_{i=1}^n c_{i,N_{eq}^k}^k \cdot \Delta t_i} \tag{3.14}$$

The second moment, μ_2^k, quantifies band broadening related e.g. to limited mass transfer kinetics. It can be estimated with Equation (3.15):

$$\mu_2^k = \sigma^2 = \frac{\int_0^\infty c_{N_{eq}^k}^k \cdot (t - t_R^k)^2 \cdot dt}{\int_0^\infty c_{N_{eq}^k}^k \cdot dt} \approx \frac{\sum_{i=1}^n c_{i,N_{eq}^k}^k \cdot (t_i - t_R^k)^2 \cdot \Delta t_i}{\sum_{i=1}^n c_{i,N_{eq}^k}^k \cdot \Delta t_i} \tag{3.15}$$

where i corresponds as in Equation (3.14) and Equation (3.15) to a specific measurement in n total measurements.

There are several phenomena ocurring within a column that affect the elution behavior of a component. The most important are axial dispersion, molecular diffusion and mass transfer. A good approximation to describe the relation between efficiency, i.e. $HETP^k$, and the flow rate, $\dot{V}$, or the mobile phase linear velocity, u, is given by the well-known Van Deemter Equation (3.16) [34]:

$$HETP^k = A + \frac{B^k}{u} + C^k \cdot u \tag{3.16}$$

The mobile phase linear velocity, u, depends on the volumetric flow rate, $\dot{V}$, the cross-sectional area of the column, A_c, and the total porosity, ε:

$$u = \frac{\dot{V}}{A_c \cdot \varepsilon} \tag{3.17}$$

And the parameters A, B^k and C^k represent the contribution of different processes to band broadening. Parameter A quantifies the influence of the stationary phase packing in causing multiple trajectories that the components will follow through the column (Eddy diffusion). The term B^k accounts for molecular diffusion. Terms A and B^k are often negligible for liquid chromatography of biomolecules [20]. Mass transfer limitations are captured by C^k [57].

3.2.2 Continuous equilibrium theory model

The equilibrium theory does not consider axial dispersion or mass transfer limitations [91]. The components in the mobile phase are at every position in the column permanently at equilibrium with the stationary phase [57]. This model assumes that

the column efficiency is infinite or $HETP^k = 0$. The only transport mechanism considered is convection. The continuous mass balance equation for component k is [119]:

$$\frac{\partial c^k}{\partial t} + F \cdot \frac{\partial q^k(c^k)}{\partial t} + u \cdot \frac{\partial c^k}{\partial x} = 0 \tag{3.18}$$

The mobile phase linear velocity, u, the phase ratio, F, are required for the solution of Equation (3.18). The solution of this partial differential equation requires the specification of initial and boundary conditions.

The initial condition is usually given in the form of Equation (3.19):

$$c^k(t = 0, x) = 0 \tag{3.19}$$

considering that the column is unloaded at $t = 0$.

Typically a rectangular pulse injection with a feed concentration, c^k_{Feed} is considered:

$$c^k(t, x = 0) = \begin{cases} c^k_{Feed} & 0 < t \leq t_{inj} \\ 0 & t > t_{inj} \end{cases} \tag{3.20}$$

This model can be solved analytically for simple isotherms and is very useful to study front propagation in highly efficient columns. For linear isotherms, it provides Equation (3.8).

3.2.3 Continuous equilibrium-dispersive model

The equilibrium-dispersive model assumes that equilibrium is established and also that all non-equilibrium effects can be lumped into an apparent axial dispersion coefficient, D^k_{ax}. This coefficient is assumed to be constant and does not take into account the concentration of the components [57].

The model formulates the mass balance equation of component k using the following partial differential equation (PDE):

$$\frac{\partial c^k}{\partial t} + F \cdot \frac{\partial q^k(c^k)}{\partial t} + u \cdot \frac{\partial c^k}{\partial x} = D^k_{ax} \cdot \frac{\partial^2 c^k}{\partial^2 x} \tag{3.21}$$

The mobile phase linear velocity, u, the phase ratio, F, are again required for the implementation of a solution.

An estimation of the additionally required apparent axial dispersion coefficient, D_{ax}^k, can be done using Equation (3.22) [57]:

$$D_{ax}^k = \frac{HETP^k \cdot u}{2} = \frac{L \cdot u}{2 \cdot N_{eq}^k} \tag{3.22}$$

Common boundary conditions (BC) in space are in the case under study, a Robin BC at $x = 0$ and a Neumann BC at $x = L$. The Robin (or Danckwerts) inlet boundary condition is [30]:

$$\frac{\partial c^k}{\partial x}(x = 0, t) = \frac{u}{D_{ax}^k} \cdot (c^k(x = 0, t) - c_{Feed}^k) \tag{3.23}$$

The Neumann outlet boundary condition is:

$$\frac{\partial c^k}{\partial x}(x = L, t) = 0 \tag{3.24}$$

The initial condition of a not preloaded column is used again according to Equation (3.19).

3.2.4 Numerical solution of the equilibrium-dispersive model

For non-linear adsorption isotherms, the solution of Equation (3.21) can be only calculated using numerical methods [53]. In this work, numerical solutions were determined using the method of lines (MOL) [71].

Numerical solutions can be obtained, using well-established methods such as finite differences or finite elements. The basic idea behind the method of lines is the replacement of the spatial derivatives in the PDE system with algebraic expressions such as finite differences while the derivatives in time remain. In doing so, a system of ordinary differential equations (ODE) is generated that approximates the original PDE system [114, 123].

More specifically, the first order space derivative term in Equation (3.21) can be replaced by a central finite difference:

$$\frac{\partial c^k}{\partial x} = \frac{c^k_{n+1} - c^k_{n-1}}{2 \cdot h} \tag{3.25}$$

The second order space derivative term in Equation (3.21) can be approximated by a central finite difference:

$$\frac{\partial^2 c^k}{\partial^2 x} = \frac{c^k_{n+1} - 2 \cdot c^k_n + c^k_{n-1}}{h^2} \tag{3.26}$$

where the subscript n refers to the position in the space grid (in the x-coordinate from $x = 0$ to $x = L$), and h is the step size in the x-direction:

$$h = \Delta x = x_n - x_{n-1} = x_{n+1} - x_n \tag{3.27}$$

The use of central finite differences for replacing first and second order space derivative terms is appropiate for approximating fictitious values found before the column inlet and column outlet, which is discussed in detail in the following paragraphs. The initial and boundary conditions required to solve the problem are also discretized. Equation (3.23) can be transformed into:

$$\frac{c^k_{n+1} - c^k_{n-1}}{2 \cdot h} = \frac{u}{D^k_{ax}} \cdot (c^k_n - c^k_{Feed}) \tag{3.28}$$

The fictitious concentration before the column, c^k_0, can be calculated from Equation (3.28):

$$c^k_0 = c^k_2 - \frac{u \cdot 2 \cdot h}{D^k_{ax}} \cdot (c^k_1 - c^k_{Feed}) \tag{3.29}$$

Replacing Equation (3.29) in the PDE Equation (3.21) at $x = 0$ or $n = 1$ provides for linear isotherms:

$$\begin{aligned} \frac{dc^k_1}{dt} = &-\frac{u^2}{1 + F \cdot H^k} \cdot \frac{(c^k_1 - c^k_{Feed})}{D^k_{ax}} \\ &+ \frac{2}{1 + F \cdot H^k} \cdot \frac{D^k_{ax} \cdot (c^k_2 - \cdot c^k_1) - h \cdot u \cdot (c^k_1 - c^k_{Feed})}{h^2} \end{aligned} \tag{3.30}$$

Analogously, Equation (3.24) at $x = L$ or $n = n_{max}$ can be transformed into:

$$\frac{c^k_{n_{max}+1} - c^k_{n_{max}-1}}{2 \cdot h} = 0 \tag{3.31}$$

The fictitious concentration after the column, $c^k_{n_{max}+1}$, can be estimated from Equation (3.31):

$$c^k_{n_{max}+1} = c^k_{n_{max}-1} \tag{3.32}$$

Replacing Equation (3.32) in the PDE Equation (3.21) at $x = L$ or $n = n_{max}$:

$$\frac{dc^k_{n_{max}}}{dt} = \frac{2 \cdot D^k_{ax}}{1 + F \cdot H^k} \cdot \frac{c^k_{n_{max}-1} - c^k_{n_{max}}}{h^2} \tag{3.33}$$

For the rest of the nodes ($n = 2$ until $n = n_{max} - 1$), the solution of the resulting ODE's Equation (3.21) is given by:

$$\frac{dc^k_n}{dt} = -\frac{u}{1 + F \cdot H^k} \cdot \frac{c^k_{n-1} - c^k_n}{2 \cdot h} + \frac{D^k_{ax}}{1 + F \cdot H^k} \cdot \frac{c^k_{n+1} - 2 \cdot c^k_n + c^k_{n-1}}{h^2} \tag{3.34}$$

The ODE system expressed by Equation (3.30), Equation (3.33), and Equation (3.34) was solved using MATLAB.

3.3 Operating modes in elution chromatography

Classical elution chromatography has become increasingly relevant for the development and purification of novel biopharmaceutical drugs [138]. In protein elution chromatography the mobile phase contains typically a modifier (salt, organic solvents) which is traveling often faster than the components in the mixture and affects the interactions between the biomolecules and the stationary phase. The use of a modifier is often mandatory to separate components characterized by a broad spectrum of retention times to facilitate the separation. Related to the presence or absence of a modifier, there are basically two operating modes in protein elution chromatography: isocratic or gradient chromatography [20].

3.3.1 Isocratic elution chromatography

In isocratic elution chromatography the concentration of the mobile phase modifier remains constant throughout the separation [20]. Due to the broad spectrum in retention times, it is not so common in protein chromatography to use isocratic elution modes. An exception is Size Exclusion Chromatography (SEC) or Gel Filtration [49]. Size exclusion chromatography separates proteins according to their molecular size. Larger molecules cannot enter the pores of the stationary phase and elute faster. On the other hand, smaller molecules go into the pores following multiple trajectories in the column and are delayed as they diffuse in and out. SEC is predominantly applied as a polishing step separating aggregates from target proteins [49].

3.3.2 Gradient elution chromatography

In gradient elution chromatography the concentration of the mobile phase is modulated over time throughout the separation [20].

The initial mobile phase (or the loading buffer) is chosen in order to create conditions for the adsorption (binding) of the target protein. Then, the mobile phase modifier is changed using an elution buffer so that the interaction between the target protein and the stationary phase becomes weaker. In this elution step, the target protein should be isolated from the other proteins or impurities present in the feed mixture [139, 140, 141].

Gradient elution chromatography can be easily applied using two different simple methods: linear (by continuously changing the mobile phase composition or modifier concentration with a constant rate) or stepwise (by discontinuously changing the mobile phase composition of modifier concentration) [44].

The chromatographic purification of antibodies and recombinant antibody fragments requires gentle and non-denaturizing conditions because proteins are extremely sensitive to higher temperatures, organic solvents, extreme pH values and high shear forces present in traditional separation processes like distillation and centrifugation [17, 70].

Classical gradient elution chromatography is made up of 5 steps [69]:

1. Equilibration: A certain amount of loading buffer is required in order to establish constant and stable conditions (conductivity, pH, absorption) where the adsorption of target proteins is favored.

2. Sample application: The sample containing the proteins to be separated is injected into the column. The volume to inject depends on the binding capacity of the column.

3. Wash away unbound proteins: After the injection of the sample, some column volumes of washing buffer (loading or washing buffer) are needed in order to wash away the unbound proteins through the column.

4. Elution: The adsorbed protein elutes using a stepwise or linear gradient based on the change in strength of the mobile phase.

A characteristic cycle time, t_{cycle} is obtained by the sum of the times for these consecutive operations in:

$$t_{cycle} = t_{equilibration} + t_{injection} + t_{wash-out} + t_{gradient} \tag{3.35}$$

Several techniques are well-established in the field of protein chromatography applying gradient elution chromatography such as Ion Exchange Chromatography (IEC), Hydrophobic Interaction Chromatography (HIC), and Affinity Chromatography (AC). Each of these techniques exploits different physical properties of the proteins. A classification can be done considering the different types of binding mechanisms that allow the components to be retained [20]. The most important techniques are briefly explained here:

1. Ion Exchange Chromatography (IEC): This type of chromatography uses the presence of electric charges on the surface of proteins. Depending on the pH value of the medium, the amino- and carboxyl-groups of the proteins may be protonated or deprotonated, causing positive or negative charges. Proteins are amphoteric substances, that means they are able to act both as an acid and as a base [48]. Since the charge of a protein can change depending on the properties of the medium, the retention can be adjusted in the loading step and elution can be carried out by modifying the pH or the ionic strength. The adsorption of components occurs by interaction of these molecules with the ionic groups of opposite charge fixed on surface of the stationary phase [66].

2. Hydrophobic Interaction Chromatography (HIC): In this case hydrophobic ligands are attached to the solid matrix. The protein retention occurs due to the interaction between the ligands and the hydrophobic patches present on the protein surface. HIC exploits the hydrophobicity of proteins [64]. The

mobile phase is an aqueous solution of salts which contributes to the formation and stability of water-water interactions. The elution of the biomolecules is carried out reducing the salt concentration of the mobile phase.

3. Affinity Chromatography (AC): The basis of affinity separations is the interaction with a natural or synthetic ligand that recognizes and binds exclusively a target protein [36]. Adsorption takes place as a result of several interactions at the same time (Van der Waals forces, hydrogen bridges, hydrophobic interactions). Depending on the ligand, there are different affinity chromatographic techniques such as Protein A, Protein G, and Immobilized Metal Ion chromatography. Polyclonal and monoclonal antibodies are currently purified using very expensive protein A chromatography resins.

3.4 Continuous counter-current multi-column chromatography

True moving beds (TMB) and simulated moving beds (SMB) form the most common and classical continuous counter-current multi-column chromatographic processes. It should be pointed out that only binary separations are possible using classical configurations, although pseudo-binary separations are feasible if the component of interest is either the slowest or fastest one in the elution train. Additionally, multicomponent separations can be achieved using more sophisticated arrangements with several connected SMB units [73, 74].

Continuous counter-current multicolumn adsorption arrangements are attractive in order to achieve a more productive and efficient configuration than provided by the discontinuous single-column processes.

The most frequently exploited continuous chromatographic separation mode is the classical isocratic closed-loop 4-zone simulated moving bed (SMB) process. This standard SMB configuration exploits several chromatographic columns arranged in a closed loop in four zones.

Counter-current multi-column separators maximize mass transfer efficiency by increasing the stationary phase exploitation and by reducing the mobile phase consumption [85, 143]. Besides, the products are typically more concentrated and the productivity is larger than for the batch operation. Possible disadvantages are the increased complexity of the design and higher costs of the equipment [91].

3.4.1 True Moving Bed (TMB)

A TMB is a theoretical concept that represents a counter-current chromatographic arrangement. The classical TMB consists of four zones. There are two inlet (feed and desorbent) and two outlet streams (extract and raffinate). This four-zone arrangement imposes on each zone a very specific task. The different zones are often designated using roman numbers (I, II, III, IV). The separation of the binary or pseudo-binary mixture into two fractions takes place in zones II and III. Regeneration of the stationary and mobile phases is carried out in zones I and IV, respectively [17, 18]. The schematical configuration is shown in Figure 3.2:

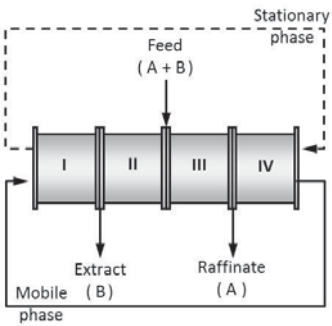

Figure 3.2: Schematic representation of the classical closed-loop 4-zone isocratic True Moving Bed (TMB)

As depicted in Figure 3.2, the mobile phase flows in one direction while the stationary phase moves in the opposite direction. The desorbent stream is introduced in zone I together with the regenerated mobile phase from zone IV. The feed stream is introduced between zone II and III. The better adsorbable component, B, will move with the stationary phase towards zone II and it will be dragged at the extract port. On the other side, the least adsorbable component, A, will travel with the mobile phase towards zone III and can be recovered at the raffinate port.

3.4.2 Simulated Moving Bed (SMB)

The TMB can not be realized practically because of the difficulties related to the continuos movement of the solid phase [91, 108]. In real applications the stationary

phase is packed into several columns and the counter-current movement is simulated by a periodic shift of the columns against the direction of the mobile phase flow [24]. That leads to the SMB configuration. In this case, equal or variable number of columns are included in each zone in order to satisfy the requirements of the specific separation. An illustration of the conventional SMB unit is shown in Figure 3.3.

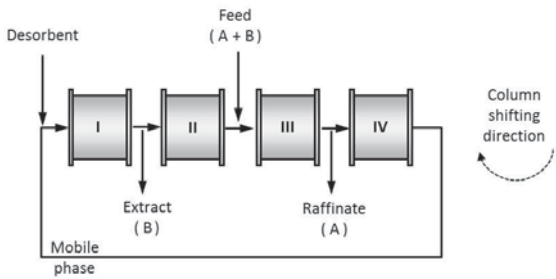

Figure 3.3: Schematic representation of classical closed-loop 4-zone isocratic Simulated Moving Bed (SMB)

SMB has proven to outperfom batch chromatography, even when a challenging purification of components with very similar retention behavior is needed [112].

The development of the SMB technology has been driven by different applications and scales. In the 1960's, SMB was used for the separation of aliphatics from olefins, m,p-xylene isomer separation and sugar separations in the range of hundred thousand tons per year [24]. In the 1990's, successful applications in the pharmaceutical industries for the separation of enantiomers opened up and spread the acceptance of the technology. Nowadays, downstream processing of high value biotherapeutics such as antibodies appears as an interesting area of application for continuous chromatography with scales in the kilogram range per year [38].

3.4.3 Design of TMB and SMB processes

The basis for the TMB and SMB design is the specification of dimensionless flow rate ratios, m_i, for each zone i. These ratios were defined by the different volumetric flow rates of the mobile phase in each zone, $\dot{V}_i$, over the volumetric flow rate of the stationary phase in the unit, $\dot{V}_s$, as given by Equation (3.36) [122]:

$$m_i = \frac{\dot{V}_i}{\dot{V}_s} \tag{3.36}$$

Under isocratic elution conditions and assuming linear adsorption isotherms, the conditions that should be fullfilled to reach complete separation of the two components, k_1 and k_2, in a TMB configuration are given by the following inequalities [122]:

$$m_I \geq H^B \geq m_{III} > m_{II} \geq H^A \geq m_{IV} \tag{3.37}$$

This at first requires a positive feedstream ($m_{III} > m_{II}$) [91]. The translation of the inequality into a m_{II}, m_{III}-plane produces a triangle, that is why, this theory is called triangle theory. Outside the triangle, at least one of the conditions will not be satisfied and thus the separation of the two components will not be complete. The vertex of the triangle, w, provides the best separation performance (least solvent consumption, most productivity and enrichment) but it is not a robust operating point. An operation point within the separation region sufficiently far from the vertex must be chosen. Details can be found in the literature [91, 108].

The basic difference between SMB and TMB configurations is related to their dynamic behavior. In the TMB, a steady state is reached. On the other hand, the SMB reaches only a periodic cyclic steady state (CSS), which is time-dependent. After every switch each section of a SMB goes through a transient state before reaching at the end again the initial state [122].

The design of SMB chromatographic separations can be done exploiting the analogy to the TMB process. The region of optimal operating conditions can be found more easily for a hypothetical TMB. The rules to convert the SMB and TMB flow rates require that the velocities of the liquid phases relative to the one of the solid are kept constant [3, 122].

It could be demonstrated that, when the following two conversion rules between both configurations are fulfilled, the separation performances are very close [24, 91]. The volumetric flow rate in zone i for the SMB, $\dot{V}_{i,SMB}$, is equivalent to the volumetric flow rate in the analogous zone of the TMB, $\dot{V}_{i,TMB}$, plus the product between the volumetric flow rate of the stationary phase, $\dot{V}_s$, and the inverse of the phase ratio, F [117]:

$$\dot{V}_{i,SMB} = \dot{V}_{i,TMB} + \frac{\varepsilon}{1-\varepsilon} \cdot \dot{V}_s \tag{3.38}$$

The switching time, t_{switch}, for the SMB process is given by the column volume, V_c, the total column porosity, ε, and the adsorbent volumetric flow rate, $\dot{V}_s$:

$$t_{switch} = \frac{1-\varepsilon}{\dot{V}_s} \cdot V_c \tag{3.39}$$

Rearranging Equation (3.38) using Equation (3.39) gives the volumetric flow rate in zone i, $\dot{V}_{i,SMB}$ in terms of the switching time, t_{switch}:

$$\dot{V}_{i,SMB} = \dot{V}_{i,TMB} + \frac{\varepsilon \cdot V_c}{t_{switch}} \tag{3.40}$$

In smalle-scale SMB units the extra-column dead volume might be comparable to the volume of the columns and must be considered [93]. This extra-column dead volume per zone, $V_{i,dead}$ can be included in Equation (3.40):

$$\dot{V}_{i,SMB} = \dot{V}_{i,TMB} + \frac{\varepsilon \cdot V_c}{t_{switch}} + \frac{V_{i,dead}}{t_{switch}} \tag{3.41}$$

As mentioned above, the design of SMB processes provides a region of feasible operating parameters to achieve the required separation performance. Thus, the following dimensionless flow rate ratios $m_{i,SMB}$ can be defined including the effect of non-negligible extra-column dead volumes [93]:

$$m_{i,SMB} = m_i + \frac{V_{i,dead}}{V_c \cdot (1-\varepsilon)} \tag{3.42}$$

3.4.4 Gradient SMB process

As mentioned above, the use of continuous counter-current multi-column gradient chromatography offers attractive opportunities in the field of protein separations due to the possibility of tuning the mobile phase strength within the simulated moving bed process [8].

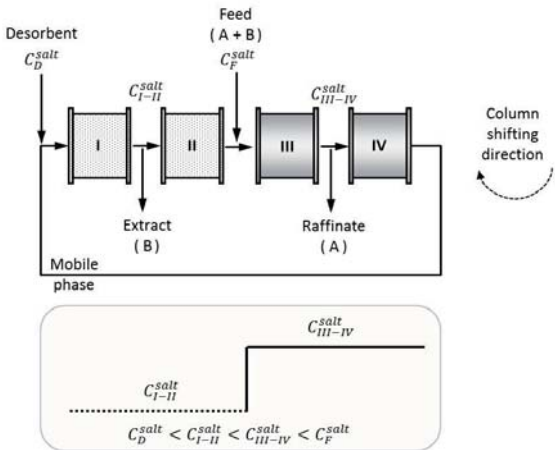

Figure 3.4: Schematic representation of closed-loop 4-zone gradient Simulated Moving Bed process

As outlined above, in the area of bioseparations, gradient elution chromatography is one of the most common unit operations. The combination of simulated moving bed and gradient elution should offer an improved separation performance by tuning the adsorption behavior of the components using adjusted eluting conditions in zones I and II, and binding conditions in zones III and IV [1].

In Figure 3.4, the principle of a closed-loop 4-zone gradient Simulated Moving Bed unit is depicted. The stepwise gradient is also illustrated. The stepwise gradient is achieved using different concentrations of a modifier or a salt in the mobile phase, C_i^{salt}, at the inlet ports. The change in mobile phase composition is produced between the zones II and III due to the introduction of the feed stream. Zones I and II operate under a certain mobile phase composition and zones III and IV operate under a different mobile phase composition indicated in Figure 3.4 by different modifier or salt concentrations, C_{I-II}^{salt} and C_{III-IV}^{salt}. The two distinct levels of mobile

phase compositions affect the adsorption behavior of the components within the SMB unit, i.e. they provide distinct favorable adsorption equilibrium constants [1, 7, 8].

In a stepwise gradient SMB process usually the weaker mobile phase is introduced with the feed and a stronger mobile phase for efficient adsorbent regeneration is introduced using the desorbent stream [7].

3.4.5 Open-loop 3-zone pH-gradient SMB process

A simplified gradient SMB configuration could be made consisting of just three zones eliminating zone IV. This open-loop 3-zone process provides an attractive option when cheap aqueous buffers can be used as mobile phase and solvent recycling is not mandatory [102].

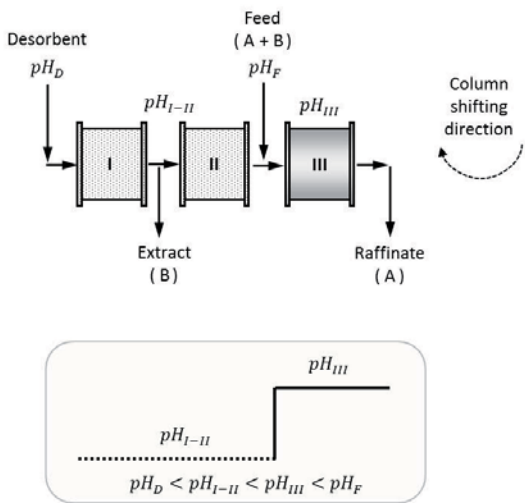

Figure 3.5: Schematic representation of open-loop 3-zone pH-gradient Simulated Moving Bed process

In this work, an open-loop 3-zone pH-gradient SMB unit as depicted in Figure 3.5 is suggested for the separation problem under investigation. This configuration exploits two different inlet fluid phases with two distinct pH values, pH_{I-II} and pH_{III}. This establishes two different pH levels in zones I and II, and in zone III.

The purification of two components, k_1 and k_2, is possible by tuning the retention behavior within the SMB unit imposing non-adsorbing conditions in zones I and II, and adsorbing conditions in zone III.

3.5 Evaluation of the performance of chromatographic processes

An evaluation of the performance of discontinuous and continuous chromatographic processes requires the definition of several performance parameters, such as final concentration, purity, productivity, yield and specific buffer consumption [120].

The specific mean component concentration over the fractionation time (discontinuous chromatography) or switching period (continuous chromatography) are the key to assess the performance of a chromatographic purification process under either isocratic or gradient conditions [36].

In the case of discontinuous chromatographic purification, the performance parameters are calculated using specific mean component concentration in the different fractions collected over the course of the chromatographic run, $\bar{c}^k_{fraction}$, during certain fractionation time (between t_{start} and t_{end}):

$$\bar{c}^k_{fraction} = \frac{1}{t_{end} - t_{start}} \cdot \int_{t_{start}}^{t_{end}} c^k(t) \cdot dt \tag{3.43}$$

The mass of product in this fractionation time is:

$$m^k_{fraction} = \bar{c}^k_{fraction} \cdot V_{fraction} \tag{3.44}$$

The purity, PUR^k_{Batch}, is defined as the specific mean component concentration of one of the components, $\bar{c}^k_{fraction}$, over the sum of the specific mean component concentration of all components ($k = A, B, ..., NC$) present in the fraction:

$$PUR^k_{Batch} = \frac{\bar{c}^k_{fraction}}{\sum_{k=1}^{NC} \bar{c}^k_{fraction}} \tag{3.45}$$

The yield, Y^k_{Batch}, is the mass of component recovered in the fraction(s) of interest, $m^k_{fraction}$, related to the mass of this component present in the feed, m^k_{Feed}:

$$Y^k_{Batch} = \frac{m^k_{fraction}}{m^k_{Feed}} \tag{3.46}$$

The productivity, PRD^k_{Batch}, is the amount of product recovered, $m^k_{fraction}$, divided by the cycle time, t_{cycle}, and the volume of stationary phase, V_s:

$$PRD^k_{Batch} = \frac{m^k_{fraction}}{t_{cycle} \cdot V_s} = \frac{m^k_{fraction}}{t_{cycle} \cdot V_c \cdot (1-\varepsilon)} \tag{3.47}$$

The specific desorbent consumption, SDC^k_{Batch}, is the total volume of mobile phase used for a complete cycle, V_{MP}, over the purified amount of target product, m^k:

$$SDC^k_{Batch} = \frac{V_{MP}}{m^k} \tag{3.48}$$

Analogously, performance parameters can also be evaluated for SMB chromatography considering the switching time and the corresponding outlet streams extract and raffinate where the purified components are collected. These parameters remain constant once the periodic cyclic steady state has been reached.

In the case of continuous chromatographic purification, the performance parameters for a component k are calculated using the specific mean component concentration at the corresponding outlet port (Extract or Raffinate), $\bar{c}^k_{port}$, collected over a switching period:

$$\bar{c}^k_{port} = \frac{1}{t_{switch}} \cdot \int_0^{t_{switch}} c^k(t) \cdot dt \tag{3.49}$$

The mass flow rate over the switching period is:

$$\dot{m}^k_{port} = \bar{c}^k_{port} \cdot \dot{V}^k_{port} \tag{3.50}$$

The purity, PUR^k_{port}, is again defined as the specific mean component concentration of one of the components, $\bar{c}^k_{port}$, over the sum of the specific mean component concentration of all components ($k = 1, 2, ..., NC$) present at the outlet port (Extract or Raffinate):

$$PUR^k_{port} = \frac{\bar{c}^k_{port}}{\sum_{k=1}^{NC} \bar{c}^k_{port}} \tag{3.51}$$

The yield, Y^k_{port}, is the mass flow rate of component recovered at the outlet port, $\dot{m}^k_{port}$, related to the mass flow rate of component entering the SMB unit at the feed inlet port, $\dot{m}^k_{Feed}$:

$$Y^k_{port} = \frac{\dot{m}^k_{port}}{\dot{m}^k_{Feed}} \tag{3.52}$$

The productivity, PRD^k_{port}, is the mass flow rate of product recovered, $\dot{m}^k_{port}$, at the outlet port (Extract or Raffinate) over the number of columns, N_c, and the volume of stationary phase, V_s:

$$PRD^k_{port} = \frac{\dot{m}^k_{port}}{N_c \cdot V_s} = \frac{\dot{m}^k_{port}}{N_c \cdot V_c \cdot (1 - \varepsilon)} \tag{3.53}$$

The specific desorbent consumption, SDC^k_{SMB}, is the total volumetric flow rate of mobile phase used within switching period over the purified mass flow rate of target product, $\dot{m}^k_{port}$:

$$SDC^k_{SMB} = \frac{\dot{V}_{Desorbent} + \dot{V}_{Feed} + (\dot{V}_{Cleaning} + \dot{V}_{Equilibration})}{\dot{m}^k_{port}} \tag{3.54}$$

In the case of an open-loop configuration, additional desorbent consumption should be considered. Thus, the volumetric flow rates corresponding to the cleaning and equilibration zone were included in Equation (3.54).

Chapter 4

Chromatographic purification of antibody fragments

The purification of biopharmaceuticals has been focused in the past on monoclonal antibodies. However, the advance of recombinant protein technology is shifting the product portfolio to small-sized and powerful biomolecules such as antibody fragments. At the same time, downstream processing technology is moving towards simple purifications taking advantange of the highly specific tags attached to target proteins and the recently developed chromatographic affinity resins [23].

This chapter summarizes the state-of-the-art in the chromatographic purification of antibodies and antibody fragments. Research in the field of recombinant protein chromatographic purification considered basically two kind of processes: (1) discontinuous multi-step processes, and, (2) continuous multi-column arrangements. The former type of processes is up to now predominantly applied and investigated.

This chapter also introduces the foundations for the purification of histidine-tagged proteins by immobilized metal ion affinity chromatography (IMAC), which was used in the experimental part of this work.

4.1 State of the art

Many reports on IMAC for antibody or recombinant protein purification have been published [11, 46, 138] but only a few are dedicated to the development of continuous chromatographic purification processes [6, 51, 113]. Previous research has been mainly focused on discontinuous chromatographic separations. Nevertheless, there are a couple of publications highlighting the possibilities of using continuous

chromatographic purification either for antibody purification or combined with IMAC for recombinant proteins such as β-glucosidase [113]. Both, discontinuous and continuous approaches are going to be summarized in this section.

Vançan et al. studied the separation of human immunoglobulin G using different metal ions chelated to an IDA-Sepharose matrix (Cu^{2+}, Zn^{2+}, Ni^{2+} and Co^{2+}), and also different adsorption buffer systems (MOPS, MMA, Phosphate and Tris-HCl). The adsorption was high irrespective of the metal ion or buffer selected [130]. A similar analysis was realized by Todorova-Balvay et al. but isolating not only the full-length antibody but two Fab fragments and the Fc fragment [128]. The fragments showed less affinity for the stationary phase than the full-length antibody.

Currently, discontinuous single-column processes are dominant for the purification of histidine-tagged single-chain antibody fragments (scFv) by IMAC. Examples of histidine-tagged antibody fragment separations using IMAC are given by Essen [39], Skerra [121], and Yan [142]. Essen and Skerra investigated the elution of the variable domains (VH and VL) of a scFv when a $(His)_6$-tail was fused to each domain. Stoichiometric elution of the domains was only possible by the introduction of an electrolyte (glycine betaine) which stabilized the non-covalent association of the domains [39]. In the latter examples, scFv antibodies with an histidine affinity tail were purified in a single-step. Antibody fragments conserved during purification their activity and functionality [121, 142].

Hexa-histidine tags or PEGylation were also used for producing several clinical-grade single-chain antibody fragments. In Casey's report, IMAC outperfomed the traditional antigen affinity chromatography with higher yield, less costly scale-up and lower risk of tumour derived from antigen leaching [21]. In Laroche's report three purification steps were necessary to obtain a single-chain fragment free from contaminants that were co-purified by IMAC [82]. Moosmann demonstrated that the combination of cation exchange and hydrophobic interaction chromatography provides an effective purification of PEGylated single-chain antibody fragments reaching purities of 98% [94].

A theoretical approach presented by Vunnum and Cramer gives an insight to understand the complex dynamics of protein chromatography using IMAC in the presence of competitive mobile phase modulators such as imidazole [135]. An accurate model for the estimation of multicomponent isotherms was developed and validated using certain model proteins. The model considers multipointed nature of protein adsorption and the adsorption behavior of imidazole [133, 134].

Antos and Seidel-Morgenstern performed systematic simulations to identify regions of feasible operating parameters as a function of the locally changing nonlinear

adsorption equilibria for a two-step solvent gradient SMB [7]. The predictions were experimentally validated by the separation of two cycloketons using normal-phase silica and applying a two-step gradient using pure n-hexane as the weak solvent in the feed stream and pure ethyl acetate as the strong solvent in the desorbent stream. The improved purities and concentrations obtained in the raffinate and extract streams using a two-step gradient SMB demonstrated the potential of the gradients compared to the common isocratic SMB separation [7].

The use of SMB configurations for protein purification has been increased in the last decade and certain specific examples can be found in the literature. Gottschlich developed a SMB system with two additional purge steps for the biospecific purification of monoclonal antibodies [51]. Purge step 1 allows the equilibration of the column going into zone I. Purge step 2 removes the fast eluting contaminants within the fist minutes of the switching interval after leaving the adsorption zone. Adsorption and desorption of the target product is performed under gradient conditions. Monoclonal antibodies were purified with a yield of 90%.

Andersson and Mattiasson [6] described the separation of lactoperoxidase and lactoferrin using an SMB configuration with cation-exchange columns. SMB was compared against batch chromatography. SMB was more productive with lower buffer consumption and higher target protein concentration.

Salt gradients can improve resin use and reduce eluent consumption during isolation of proteins by ion-exchange in simulated moving beds (IE-SMB). The gradients are created using feed and desorbent solutions with different salt concentrations. This case was described and experimentally validated by Houwing and van der Wielen for successful fractionation of a dilute binary mixture of proteins using a salt gradient [59].

Nowadays, there is an increasing interest in using more productive and advanced multi-column configurations, in which biological multi-component mixtures are fed uninterruptedly and the target biomolecules are withdrawn continuously at two or more characteristic outlet ports.

Alternative configurations have been suggested and were successfully applied for protein purification, such as a multicolumn countercurrent solvent gradient purification (MCSGP) process [10, 95, 97], size exclusion simulated moving bed (SE-SMB) chromatography [19, 101], and the open-loop simulated moving bed (SMB) chromatography as an adaptation of the classical SMB principle [18, 55, 75]. In contrast to SMB, the MCSGP process offers the possibility to isolate more than two fractions. It is an attractive gradient-concept exploiting an elegant but complex combination between continuous steps connecting all columns and batch-wise elution

steps [78, 98].

Recently, an interesting article on SMB for the purification of histidine-tagged recombinant proteins appeared. In this paper, Sahoo et al. studied an open-loop imidazole-gradient SMB configuration of IMAC columns for the separation of histidine-tagged β-glucosidase expressed in *E.Coli* [113]. The process design was based on an optimized single-column protocol considering each step in the chromatography cycle (load, wash, elution and regeneration) as a set of columns in the SMB. The target product was purified with a recovery of 91% using less buffer and obtaining higher productivity than a comparable batch process.

Table 4.1 illustrates the main differences between batch, SMB and MCSGP processes:

Table 4.1: Advantages and disadvantages of discontinuous and continuous chromatography according to Mueller-Spaeth in [96]

Technology	Batch	SMB	MCSGP
Advantages	Multi-component separations Single-column Linear or stepwise gradients	High efficiency Continuous process Countercurrent operation	High efficiency Continuous process Linear or stepwise gradients Countercurrent operation
Disadvantages	Low efficiency Discontinuous process	Only binary separations Only stepwise gradients Multi-column set-up	Multi-column set-up Complex

Based on the previous work, the combination of IMAC and SMB techniques should provide a unique strategy for simplifying the current multi-step discontinuous approach and thus, reducing the cost of the whole purification process. In the next section, the mechanism of IMAC is explained in more detail.

4.2 Immobilized Metal Ion Affinity Chromatography (IMAC)

A strategy for the purification of recombinant proteins expressed in prokaryotic expression systems such as antibody fragments is the use of affinity peptide tags (e.g. histidine tags) that are genetically engineered into the protein facilitating its purification by immobilized metal ion affinity chromatography (IMAC) [11]. IMAC

is a very powerful tool for the purification of recombinant proteins in a single-step purification procedure [77].

Histidine is one of the 20 naturally ocurring amino acids commonly found in proteins. Natural histidine clusters are quite unlikely, that is why, the introduction of artificially-made histidine tags for the specific binding makes the separation easier and more selective [47]. Histidine tags are widely used because they have a small size (1 kDa of molecular weight) and do not interfere with the activity or structure of the target protein [106].

IMAC can be classified within the diverse group of affinity chromatographic techniques. This technique was developed by Porath and colleagues in 1970's and exploits the ability of some protein groups such as histidines, cysteines or tryptophans to form rather stable complexes with metal ions in nearly neutral aqueous solutions [107]. The strength of binding will depend on factors such as length, position and surface-exposure of this groups, on the metal ion type or on the pH of the buffers involved [47].

Multivalent transition metal ions such as Cu^{2+}, Zn^{2+}, Ni^{2+} or Co^{2+}, also called "intermediate" metal ions, are commonly used as IMAC ligands [137]. The strength of protein adsorption can be tuned by changing the transition metal ion [126]. The strength sequence was determined by Sulkowski ($Cu^{2+} > Ni^{2+} > Zn^{2+} > Co^{2+}$). Copper ions bind his-taggged proteins more strongly than nickel or cobalt. Nickel ions are the most common choice for purifying histidine-tagged proteins. Nickel ions provide good binding to His-tagged proteins but tend to bind non-specifically to certain proteins that contain histidine clusters [127].

In IMAC, the metal ion acts as an electron acceptor while the exposed histidines of the protein act as electron donors. Complexation with chelate-forming functional groups as iminodiacetic acid (IDA), or nitrilotriacetic acid (NTA) allows the metal ions linking to the stationary phase of the chromatographic column. Figure 4.1 represents schematically the metal ions disposition in the stationary phase and the interaction with the histidine-tagged protein:

In the Figure 4.1, the stationary phase consists of the matrix, M, the ligand, L, and the metal ion, Me^{n+}. The target product or histidine-tagged protein is represented by XP. And the concentration of a modifier usually imidazole is given by [M].

The ligand favors the anchor of the metal ion and provides an exposed position on the stationary phase [77]. Additionally, the matrix (usually cross-linked agarose or sepharose) should be permeable to proteins, strongly hydrophilic, chemically inert and microbiologically resistent under operational conditions. In order to promote

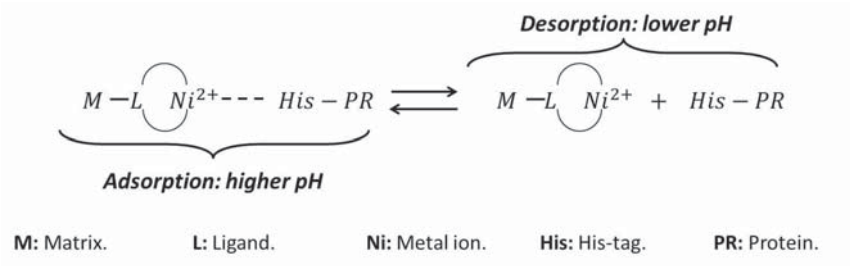

Figure 4.1: Schematic representation of IMAC reversible binding adapted from Porath [107]

protein adsorption and to reduce unspecific electrostatic interactions, equilibrium buffers with high ionic strength should contain high concentrations of sulfate or chloride salts [106].

The desorption-step in IMAC is carried out by two mechanisms: lowering the pH (at lower pH in the case of intermediate and soft metal ions, the metal chelate complex is disrupted and the protein eluted) or by the introduction of a competing electron donor species (i.e. imidazole, other metal ions or a chelator) maintaining in this case pH and ionic strength nearly constant [106, 133].

There are two kinds of binding in immobilized metal ion affinity chromatography (IMAC), specific and non-specific. The specific one involves only the target component and the metal ion. And the non-specific is an undesirable side-effect, caused by electrostatic or hydrophobic interactions.

Histidine is a weak polyprotic acid and the degree of dissociation depends on the pH of the medium[48]. At low pH, the ionic species of histidine depend on the ionisation state of the carboxyl group and the histidine side-chain is positively charged, $[His^{2+}]$. If the pH is increased around the neutral pH, the ionic species of histidine depend on the ionic state of the imidazole side chain and have a net positive charge, $[His^{1+}]$. If the pH is further increased above the $pK_{a2} = pK_{Imidazole} = 6.0$, histidine is uncharged, $[His^{0}]$. Finally, a further increase in pH results in the dissociation of the amino group to yield the negatively charged histidine, $[His^{1-}]$.

Advantages of IMAC are numerous: low costs, high stability and reproducibility, durable and easily regenerated adsorbents, gentle elution conditions [23]. Very dilute protein solutions can be effectively purified in a single-step procedure. Purities over 90% are often possible, which is desirable for continuous process like SMB

and large-scale purifications at industrial scale [9, 46, 47]. Table 4.2 compares characteristic features of HIC, IEC, and AC against IMAC:

Table 4.2: A comparison of the different gradient elution chromatographic techniques against IMAC according to Chaga [23]

Property	HIC	IEC	AC	IMAC
Capacity	High (Medium)	High	Low	High (Medium)
Recovery	Medium	High	Medium	High
Loading	Sometimes harsh	Mild	Mild	Mild
Elution	Mild	Mild	Harsh	Mild
Regeneration	Incomplete	Complete	Incomplete	Complete
Selectivity	Low-medium	Low-medium	High	Medium-high
Cost	Low	Low	High	Low

IMAC stationary phases are currently produced by several companies such as GE Healthcare Bio-Sciences AB, Merck KGaA, Dionex Corporation, and Bio-Rad Laboratories, Inc among others. The resins produced by these companies are summarized in Table 4.3:

Table 4.3: Companies producing IMAC stationary phases and their corresponding references on the market

Company	Resin
Dionex Corporation	Dionex ProPac® IMAC-10
Bio-Rad Laboratories, Inc	Profinity™ IMAC
Merck KGaA	Fractogel® EMD Chelat (M)
GE Healthcare Bio-Sciences AB	HisTrap™ - Ni Sepharose™

The specific materials used in this work will be explained in the next chapter.

Chapter 5

Materials and methods

This chapter deals with the materials, the analytical methods and the chromatographic equipment used in the experimental part of this work. First, the cell culture supernatant containing the single-chain antibody fragment is described. After that, the chapter addresses key issues for choosing a suitable chromatographic system (mobile and stationary phases) and the analytical methods necessary for quantifying the purification of the antibody fragments by immobilized metal ion affinity chromatography.

5.1 Materials

This section introduces the cell culture supernatant containing the target product, the single-chain antibody fragment, the buffer solutions, the stationary phase, and the equipment used for the discontinuous and continuous chromatographic experiments.

5.1.1 Cell culture supernatant

In the frame of the Collaborative Research Center SFB 578, "From Gene to Product", funded by the German Research Foundation, the groups of Prof. Duebel and Dr. Hust at the Institute of Biochemistry and Biotechnology and the group of Dr. Franco-Lara and Dr. David at the Institute of Biochemical Engineering at the Technical University of Braunschweig have succesfully expressed the lysozyme specific histidine-tagged single-chain fragment variable in *Bacillus Megaterium*.

B. megaterium, a gram-positive bacterium, is a useful industrial production strain and expression host with high secretion capacities [132]. The lack of an outer membrane allows the harvest of secreted functional single-chain antibody fragments directly from the cell culture supernatant and is a considerable advantage of *B. megaterium* compared to gram-negative organisms such as *E. Coli* [31].

The single-chain fragment variable antibody fragment is directly secreted in the cell culture medium characterized by a composition given in Table 5.1:

Table 5.1: Composition of the medium containing the single-chain antibody fragment adapted from [31]

Composition	Amount [g/L]
Sulfates	24.00
Phosphates	8.82
Chlorides	0.41
Xylose	5.00
$(NH_4)_6MoO_{24}{\cdot}4H_2O$	0.02
H_3BO_3	0.0002

Characterization of the target protein was carried out at the Institute of Biochemical Engineering of the Technical University of Braunschweig and it is presented in Table 5.2:

Table 5.2: Properties of the single-chain antibody fragment adapted from [31]

Property	Description
Formula	$C_{1164}H_{1775}N_{329}O_{369}S_6$
Aminoacids number	246
Molecular weight	27 KDa
Isoelectric Point	8.3

The production of the single-chain antibody fragment was carried out in shaking flasks using a medium with pH 7.2. After that, 2 mL /L of sterilized filtered trace element solution was added. The preculture was prepared in overnight cultures in shake flasks at 37°C and 250 rpm. The induction was started by adding 0.5% xylose. The culture was shaken at 250 rpm and 37°C for up to 48 h. At different times, the supernatant was directly used for analysis and control. The details for

the production of the antibody fragment can be found in the literature [31, 32, 33, 68].

It is worth to mention that more than 30 components, most of them proteins, are present in the cell culture supernatant making the purification of the target product a very difficult task. The antibody fragment has a molecular weight around 27 kDa and the estimated concentration of the antibody fragment in the cell culture supernatant was around 1 mg/L.

5.1.2 Stationary phase

The chromatographic technique selected in this work for the antibody fragment purification was IMAC as explained in detail in Section 4.2, which is based on the interaction of histidine-tagged proteins with metal ions, such as Ni^{2+}, present on the surface of the IMAC's stationary phases [26, 58, 77, 107].

The commercial ready-to-use chromatographic columns, HisTrap™ HP (GE Healthcare Bio-Sciences AB, Uppsala, Sweden), were used in the experimental part of this work. These columns were prepacked and precharged with Ni Sepharose™ High Performance (highly cross-linked agarose beads with nickel as metal ion). According to the manufacturer [2], the stationary phase exhibits low nickel ion leakage and is compatible with a wide range of additives.

The column properties are presented in Table 5.3:

Table 5.3: Properties of the ready-to-use HisTrap™ HP columns [2]

Property	Description
Matrix	Highly cross-linked spherical agarose, 6%
Average particle size	34 μm
Dynamic binding capacity	40 mg of $(His)_6$-tagged protein/mL of medium
Column Volume	aprox. 1 mL
Column Dimensions	2.5 cm x 0.7 cm i.d.
Max. Flow rate	4 mL/min
Max. Back pressure	3 bar

Although microbial growth in the medium is not expected, as precaution and to avoid fouling, the columns were always washed first with water and then with a solution of 20% ethanol after operation. Finally, the columns were stored at 4°C.

5.1.3 Mobile phase

Aqueous buffers are often used as mobile phase for purifying proteins. Buffers keep proteins soluble and active, and also prevent unfolding or aggregation. When working with buffers, it is important to take into account parameters such as pH, salt composition, stabilizing elements, and reducing agents among others [20].

Downstream processing costs become an extremely relevant issue when purifying proteins. That is why, the concentration of the buffer should be kept as low as possible, usually around 10 - 20 mM [35]. Another significant issue is the absorbance of the buffer in the UV spectral region when using an UV signal for detection [37]. It is strongly recommended to use high quality water (deionised and filtered through a sterile ultrafiltration system) to prevent bacterial growth [72].

The definition of pH is based on the fact that the dissociation of water into hydrogen ions and hydroxyl ions is stoichiometric and occurs to the extent that 10^{-7} mol of $[H^+]$ and 10^{-7} mol of $[OH^-]$ are present at equilibrium in 1 liter of water at 25 °C and at neutral pH 7.0 [48]. In 1909, the Danish biochemist Søren Sørensen, introduced the pH-scale to simplify the troublesome use of negative exponents to express the hydrogen ion concentrations within a range between 10^0 and 10^{-14} and defined pH as the negative logarithm with base 10 of the hydrogen ion concentration [48]:

$$pH = -\log_{10}[H^+] \tag{5.1}$$

It is worth noting that pH scale, as expressed in Equation (5.1), is a logarithmic scale, which means that pH values differing by one pH unit exhibit a ten-fold difference in the hydrogen ions concentration $[H^+]$.

The observation that partially neutralized solutions of weak acids or weak bases are resistant to pH changes usually over a range of +/- 1 pH unit around the pK_a on the addition of small amounts of acids leads to the discovery of buffers [105]. Buffer solutions are made up of an acid and its conjugate base. Thus, the pH value is kept almost constant in certain range.

In this work, phosphate buffers were used as mobile phase, which are a major intracellular buffering system. In order to generate a stepwise and descending pH-gradient through the IMAC column, loading and elution buffers are needed. Loading and elution buffers were prepared by dissolving 10 mM of sodium dihydrogen phosphate monohydrate ($NaH_2PO_4 \cdot H_2O$, Merck KGaA, Darmstadt, Germany), 10 mM of di-sodium hydrogen phosphate anhydrous (Na_2HPO_4, Merck KGaA,

Darmstadt, Germany) and 0.5 M sodium chloride ($NaCl$, Sigma-Aldrich Chemie GmbH, Steinheim, Germany) in water. Finally, pH value was adjusted either to 6.5 (Loading buffer) or 4.0 (Elution buffer) with either concentrated solutions of sodium hydroxide or hydrochloric acid.

Buffers were filtered prior to chromatography (Cellulose nitrate filters 0.20 μm, Sartorius Stedim Biotech, Goettingen, Germany). Water used in all experiments was purified in a Milli-Q® ultrapure water purification system (Milli-Q® gradient, Millipore SAS, Molsheim, France). The composition of the buffers is summarized in Table 5.4.

Table 5.4: Mobile phase composition

Buffer	Composition
Loading buffer	20mM $NaH_2PO_4 \cdot H_2O$, 0.5 M NaCl, pH 6.5
Elution buffer	20mM $NaH_2PO_4 \cdot H_2O$, 0.5 M NaCl, pH 4.0

When using pH-gradient together with IMAC, adsorption of a his-tagged recombinant protein to the IMAC stationary phase is performed at a neutral or close to neutral pH at which histidine is in the nonprotonated form. The use of strong electrolytes, such as $NaCl$ that dissociates completely in water, reduces the nonspecific electrostatic interactions and focuses the binding on the chelated metal ion. Elution of the target recombinant protein is achieved by protonation using an elution buffer with lower pH [46].

5.1.4 Chromatographic equipment

This section introduces the chromatographic equipment used for the discontinuous and the continuous purification of the antibody fragments.

Discontinuous chromatography

Batch chromatographic experiments were carried out in an ÄKTA Purifier 100 controlled by Unicorn software (GE Healthcare Bio-Sciences AB, Uppsala, Sweden). The pH-gradient was monitored online at the column outlet using an 88 μl flow cell equipped with a flow-through pH electrode (GE Healthcare Bio-Sciences AB, Uppsala, Sweden). Offline pH measurements of buffers were done using a Mettler Toledo pH meter (Mettler-Toledo GmbH, Schwerzenbach, Switzerland).

The device incorporates a binary pump which has four pump heads in two modules A and B. Usually only the buffers contained in A (loading buffer) and B (elution buffer) are used. This pump is able to reach a flow-rate up to 100 ml/min and a pressure up to 10 MPa. Switch valves are responsible of selecting the solutions required and leading them to the pump. The election between linear or stepwise elution gradients can be programmed with the *UNICORN* software.

The streams are mixed in the mixer installed just after the pump. A filter of 2 μm pore size is installed after the mixer to avoid the entrance of particles into the column. The injection of the sample is carried out by a 7-way valve. This valve connects the different ports with the column or to the waste vessel.

After the column, the flow cells installed on-line provide data about the UV absorption (up to three wavelengths in the range 190-700 nm), the conductivity and the pH of the mobile phase. With the unit it was also possible to collect samples coming out from the column using the fraction collector. This device can collect up to 95 fractions with fixed or variable volume.

Continuous chromatography

SMB experiments were carried out with in a lab-scale system CSEP® C916 Simulated Moving Bed unit (Wissenschaftliche Gerätebau Dr. Ing. Herbert Knauer GmbH, Berlin, Germany).

64 ports connected in pairs are located in a multi-function valve and offer the possibility to use maximum 4 columns in each of the zones for a 4-zone set-up. Up to 16 chromatographic columns can be installed in this system. The multi-function valve is the heart of the unit and is made of Hastelloy and equipped with 1/16 inches connections. The upper part of the valve is static and is connected from and to the pumps. While the lower part of the valve is able to rotate and is connected from and to the columns. All capillaries have to be fixed at the multi-function valve, input and outputs of the pumps, or low dead volume couplings with the peek fittings and screwed joints.

Four or more WellChrom HPLC-pumps K-501, one HPLC-Interface Box, one control box, and two UV-Detectors are part of the system. The interface box connects the system to the personal computer for monitoring the continuous product streams. The switching time can be set with the control box.

The details regarding the connections of the simulated moving bed unit used for the experimental validation will be shown later in Section 8.1.

5.2 Methods

This section gives an overview of the offline analytical assays required to evaluate the performance of the discontinuous or continuous chromatographic separation.

5.2.1 Preparation of samples prior to chromatography

The non-clarified cell culture supernatant coming from the bioreactor were pretreated and clarified prior to chromatography as depicted in Figure 5.1. In the primary recovery, particles were removed by a combination of centrifugation and filtration processes [85].

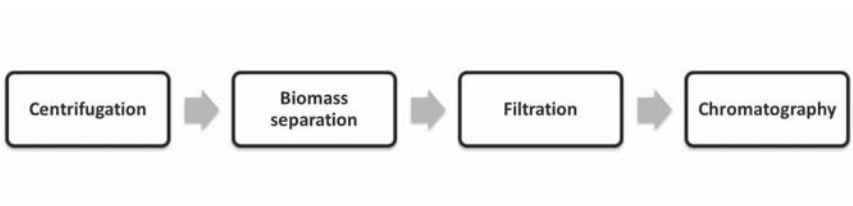

Figure 5.1: Schematic representation of the cell culture supernatant preatreatment

In the first clarification step, the supernatant was centrifugated for 30 minutes at 4°C and 4000 rpm, in order to remove the biomass present in the harvested cell culture fluid (Thermo Scientific Heraeus® Biofuge Stratos Centrifuge, Heraeus Holding GmbH, Hanau, Germany).

Next the supernatant was separated carefully from the precipitate. The particulate matter still present was removed by filtration (Pall® Acrodisc® 32 mm syringe filter with 0.2 μm Supor® Membrane, Pall Life Sciences, Ann Arbor, MI, USA). Filtration is the most common second clarification step in order to prevent the plugging of chromatographic columns [85].

The clarified cell culture supernatant was aliquated, stored frozen at -30°C, in order to preserve completely the protein structure and activity and thawed before the chromatographic runs.

5.2.2 Analytical assays

Analytical assays are time-consuming but necessary methods to quantify the performance of the separation.

Sodium dodecyl sulphate-polyacrylamide gel electrophoresis (SDS-PAGE)

This method uses a discontinuous polyacrylamide gel as a support medium and sodium dodecyl sulfate to denature the proteins. The method is called sodium dodecyl sulfate polyacrylamide gel electrophoresis (shortly SDS-PAGE).

In gel electrophoresis, the gel acts as a sieve for the proteins in the sample, small proteins will move faster and large proteins will move slower. Thus, the separation of proteins is based on their molecular size and is a valuable tool in the identification of proteins [72]. The protein sample must be unfolded and coated with sodium dodecyl sulfate molecules under denaturing and reducing conditions. The number of molecules bound by a protein is proportional to the length of its polypeptide chain and the protein acquires a net negative charge that overwhelms any intrinsic charge that the protein might have. The movement of the negatively charged and unfolded proteins in an electrical field towards a positively charged electrode can be related with its molecular size. The visualization of the proteins is carried out using a protein-specific staining technique. Finally, the size of the protein can be estimated by comparison of its migration distance on the gel against the standard proteins of known molecular weights [81].

The collected chromatographic samples were ultrafiltrated to concentrate the proteins prior to electrophoresis (Amicon® Ultra-4 Centrifugal filters with Ultracel®-10k, Millipore Ireland Ltd, Cork, Ireland). Following this, the samples were mixed with the Laemmli buffer and heated at 99°C and shaked at 750 rpm for 10 min (Thermomixer comfort, Eppendorf AG, Hamburg, Germany). The electrophoresis was done using 12% SDS-PAGE gel according to the method of Laemmli [81]. Samples were compared to the standard protein marker (PageRuler™ Unstained Protein Ladder, Fermentas GmbH, St. Leon-Rot, Germany). Clarified cell culture supernatant and collected samples were resolved on SDS-PAGE and stained with Coomassie blue (Coomassie® Brilliant Blue R-250, AppliChem GmbH, Darmstadt, Germany). Up to 20 μl of the mixture was loaded onto the wells of 12% precasted SDS-PAGE gels and separated at 50 mA for 1 h (Biometra® Power Pack P25 T, Biomedizinische Analytik GmbH, Goettingen, Germany). See Appendix A for details of the SDS-PAGE procedure.

Purity estimation by densitometry

The purity of the single-chain antibody fragment was estimated by densitometric analysis of the Coomasie-stained gels using the image processing software ImageJ IJ1.46r (National Institutes of Health, MD, USA). ImageJ is used to analyze and process all types of images in biology-related research.

Basically, the densitometric method translates each lane of the SDS-PAGE gel into a lane profile plot as is illustrated in Figure 5.2:

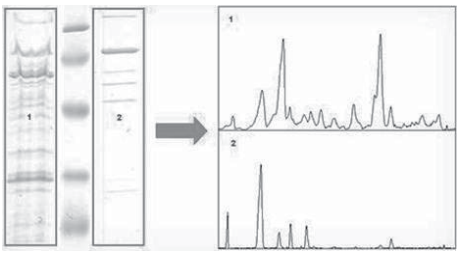

Figure 5.2: Schematic representation of the purity estimation by densitometry

The purity measurement is based on the analysis and quantification of the lane profile plots from the SDS-PAGE gel by measuring peak areas corresponding to each of the bands found on the gel using the Image Processing software ImageJ [65].

Each SDS-PAGE gel for purity analysis was scanned on a flat-bed scanner as grayscale image with a medium value resolution around 300 dpi. The image of the scanned gel was processed by surrounding the lane of interest for analysis. The image was improved by substracting the background and enhancing the contrast. The lane profile plot was generated and the area of each peak of the lane profile plot was determined. The purity of the antibody fragment was estimated as the normalized value of the area of the band around 27 KDa to the total area of the lane profile plot. Purity was expressed as percentage of the total area of the lane profile plot.

Quantification of the single-chain antibody fragment concentration by Enzyme-linked immunosorbent assay (ELISA)

The activity and concentration of specific antibodies and antibody fragments can be measured by the use of a defined antigen [29]. Enzyme-linked Immunosorbent Assay (ELISA) is used for the estimation of the single-chain antibody fragment concentration.

This analytical assay involves different steps such as addition, reaction, and incubation, followed by the separation of bound and free reagents using washing steps. Antigen binding ELISA was done according to previosly established protocol by Jordan [68]. First, hen egg white lysozyme is immobilized on the wells of a 96-well Maxisorp® microtiter plates (Nunc GmbH & Co.KG, Wiesbaden, Germany) overnight at 4°C. Coated wells were washed three times with PBST (PBS + 0,1% (v/v) Tween 20) and blocked with 2% (w/v) skim milk powder in PBST for 1.5 h at room temperature, followed by three times washing with PBST. Soluble antibody fragments were diluted in blocking solution and incubated for 1.5 h, followed by three times washing with PBST. Soluble antibody fragments were detected with mAb mouse anti-penta His-tag (Qiagen, Hilden, Germany) and polyclonal goat anti-mouse IgG conjugated with horse radish peroxidase (Sigma, Taufkirchen, Germany) and visualised with 3,3',5,5'-tetramethylbenzidine substrate. The staining reaction was stopped by adding 1 N sulphuric acid. The absorbances at 450 nm and scattered light at 620 nm were measured using a microtitre plate reader SUNRISE (Tecan, Crailsheim, Germany). The absorbance at 620 nm was subtracted. The method is illustrated in Figure 5.3.

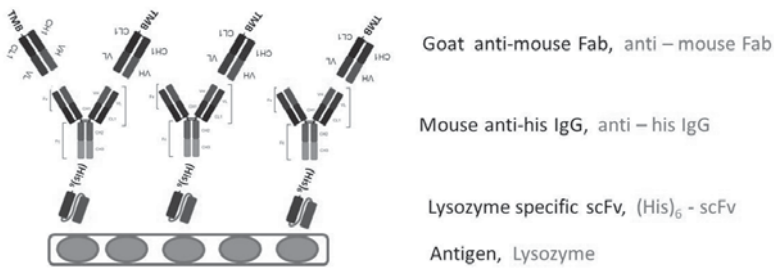

Figure 5.3: Schematic representation of the ELISA assay for the estimation of the antibody fragment concentration

Determination of the concentration of the functional folded single-chain Fragment

variable antibody was carried out by parallel measuring different known concentrations made by serial dilutions of the antibody fragment on the microtiter plate. In this way, it was possible to measure the functional and active amount as the concentration of the single-chain antibody fragment present in the different collected samples [31]. See also Appendix B for details of the ELISA procedure.

Chapter 6

Discontinuous chromatography: Single-column Experiments

This chapter describes the adsorption-desorption behavior of the histidine-tagged single-chain fragment variable antibody on a commercial IMAC column. First, the cell culture supernatant originating from *B. Megaterium* was characterized using single-column experiments in a pH-gradient elution mode.

Subsequently, an empirical approach was proposed capable to describe the course of the pH-profile as a function of time and position within the batch column under stepwise pH-gradient elution conditions. The dependence of the adsorption equilibrium constants on the pH was determined by stepwise pH-gradient elution experiments analyzed with the equilibrium-dispersive model. Finally, the performance parameters evaluating the discontinuous single-column process were determined.

6.1 Chromatographic elution behavior

In downstream processing, it is very common to find after bacterial fermentation highly diluted target recombinant proteins in the range of milligrams per liter coming from large bioreactors having volumes in the order of thousands of liters [38]. The goal is to recover such high-value target biopharmaceuticals from complex mixtures of proteins.

The purification of the antibody fragment by immobilized metal ion affinity chromatography was carried out using a stepwise descending pH-gradient. This IMAC pH-gradient was generated using a non-retained buffer system as described in Section 5.1.3. The IMAC column was equilibrated initially using 10 mL of

mobile phase (pH = 6.5) which promotes the binding of the histidine-tagged single-chain antibody fragment. After equilibration with the loading buffer, 2 mL of diluted cell culture supernatant feed mixture were injected using a 2 mL injection loop (GE Healthcare Bio-Sciences AB, Uppsala, Sweden). For the discontinuous single-column experiments, this feed mixture containing the single-chain antibody fragment was diluted to 1:1 in the loading buffer. The feed concentration of the single-chain antibody fragment for the batch experiments was 0.88 mg/L. Dilution of the feedstock may help to promote binding between the histidine-tagged antibody fragment and the IMAC adsorbent by adjusting the pH of the feed mixture. After injection of the sample, the stepwise pH-gradient was realized by a sudden change from 0% to 100% of elution buffer (pH = 4.0) which was maintained over 30 mL to elute the target protein. The flow rate was kept constant at 1.28 mL/min during the whole experiment. UV-signals for the chromatograms were measured at 214 nm.

The chromatographic conditions of the discontinuous single-column stepwise pH-gradient experiments are summarized in Table 6.1:

Table 6.1: Chromatographic conditions of the discontinuous single-column stepwise pH-gradient elution experiments using IMAC

Chromatographic condition	Description
Stationary phase	Ni Sepharose™ High Performance
Column Volume	V_c = 0.96 mL
Column Dimensions	L = 2.5 cm, D = 0.7 cm
Mobile Phase	Loading Buffer: Sodium phosphate (20 mM), sodium chloride (500 mM), pH 6.5; Elution Buffer: Sodium phosphate (20 mM), sodium chloride (500 mM), pH 3.8 - 5.0
Gradient	Step 0 - 100 %
Flow rate	$\dot{V}$ = 0.64 - 1.28 mL/min
Sample	Diluted cell culture supernatant containing the antibody fragment
Sample volume	$V_{injection}$ = 0.1 - 2 mL
Absorbance	214 nm
Concentration antibody fragment, Feed	c_{Feed}^{scFv} = 0.88 mg/L
Fraction volume	$V_{fraction}$ = 2 - 4 mL

The antibody fragment was eluted by lowering the pH. This kind of recombinant proteins may not be stable at low pH values, resulting in aggregation, degradation, and product inactivation [96]. For this reason, the fractionation over the elution step was carried out pouring 0.5 mL of neutralization buffer (Tris-HCl, pH 8.6) in

the tubes used for fractionation before the samples were collected.

A characteristic single-column batch chromatogram is shown in Figure 6.1. Several fractions were collected over the course of the whole chromatographic run for subsequent analytical assays. The proteins in the cell culture supernatant migrate with different rates as they pass through the IMAC-column. Basically, there are two characteristic fractions, an impurity fraction, IMP, and the antibody fragment fraction, ABF, displaying different degrees of affinity to the stationary phase as depicted in Figure 6.1. The lane numbers in the SDS-PAGE shown in Figure 6.2 correspond to the fractions in Figure 6.1.

After these results, the purification of the antibody fragment fraction, ABF, was considered as a pseudo-binary separation problem. The pseudo-binary feed mixture consists of the protein impurity fraction, IMP, as the faster eluting fraction and the antibody fragment fraction, ABF, as the slower eluting fraction.

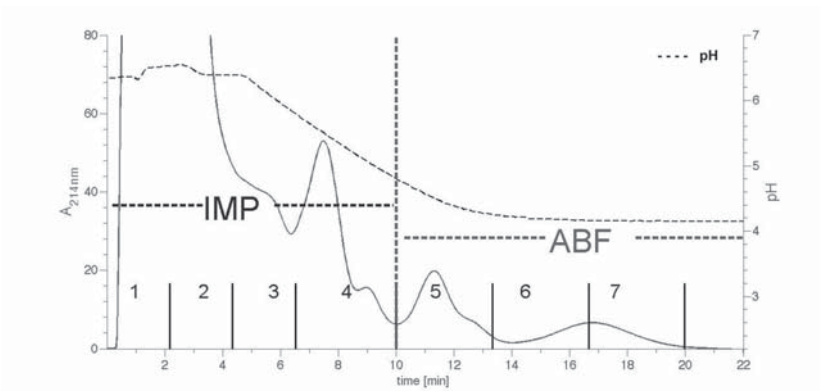

Figure 6.1: Chromatographic elution profile of diluted cell culture supernatant containing the single-chain antibody fragment using a stepwise pH gradient. Conditions as given in Table 6.1: Sample Load = 2 mL; Flow rate = 1.28 mL/min; Loading Buffer: Sodium phosphate (20 mM), sodium chloride (500 mM), pH 6.5; Elution Buffer: Sodium phosphate (20 mM), sodium chloride (500 mM), pH 3.8

The major eluting protein impurity fraction, IMP, was formed by the large amount of unretained proteins and the non-specifically bound proteins. The IMP fraction passed rapidly through the column during the sample loading and at the beginning of the descending pH-gradient due to the lack of exposed histidine clusters (see Figure 6.1 and Figure 6.2; fractions 1 to 4).

The results of SDS-PAGE analysis of fractions 1 to 4 reveal that the protein impurity fraction IMP (see Figure 6.2; lanes 1 to 4) contains a significant amount of different proteins with larger and lower molecular weights compared to the target single-chain antibody fragment band at 27 KDa. Fractions and lanes 1, 2 and 3 illustrated the fact that most of proteins in the cell culture supernatant have no affinity to the IMAC-column. The non-specifically retained proteins can be seen in fraction and lane 4.

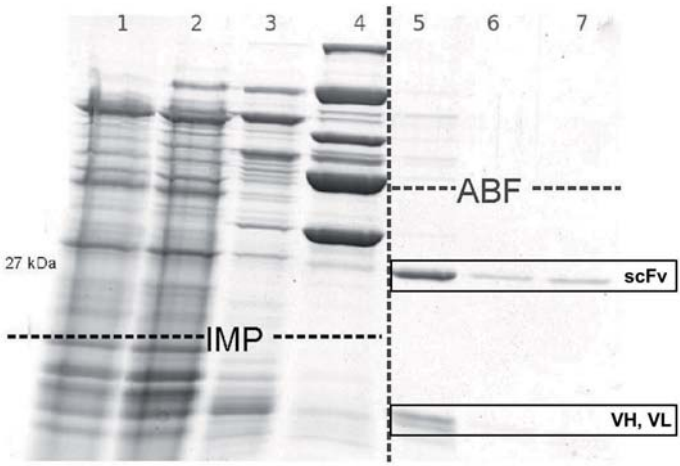

Figure 6.2: SDS-PAGE analysis of fractions collected over the course of chromatogram in Figure 6.1. The lane numbers correspond to the fraction numbers indicated in the chromatogram. Protein impurity fraction IMP (lanes 1 to 4) and antibody fragment fraction ABF (lanes 5 to 7)

As the pH value was further decreased the antibody fragment fraction, ABF, elutes in two distinct and separated peaks as the the most retained component with the highest affinity (see Figure 6.1; fractions 5 to 7). Elution of the strongly bound ABF fraction required an extense elution step. ABF was mainly composed by the 27 kDa single-chain antibody fragment band as shown in lanes 5 to 7 in Figure 6.2.

Two additional bands around 15 kDa corresponding to the histidine-tagged variable domains of the antibody fragment, VH and VL domains, eluted more concentrated in fraction 5 than in fractions 6 and 7 as illustrated in Figure 6.2. The presence of

the histidine-tagged variable domains in the ABF fraction could be explained due to the disruption of the peptide linker during purification or bacterial fermentation. Some conditions at the bioreactor when proteins are extracellularly secreted by *B. Megaterium* may lead to product degradation or even aggregation.

VH and VL domains bands were found in the ABF fraction. The variable domains were strongly bound to the IMAC-column but not stronger than the single-chain antibody fragment. The single-chain antibody fragment and its variable domains elute together only at the beginning of the elution of the antibody fragment, while the rest of the antibody fragment is more strongly adsorbed and elutes at the end of the chromatogram.

It can be assumed that the disrupted VH and VL domains were paired in solution through hydrophobic and ionic interactions [96]. Thus, the isolation of such domains from the correctly paired histidine-tagged single-chain antibody fragment by discontinuous single-column IMAC was not possible.

6.1.1 Column characterization

After these preliminary results the columns were characterized in more detail. The total column porosity was estimated experimentally using small pulses, 50 μL, of unretained protein collected in preliminary runs under isocratic conditions at different pH values and using a flow rate of 1 mL/min. Both hold-up times of the column and the apparatus were determined in this manner.

As a result of these quantitative evaluations, the hold-up time of the apparatus, $t_{0,a}$, was found to be equal to 0.19 min for a volumetric flow rate of 1 mL/min. The total hold-up time of the column and the apparatus, t_0, was 0.54 min. The difference between both values describes the hold-up time of just the column, $t_{0,c} = t_0 - t_{0,a}$. Equation (3.2) was used to estimate the total porosity of the column or the total void volume of the column, ε, using the volumetric flow rate, $\dot{V}$, and the column volume, V_c:

$$\varepsilon = \frac{\dot{V} \cdot t_{0,c}}{V_c} \tag{6.1}$$

The corresponding total porosity of a column was estimated to be $\varepsilon = 0.35$.

6.1.2 Influence of the elution pH

The elution pH plays a relevant role in the adsorption-desorption behavior of the proteins and the kinetics of the process. Optimization of this parameter makes possible to adjust the elution of the proteins under stepwise pH-gradients due to the different protonation degrees of the histidine at different pH values. The length and the strength of the stepwise pH-gradient under different elution conditions affects significantly the retention behavior of the proteins of interest.

Taking into account the pK_a value for the imidazole side chain of histidines ($pK_a = 6.0$), it can be concluded that the optimal binding conditions (i.e. pH) for the antibody fragment are above the pK_a and the elution conditions below the pK_a. Therefore, the elution of his-tagged proteins could be controlled by setting the pH of the elution buffer keeping the pH of the loading buffer above pH = 6.0.

The pH range for the discontinuous single-column experiments was chosen between the loading (pH = 6.5) and elution (pH = 3.8) buffer conditions. Selected stepwise pH-gradient elution profiles are depicted at three distinct elution pH values in Figure 6.3. The pH of the loading buffer was kept constant during these experiments at pH = 6.5. Although, the loading pH is also an important parameter, its effect was not studied in this work.

For an elution pH = 3.8, both fractions ABF and IMP eluted relatively fast and were less separated from each other as shown in Figure 6.3 (a). As the elution pH increased (pH = 4.6 and 5.0), the binding of the proteins became stronger resulting in larger retention times, broader and more separated peaks as illustrated in Figure 6.3 (b) and (c).

The peaks of the protein impurity fraction, IMP, were sharper and eluted faster than those of the antibody fragment fraction, ABF, and their retention times changed barely with the variations of the pH of the elution buffer.

In contrast, the peaks of the ABF fraction were more sensitive to the changes of the pH of the elution buffer. At pH = 5.0, the strength of the elution buffer was very weak for the elution of the antibody fragment resulting in very large retention times, very broad peaks and very diluted ABF fraction as depicted in Figure 6.3 (c).

The lowest elution pH was set to be 3.8 because lower pH values would result in damage of the stationary phase and a loss of reproducibility of the runs.

Summarizing, the characteristic peak of the IMP fraction contains the non-specifically bound proteins having some exposed histidine residues available for adsorption and displaying an intermediate affinity to the stationary phase. Those critical impurities are lumped in the characteristic peak of the IMP fraction.

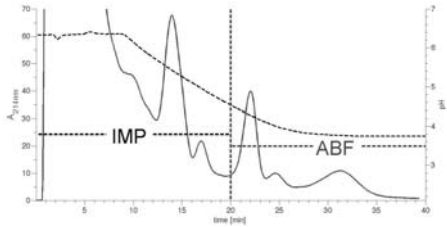

(a) $pH_{Elution} = 3.8$

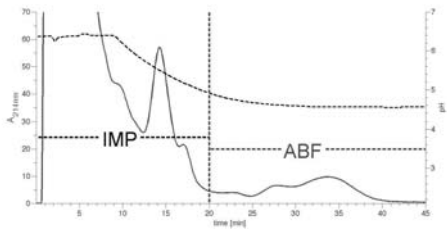

(b) $pH_{Elution} = 4.6$

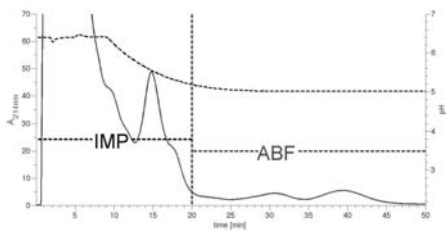

(c) $pH_{Elution} = 5.0$

Figure 6.3: Influence of the elution pH at (a) $pH_{Elution} = 3.8$, (b) $pH_{Elution} = 4.6$ and (c) $pH_{Elution} = 5.0$. Conditions as given in Table 6.1: Sample Load = 2 mL; Flow rate = 0.64 mL/min; Loading Buffer: Sodium phosphate (20 mM), sodium chloride (500 mM), pH 6.5; Elution Buffer: Sodium phosphate (20 mM), sodium chloride (500 mM), pH 3.8 - 5.0

Analogously, the characteristic peak of antibody fragment fraction corresponds to the first peak of the ABF fraction where most of the single-chain antibody fragment elutes. This pseudo-binary separation problem is illustrated in Figure 6.3 under different pH eluting conditions.

6.1.3 Influence of the sample load

The amount of sample injected into the column determines significantly not only the productivity but the peak resolution of the discontinuous single-column separation process. Samples injected in gradient elution protein chromatography have typically larger volumes and target proteins are highly diluted. The influence of the sample load or injection volume, $V_{injection}$, under the same stepwise pH-gradient elution conditions is discussed in this section.

As reference, the last peak of the IMP fraction and the first peak of the ABF fraction were considered when measuring retention times of the fractions.

Figure 6.4 shows three chromatograms with three distinct injection volumes. In all chromatograms can be observed that decreasing the injection volume, $V_{injection}$, decreases also the intensity of the UV-signal and the peaks are significantly smaller. With an injection volume of 0.1 mL, the proteins were hardly detectable by the UV detector as shown in Figure 6.4 (c). As expected, larger retention times were obtained when increasing the sample load.

The evaluation of the retention times of the components should take into account a correction considering the sample load in Equation (3.8). This correction was carried out subtracting the injection time, $t_{injection}$, from each retention time of the peaks of IMP and ABF, t_R^k, at the distinct sample load experiments. Retention times were determined using the method of moments as described in Section 3.2. The corrected retention times, $t_{R,corr}^k$, are given by Equation (6.2):

$$t_{R,corr}^k = t_R^k - t_{injection} \qquad k = IMP, ABF \tag{6.2}$$

The corrected retention times, $t_{R,corr}^k$, are summarized in Table 6.2:

Table 6.2: Evaluation of the retention times regarding the sample load using Equation (6.2)

Sample load	t_R^{IMP}	t_R^{ABF}	$t_{injection}$	$t_{R,corr}^{IMP}$	$t_{R,corr}^{ABF}$
2.0	13.9	22.0	6.5	7.4	15.5
1.0	10.3	18.7	3.4	6.9	15.3
0.5	8.7	17.2	1.8	6.9	15.4
0.1	7.2	15.7	0.6	6.6	15.1

In Table 6.2 can be observed that the effect of the sample load on the corrected retention times for IMP and ABF was negligible suggesting that the adsorption

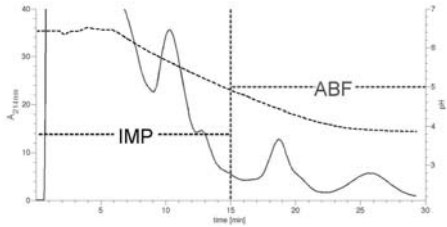

(a) $V_{injection} = 1.0$ mL

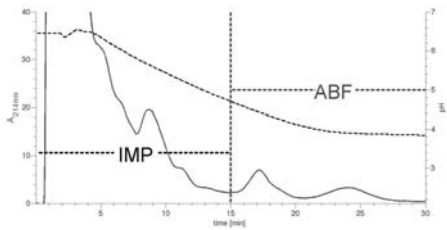

(b) $V_{injection} = 0.5$ mL

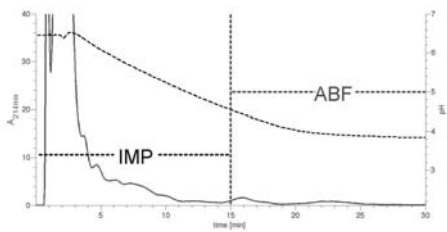

(c) $V_{injection} = 0.1$ mL

Figure 6.4: Influence of the sample load: (a) $V_{injection} = 1.0$ mL, (b) $V_{injection} = 0.5$ mL and (c) $V_{injection} = 0.1$ mL. Conditions as given in Table 6.1: Flow rate = 1.28 mL/min; Loading Buffer: Sodium phosphate (20 mM), sodium chloride (500 mM), pH 6.5; Elution Buffer: Sodium phosphate (20 mM), sodium chloride (500 mM), pH 3.8

equilibrium constants of the ABF and IMP behave linearly for these injection volumes and elution conditions. This justifies the application of the linear isotherm model using the adsorption equilibrium constants according to Equation (3.1).

6.2 Description of the pH-profile

This section deals with the description of the stepwise pH-profile used for the discontinuous chromatographic purification of the antibody fragment from the cell culture supernatant.

The principle of the IMAC technique is based on the formation of a chelate complex between the histidine-tagged protein and the metal ion immobilized on the stationary phase as explained in Section 4.2. High pH values above 6.0 favors the formation of the chelate complex between the histidine-tags attached to the protein and the metal ion. The reduction of pH leads to the resolution of the complex and the protonation of the histidines. This phenomenon allows the elution of proteins from the stationary phase.

The implementation of the stepwise pH-profile was carried out by a sudden change from 0% to 100% content of elution buffer. At the beginning of the stepwise pH-gradient elution, the loading and elution buffers were mixed in the 2mL-mixing chamber for a short period of time until the chamber was full with elution buffer. This unavoidable effect takes certain time and affects the final shape of the pH-gradient.

Figure 6.5 shows a theoretically expected ideal square-shaped stepwise pH-gradient and the experimentally obtained stepwise pH-profiles in the presence and absence of the column.

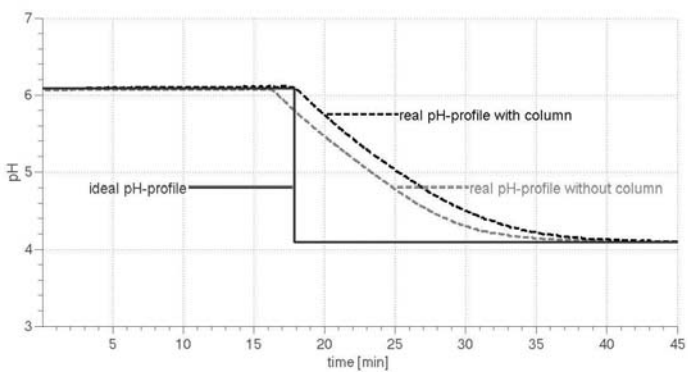

Figure 6.5: Schematic representation of the ideal and real pH-profiles

In reality, the pH-profiles observed were distorted and delayed due to dispersion and dead volumes between the injection valve, the mixing chamber and the pH-meter located at the column outlet. The experimentally pH-profiles decreased in an exponential manner after the sudden change of pH conditions between the loading and the elution buffer.

Figure 6.5 shows that the shape of the pH-gradient is not affected by the presence of the columns. The pH-profiles were only shifted according to the additional column volume. It is worth mentioning that the pH-gradient was established at the same flow rate much faster when the pH of the elution buffer was closer to the pH of the loading buffer.

An accurate description of the dynamic of the pH-profile must consider time, t, and position, x. The shape of the pH-profiles was described using the following empirical relationship respecting the linear velocity, u [42]:

$$pH(x,t) = p_1 + p_2 \cdot erf \frac{-(t - \frac{x}{u}) + p_3}{\sqrt{2} \cdot p_4} \tag{6.3}$$

In Equation (6.3), erf stands for the error function which can be easily estimated using numerical techniques provided by commercial software such as MATLAB. The parameters p_1, p_2, p_3, and p_4 were adjusted as a function of the elution pH using measured pH-profiles shown in Figure 6.3. The adjustment of the pH-profiles was carried out using the least squares approximation method [124].

$$p_1 = 3.25 + 0.54 \cdot pH_{Elution} \tag{6.4}$$
$$p_2 = 3.18 - 0.45 \cdot pH_{Elution} \tag{6.5}$$
$$p_3 = 19.64 - 2.96 \cdot pH_{Elution} \tag{6.6}$$
$$p_4 = 9.05 - 0.60 \cdot pH_{Elution} \tag{6.7}$$

The courses of the parameters p_1, p_2, p_3, and p_4 are depicted in Figure 6.6 as function of the elution pH.

Parameter p_1 is the only one with a positive slope. Parameters p_2, p_3, and p_4 have a negative slope. The most sensitive parameter is p_3, with respect to the elution pH.

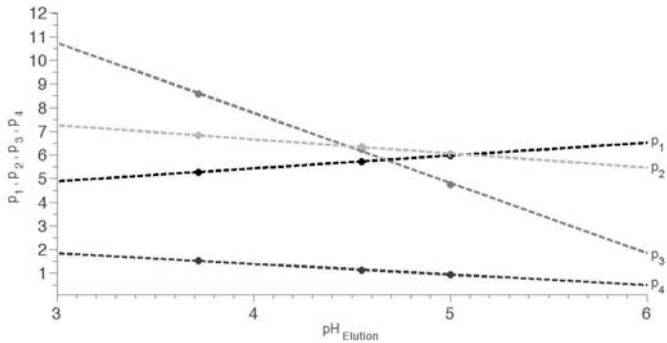

Figure 6.6: Parameters used for description of stepwise pH-profiles as a function of $pH_{Elution}$ in Equations (6.4) to (6.7)

6.3 Adsorption equilibrium constants as a function of pH

As mentioned before, knowledge regarding the adsorption equilibrium is most instructive when designing chromatographic processes [56]. An adsorption isotherm relates, at a certain constant temperature, the concentration of a component k in solution, c^k, to the concentration of the same component adsorbed on the stationary phase, q^k. For diluted protein solutions, as studied here, linear adsorption isotherms characterized by adsorption equilibrium constants are typically applicable [57]. This was supported by the fact that retention times were not affected significantly by the sample loads in the concentration range covered as mentioned in Section 6.1.3.

Nevertheless, a problem arise during pH-gradient elution processes. In those cases, the adsorption equilibrium constants depend on time, t, and position, x as given here in Equation (6.8):

$$q^k = H^k(pH(x,t)) \cdot c^k \qquad k = IMP, ABF \tag{6.8}$$

In order to predict the elution profiles of the components in the stepwise pH-gradient elution, a quantitative description of the influence of the pH of the mobile phase on the adsorption equilibrium constants of the components is required.

6.3.1 Modeling discontinuous single-column stepwise pH-gradient elution chromatography

The equilibrium-dispersive model described in Section 3.2.3 is applied under linear conditions for modeling the discontinuous single-column stepwise pH-gradient elution chromatography.

Gradient elution chromatography is the most common elution mode for purification of proteins and peptides. Consequently, modeling is an important and useful step in the development and optimization of experimental conditions in preparative protein chromatography [44].

The main difficulty encountered in modeling pH-gradient elution chromatography originates from the need of an accurate estimation of the adsorption equilibrium constants as a function of pH [40].

The equilibrium-dispersive model in Equation (3.21) considers the mass balance equation of component, k, as a partial differential equation:

$$\frac{\partial c^k}{\partial t} + F \cdot \frac{\partial q^k}{\partial t} = -u \cdot \frac{\partial c^k}{\partial x} + D_{ax}^k \cdot \frac{\partial^2 c^k}{\partial^2 x} \tag{6.9}$$

Hereby the adsorption equilibrium constant depends on pH. If linear condition are considered as in Equation (6.8) the mass balance equation Equation (6.9) yields:

$$\frac{\partial c^k}{\partial t} = -\frac{u}{1 + F \cdot H^k(pH(x,t))} \cdot \frac{\partial c^k}{\partial x} + \frac{D_{ax}^k}{1 + F \cdot H^k(pH(x,t))} \cdot \frac{\partial^2 c^k}{\partial^2 x} \tag{6.10}$$

The numerical solution of Equation (6.10) was implemented in MATLAB using the method of lines as described in Section 3.2.4 and the pH-profiles were considered using Equation (6.3).

6.3.2 Determination of adsorption equilibrium constants using pH-gradients

Selected downward pH-gradient elution experiments were used for the determination of the adsorption isotherm parameters. It is rather clear from Section 6.1.2 that there is a strong influence of the pH on the adsorption behavior of the pseudo-components (IMP and ABF) expressed in the corresponding adsorption equilibrium constants.

At low pH, both components eluted very fast because these are non-adsorbing conditions. As the pH increased towards adsorbing conditions, the adsorption of the components was stronger resulting in wider and separated peaks and also larger retention times.

As a reference, two characteristic peaks were chosen for the pseudo-binary separation as described in Section 6.1.2. The protein impurities are lumped together in the characteristic peak of the IMP fraction. And the antibody fragment fraction, ABF, is represented by the first eluting peak in the ABF fraction. Between those peaks a critical boundary for the purification of the ABF fraction is defined as depicted in Figure 6.3 under different pH eluting conditions. Thus, two adsorption equilibrium constants, H^{IMP} and H^{ABF}, were estimated from the experimental retention times using the characteristic peaks of IMP and ABF (Equation (3.8)).

In order to consider the effects of the pH of the mobile phase on the adsorption equilibrium constants, a pH-dependent adsorption equilibrium constant was derived for each pseudo-component, IMP and ABF. In the case of linear adsorption isotherms, a simple semi-empirical power function can be then used to describe the dependency of the adsorption equilibrium constant on the pH of the mobile phase:

$$H^k(pH) = a^k \cdot pH^{b^k} \qquad k = IMP, ABF \tag{6.11}$$

where a^k and b^k are constant real numbers and $pH(x, t)$ is described by Equation (6.3). In these functions the key thermodynamic information regarding the adsorption-desorption behavior of IMP and ABF is condensed. A similar approach was already suggested and described by Antos and Seidel-Morgenstern [8].

As mentioned before, selected chromatograms of the stepwise pH-gradient elution of the cell culture supernatant were applied for the estimation of the adsorption parameters, a^k and b^k, in Equation (6.11). For the sake of simplicity, it was assumed that the parameter a^k had the same value for both pseudo-components, IMP and ABF, which basically means that at very low pH values (i.e. pH 2.0) the components will not be retained and just pass together through the column.

The adsorption parameters were found by minimizing the error between the experimental and the retention times predicted by the equilibrium-dispersive model using an objective function evaluating all measurements available ($j = 1, ..., n$):

$$OF^k = \sum_{j=1}^{n} (t_{R,j}^{k,the} - t_{R,j}^{k,exp})^2 \qquad k = IMP, ABF \tag{6.12}$$

where n is the number of experiments or measurements available.

The adjusted parameters found by minimizing the objective function are given in Table 6.3:

Table 6.3: Adjusted parameters, a^k and b^k, to be used in Equation (6.11)

a^{IMP}	b^{IMP}	a^{ABF}	b^{ABF}
0.79	1.43	0.79	2.01

Figure 6.7 shows the dependency of adsorption equilibrium constants on the pH of the mobile phase. At low pH, the adsorption equilibrium coefficients for IMP and ABF are low and very close to each other and the components are slightly retained. As the pH increases, the adsorption equilibrium coefficients are increasing and the distance between the curves is becoming larger which improves selectivity of the separation.

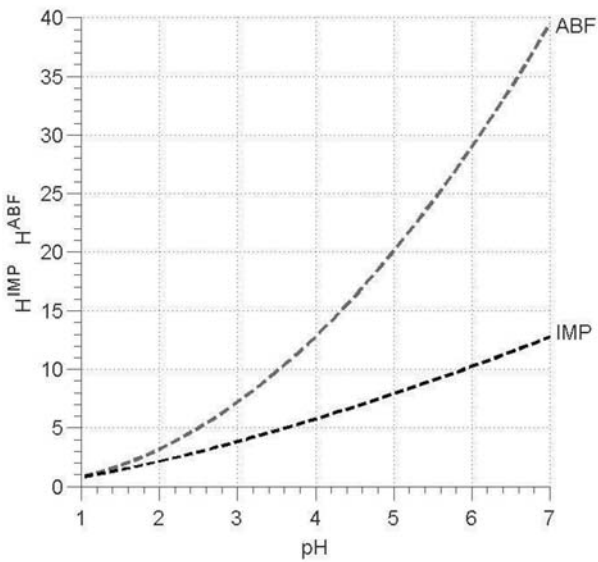

Figure 6.7: Dependency of adsorption equilibrium coefficients on the pH of the mobile phase according to Equation (6.11) and Table 6.3

Comparing the curves of the dependency of the pseudo-components Figure 6.7, it can be seen that the effect of the pH on the adsorption equilibrium constant of the antibody fragment fraction, ABF, is larger than on the adsorption equilibrium constant of the impurity fraction, IMP. Thus, ABF is more sensitive than IMP to changes in the pH of the mobile phase.

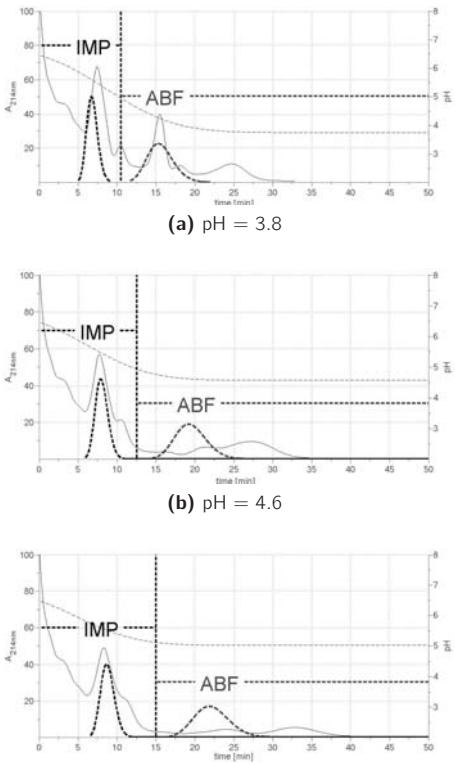

(a) pH = 3.8

(b) pH = 4.6

(c) pH = 5.0

Figure 6.8: Comparison between predicted (dotted lines) and experimental (continuous lines) elution profiles for three different stepwise pH-gradient elution. Elution buffers at (a) $pH_{Elution} = 3.8$, (b) $pH_{Elution} = 4.6$ and (c) $pH_{Elution} = 5.0$. For the experimental profiles, the conditions are given in Figure 6.3

In Figure 6.8, the elution profiles of previous experiments in Section 6.1.2 were compared with those predicted by the numerical solution of the equilibrium-dispersive model as described in Section 6.3.1.

The predicted profiles were consistent with the assumption of linear adsorption equilibria and in a relatively good agreement with the experimental elution profiles of the characteristic peaks of IMP and ABF. Additionally, it can be observed in Figure 6.8, that the fitting of the characteristic peak of IMP was better than the fitting of the characteristic peak of ABF due to the fact that all non-equilibrium effects were only described in the equilibrium-dispersive model by the axial dispersion coefficient which is also a function of the pH. The influence of the pH on the axial dispersion coefficient was neglected. But it is clear that this influence affected ABF more than IMP.

However, a more challenging separation was considered by simulation of the elution profiles of the pseudo-components in order to have an extra safety factor for the design of the continuous separation process.

6.4 Evaluation of the performance of batch chromatography

In this section, several performance parameters like the final concentration (i.e. biological activity), purity, yield, specific buffer consumption, and specific productivity, regarding only the single-chain antibody fragment (scFv) were evaluated using experimental data available from batch runs. The analysis was based on the expressions introduced in Section 3.5.

The average final concentration per fraction, $\bar{c}^{scFv}_{fraction}$, or the biological activity of the single-chain antibody fragment were estimated by ELISA (see Section 5.2.2). The concentration of the rest of proteins present in the cell culture supernatant were not determined. The purity per fraction, $PUR^{scFv}_{fraction}$, of the single-chain antibody fragment was estimated by densitometry of Coomassie blue-stained SDS-PAGE gels run under reducing conditions as described in Section 5.2.2.

For the performance analysis, the elution of ABF was examined in more detail. Fraction volumes of 2 mL were pooled out, collected and analyzed over a batch stepwise pH-gradient chromatographic experiment as depicted in Figure 6.9. The smallest fraction volume allowing an accurate estimation of the performance parameters for the single-chain antibody fragment was equal to 2 mL. Using smaller fraction volumes do not allow the measurement of the concentration of the target

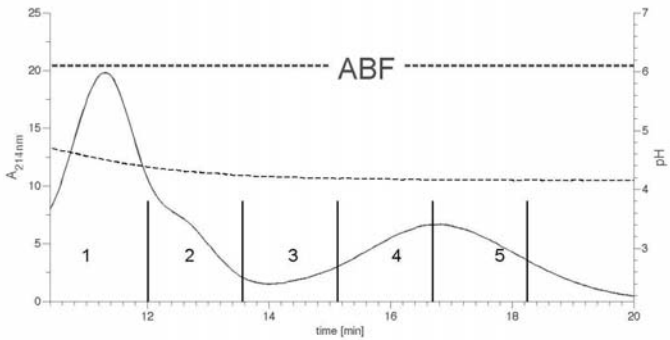

Figure 6.9: Chromatographic elution profile of the antibody fragment fraction, ABF, for evalution of the performance of batch chromatography. The collected fractions 1 to 5 are indicated between continuous lines. Conditions as given in Table 6.1: Sample Load = 2 mL; Flow rate = 1.28 mL/min; Loading Buffer: Sodium phosphate (20 mM), sodium chloride (500 mM), pH 6.5; Elution Buffer: Sodium phosphate (20 mM), sodium chloride (500 mM), pH 3.8

because the concentrations of some samples were below the minimum detectable concentration.

Table 6.4 summarizes the evaluation of the performance parameters for the discontinuous single-column chromatographic purification obtained from the different pooled samples corresponding to the ABF fraction as illustrated in Figure 6.9:

Table 6.4: Evaluation of the performance parameters of ABF over the fractions 1 to 5 as shown in Figure 6.9 according to Section 3.5

Parameters	Unit	1	2	3	4	5	Overall
$\bar{c}^{scFv}_{fraction}$	[mg/L]	0.30	0.42	0.06	0.05	0.04	0.17
$PUR^{scFv}_{fraction}$	[%]	41.00	52.00	99.00	99.00	99.00	59.10
$Y^{scFv}_{fraction}$	[%]	34.09	47.73	6.82	5.68	4.55	98.90
$SDC^{scFv}_{fraction}$	[L_{MP}/mg]	64.00	45.71	320.00	384.00	480.00	22.10
$PRD^{scFv}_{fraction}$	[mg/day·L_{SP}]	43.05	60.28	8.61	7.18	5.74	124.86

The last column in Table 6.4 considered an overall fraction, a hypothetical fraction consisting of all samples pooled together (samples from 1 to 5). In that case, an antibody fragment might be isolated with a purity of 59%, a total yield above 98%,

a specific desorbent consumption around 22 L_{MP}/mg_{scFv} and a specific productivity close to 125 mg_{scFv}/day·L_{SP}.

Figure 6.10 illustrates the evaluation of the purity, yield and productivity at the collected fractions:

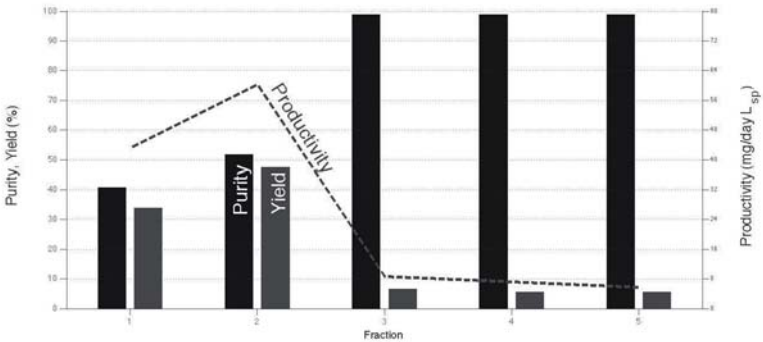

Figure 6.10: Evaluation of the purity, yield and specific productivity of ABF at the different collected fractions from 1 to 5 for the discontinuous chromatographic purification as shown in Figure 6.9

In Figure 6.10, it can be observed that fraction 3, 4 and 5 reached higher purities but extremely low yields due to the small concentrations of antibody fragment present in those fractions. In contrast, fractions 1 and 2 outperformed the other fractions when comparing performance parameters such as yield, specific productivity, and specific buffer consumption.

Although the highest yield, $Y^{scFv}_{fraction}$, corresponds to fraction 2. The largest possible yield using 2 mL fraction was still under 50%.

Additionally, it is worth noting that the estimated values for the specific buffer consumption per fraction, $SDC^{scFv}_{fraction}$, were extremely large when very small quantities were purified such as in fractions 3, 4 and 5.

Nevertheless, in fraction 2 a specific productivity, PRD^{scFV}_{Batch} equal to 52 mg_{scFv}/day·L_{SP}, for the batch pH-gradient elution chromatography was reached.

Therefore, the analysis of the individual fractions against each other illustrated the trade-off among purity versus yield and versus productivity. If a less pure target product is required the yield and the productivity can be significantly incremented using less desorbent for the purification.

For subsequent comparison of the performance of the batch process against the continuous process, the hypothetical overall fraction will be considered. The performance of the batch process can be summarized as follows: the purity, PUR^{scFv}_{Batch}, was 59.10 %, the yield, Y^{scFv}_{Batch}, was 98.90 %, the specific buffer consumption, SDC^{scFv}_{Batch}, was 22.10 L_{MP}/mg_{scFv}, and the specific productivity, PRD^{scFV}_{Batch}, was 124.86 $mg_{scFv}/day{\cdot}L_{SP}$.

6.5 Concluding remarks

It should be pointed out that there are two different views characterizing the cell culture supernatant feed mixture. At first, the mixture can be considered as multi-component due to the relative large number of main components present in the feed mixture. The second view regards the mixture as pseudo-binary related to the number of fractions achievable in a feasible continuous SMB separation process, which should allow collecting the IMP fraction at the raffinate port and the ABF fraction at the extract port. Thus, the purification of the antibody fragment fraction, ABF, was considered as a pseudo-binary separation problem. The pseudo-binary feed mixture consists of the protein impurity fraction, IMP, as the faster eluting fraction and the antibody fragment fraction, ABF, as the slower eluting fraction.

The results in Section 6.1 suggested that an effective purification of the target antibody fragment fraction, ABF, from a significant amount of unretained and non-specifically bound proteins by immobilized metal ion affinity chromatography using stepwise pH-gradient was feasible. Different elution pH conditions and sample loads were explored to estimate the most appropiate range of applicable operating parameters.

Despite the presence of the variable domains, the ABF fraction accessible through the IMAC batch process was proven biologically active with full functionality by the ELISA test. Thus, the antibody fragment fraction, ABF, purified by IMAC using a stepwise pH-gradient was a very attractive fraction containing a high-value product, the single-chain antibody fragment.

The lower the pH in the elution buffer, the steeper was the gradient and the sooner eluted the components in sharper peaks. Thus, the pH of the elution buffer had a strong influence on the retention times and peak shapes of ABF and IMP fractions. The adsorption behavior of the components was affected when other combinations of the loading and elution buffer at different pH were used.

The different shapes of the pH-gradient as a function position and time were

obtained at a certain pH of the elution buffer using the estimated parameters in Equation (6.3). In IMAC, the elution strength was strongly influenced by the pH. The retention behavior when decreasing the pH of the mobile phase was described by an exponential decay of the adsorption equilibrium constant as depicted in Figure 6.7.

The thermodynamic information contained in the dependency of the adsorption equilibrium constants on the pH is the key for designing a continuous purification process in which the determination of the migration speeds of the components at different pH conditions is essential.

This dependency was successfully applied to model the discontinuous stepwise pH-gradient elution of ABF and its nearest contaminant IMP. Although, the elution of both fractions, IMP and ABF, were simulated only as the characteristic peaks in IMP and in ABF fractions.

The experimental elution profiles of the components were in relatively good agreement with those predicted by the equilibrium-dispersive model at different stepwise pH-gradient elution conditions. The implemented numerical solution succeeded in showing the influence of the different imposed stepwise pH-gradients on the elution behavior of the key fractions IMP and ABF.

It is rather clear that in the continuous purification process IMP will travel together with the relatively large amount of unretained proteins towards the raffinate port. And ABF fraction containing the strongly retained single-chain antibody fragment will be recovered at the extract port.

Finally, it can be stated that the non-optimized single-column batch process was capable of isolating the biologically active single-chain antibody fragment from a complex medium containing large amount of protein and non-protein impurities. Additionally, the performance of the such non-optimized discontinuous single-column chromatographic purification process was evaluated under specific conditions as described in Section 6.4.

Chapter 7

Continuous chromatographic purification: Theoretical Design

This chapter deals with the theoretical design of an open-loop 3-zone pH-gradient simulated moving bed process introduced in Section 3.4.5 using immobilized metal ion affinity chromatography for the purification of a single-chain antibody fragment from a cell culture supernatant.

The process design was based on an equilibrium stage model using a recursive solution which describes the steady state of the equivalent true moving bed (TMB) under linear conditions [12]. The basic stage model was presented in Section 3.2.1.

Detailed simulations were carried out to study the influence of the number of equilibrium stages, purity constraints and concentrations of impurities on the region of feasible operating parameters and to predict the performance of the open-loop 3-zone pH-gradient SMB.

7.1 Design of the open-loop 3-zone pH-gradient SMB

Modulation of the elution strength by salt-gradient or pH-gradient within simulated moving bed process is a powerful concept for the separation of biomolecules [54]. One of the simplest SMB configurations suitable for the implementation of gradients is the open-loop arrangement with three zones. In this specific case, zone IV is not taking part anymore in order to avoid cross-contamination of the products and the raffinate outlet stream leaves the SMB unit at zone III.

The open-loop 3-zone SMB process is an economical and promising alternative to the classical closed-loop 4-zone SMB system when the eluent consumption is not critical or cheap aqueous buffers are used as mobile phase e.g. bioseparations [3, 75].

In the pH-gradient mode, the mobile phase entering the SMB unit at the feed and desorbent inlet ports consists of two aqueuous buffer solutions with two different pH values as illustrated in Section 3.4.5.

The pH-gradient SMB configuration enhances the purification performance by applying a pH-gradient using distinct pH values in contrast to the classical isocratic SMB chromatography. The use of mobile phases with different pH values affect the adsorption-desorption behavior of the biomolecules in great extent, i.e. different adsorption equilibrium constants in the different zones of the SMB unit. Thus, a stepwise pH-gradient is established within the SMB system with distinct pH values in zones I and II, and in zone III.

7.1.1 Mass balances

For illustration, the schematic representation of the open-loop 3-zone pH-gradient SMB was given in Figure 3.5. Overall mass balances for an open-loop 3-zone SMB process with an established stepwise pH-gradient are conveniently given in terms of the external and internal volumetric flow rates.

The outlet streams are Extract, E, and Raffinate, R. The inlet streams are Feed, F, and Desorbent, D. The volumetric flow rates of the zones are given by $\dot{V}_i$ with $i = I, II, III$.

$$\dot{V}_I = \dot{V}_D \tag{7.1}$$

$$\dot{V}_{II} = \dot{V}_I - \dot{V}_E \tag{7.2}$$

$$\dot{V}_{III} = \dot{V}_R = \dot{V}_{II} + \dot{V}_F \tag{7.3}$$

Within the SMB unit the pH values alternate between two distinct pH values, pH of the desorbent, pH_D, and pH of the feed, pH_F, where the desorbent has a lower pH value than the feed, i.e. $pH_F > pH_D$.

Since the inlet stream entering zone I is the desorbent stream, it holds $pH_{I-II} = pH_D$. Analogously, the outlet stream leaving zone III is the raffinate stream. Thus, it holds $pH_{III} = pH_R$. It is rather clear that any pH value in zone III can be expressed by the inequality $pH_{I-II} < pH_{III} < pH_F$ or $pH_D < pH_R < pH_F$.

An ideal stepwise pH-gradient is established within the SMB unit with two distinct internal pH values, pH_{I-II} in zones I and II, and pH_{III} in zone III. According to Chapter 6, a greater elution strength is established in zones I and II (low pH) than in zone III (high pH). The following steady state mass balance is based on the pH definition as hydrogen ion concentration $[H^+]$ in Equation (5.1) and is valid only if the mobile phase does not interact with the stationary phase. For the sake of simplicity, the role of the buffer capacity is neglected.

$$[H^+]_R \cdot \dot{V}_{III} = [H^+]_D \cdot \dot{V}_{II} + [H^+]_F \cdot \dot{V}_F \tag{7.4}$$

For given inlet streams, feed and desorbent with two distinct pH values, pH_D and pH_F, the internal pH in zone III, $pH_{III} = pH_R$ or $[H^+]_{III} = [H^+]_R$, depends on the external and internal pH values and volumetric flow rates, and can be estimated using the mass balance of the hydrogen ion concentration at zone III as shown in Equation (7.5):

$$[H^+]_R = \frac{[H^+]_D \cdot \dot{V}_{II} + [H^+]_F \cdot \dot{V}_F}{\dot{V}_{II} + \dot{V}_F} \tag{7.5}$$

From Equation (7.1) and Equation (7.4), it is possible to derive a relationship between m_{II} and m_{III}. This relationship represents an operating line in the m_{II},m_{III}-plane as a function of the distinct pH values (i.e. $[H^+]$) established within the unit:

$$m_{III} = \frac{[H^+]_D - [H^+]_F}{[H^+]_R - [H^+]_F} \cdot m_{II} \tag{7.6}$$

The dimensionless flow-rate ratios for each zone, m_i, are the basis for the TMB and SMB design as defined in Section 3.4.3 together with the pH values introduced into the mass balances as hydrogen ion concentration using Equation (5.1).

As mentioned in Section 3.4.3, the results of the modeling of the TMB process typically match closely the performance of the more complex SMB process [67]. The solid-phase flow-rate of the TMB process, $\dot{V}_s$, can be simply converted into the corresponding switch time of an equivalent SMB process.

7.1.2 Equilibrium stage model and solution method

The equilibrium stage model was described in Section 3.2.1. The model considers each zone of the continuous counter-current chromatographic SMB process as a cascade of equilibrium stages in series where adsorption equilibrium is reached in every single stage in a negligible time.

The mass balances for every single stage, j, within a zone, i, enables us to calculate the concentration of the components at each point of the unit, and thus the extract and raffinate purities [12]. Mass transfer and hydrodynamic effects are lumped together into the number of equilibrium stages per zone i, $N_{eq,i}$. An equilibrium stage under permanent local equilibria between the mobile and stationary phases is depicted in Figure 7.1.

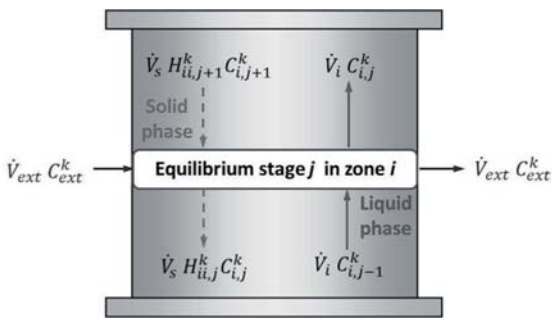

Figure 7.1: Schematic representation of a single equilibrium stage

For designing the open-loop 3-zone pH-gradient SMB, the three zones are assumed to have identical number of equilibrium stages:

$$N_{eq,I} = N_{eq,II} = N_{eq,III} = N \tag{7.7}$$

It is rather clear that the number of equilibrium stages could be in principle different in each zone according to the internal volumetric flow rates. The total number of equilibrium stages of the TMB unit is:

$$N_{eq,total} = 4 + N_{eq,I} + N_{eq,II} + N_{eq,III} \tag{7.8}$$

The mass balance for a single equilibrium stage, $j = 1, ..., N$, located in zone, i, for a component, k, is based on the stage model described in Equation (3.10), but assuming steady state conditions and introducing the counter-current movement of the solid phase as follows:

$$\dot{V}_s \cdot q^k_{i,j+1}(c^k_{i,j+1}) + \dot{V}_i \cdot c^k_{i,j-1} - \dot{V}_s \cdot q^k_{i,j}(c^k_{i,j}) - \dot{V}_i \cdot c^k_{i,j} = \dot{V}_{ext} \cdot c^k_{ext} \tag{7.9}$$

Under linear conditions, the use of the adsorption equilibrium constants offers a simplified solution. Thus, the mass balance of each component can be solved separately without considering the rest of the components present in the mixture:

$$\dot{V}_s \cdot H^k_{ii,j+1} \cdot c^k_{i,j+1} + \dot{V}_i \cdot c^k_{i,j-1} - \dot{V}_s \cdot H^k_{ii,j} \cdot c^k_{i,j} - \dot{V}_i \cdot c^k_{i,j} = \dot{V}_{ext} \cdot c^k_{ext} \tag{7.10}$$

The term, $\dot{V}_{ext} \cdot c^k_{ext}$, could be either positive for outlet streams such as Extract, E, or Raffinate, R, or negative for inlet streams such as Feed, F, or Desorbent, D. Summarizing this term holds:

$$\dot{V}_{ext} \cdot c^k_{ext} = \begin{cases} \dot{V}_R \cdot c^k_R & \text{for } j = R; \\ \dot{V}_E \cdot c^k_E & \text{for } j = E; \\ -\dot{V}_D \cdot c^k_D & \text{for } j = D; \\ -\dot{V}_F \cdot c^k_F & \text{for } j = F. \end{cases} \tag{7.11}$$

For all other stages, j, it holds:

$$\dot{V}_{ext} \cdot c^k_{ext} = 0 \tag{7.12}$$

The equilibrium stage model used in this work assumes an ideal stepwise pH-profile within the unit as illustrated in Figure 3.5. The real pH-profile established within the SMB unit will depend on the choosen operating conditions.

As will be demonstrated below for the case of an open-loop 3-zone pH-gradient TMB process a linear system of 11 equations with 11 unknowns can be derived per component k from Equation (7.10). The dimensionless factor, χ_i, considers the ratio among the internal flow rate in zone i, the solid phase flow rate and the adsorption equilibrium constant in zone ii:

$$\chi_i^k = \frac{\dot{V}_i}{\dot{V}_s \cdot H_{ii}^k} \tag{7.13}$$

with $i = I, II, III$ and $ii = I - II, III$. The introduction of the χ_i simplifies the system of linear equations represented by Equation (7.10).

An adaptation of the recursive technique suggested by Kremser [79] to analyze multi-stage counter-current adsorption processes is illustrated in Figure 7.2.

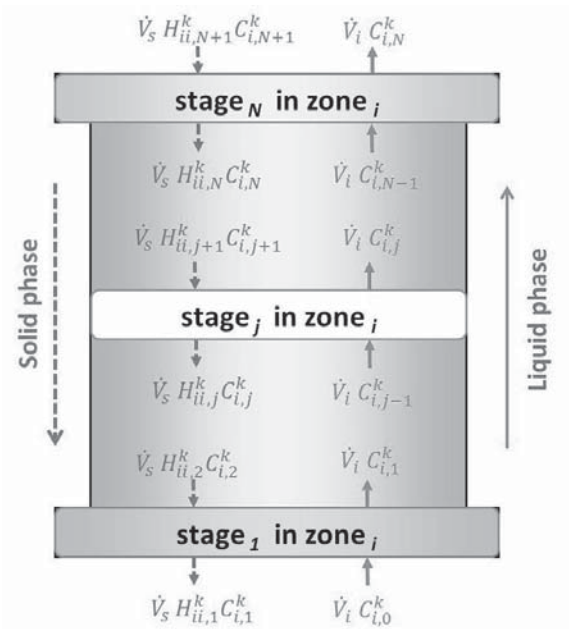

Figure 7.2: Schematic representation of the adaptation of Kremser's recursive technique for solving the linear system of equations within a zone, i, derived from Equation (7.10)

Kremser's recursive solution is a very attractive and powerful tool for the analysis of processes, in which relative large number of stages in equilibrium must be evaluated stage by stage [12]. This time-consuming evaluation can be avoided by "jumping" over all the stages, using either the recursive solution in the mobile phase direction or the recursive solution in the solid phase or opposite direction.

Considering the solid phase direction, it is possible to obtain [12]:

$$c_{i,N+1}^{k} = (\chi_i^{k^N} + \chi_i^{k^{N-1}} + \cdots + \chi_i^{k} + 1) \cdot c_{i,1}^{k} \tag{7.14}$$

$$-(\chi_i^{k^N} + \chi_i^{k^{N-1}} + \cdots + \chi_i^{k^2} + \chi_i^{k}) \cdot c_{i,0_i}^{k} \tag{7.15}$$

The sum of χ_i terms can be simplified leading to:

$$c_{i,N+1}^{k} = \gamma_i^{k} \cdot c_{i,1}^{k} - (\gamma_i^{k} - 1) \cdot c_{i,0}^{k} \tag{7.16}$$

using a dimensionless factor, γ_i, equal to:

$$\gamma_i^{k} = \frac{\chi_i^{k^{N+1}} - 1}{\chi_i^{k^1} - 1} \tag{7.17}$$

Analogously, the recursive solution in the mobile phase direction is [12]:

$$c_{i,0}^{k} = \eta_i^{k} \cdot c_{i,N}^{k} - (\eta_i^{k} - 1) \cdot c_{i,N+1}^{k} \tag{7.18}$$

using an extra dimensionless factor, η_i, equal to:

$$\eta_i^{k} = \frac{\chi_i^{k^{-(N+1)}} - 1}{\chi_i^{k^{-1}} - 1} \tag{7.19}$$

The complete mathematical description of all stages is given by 11 equations forming a linear system of equations resulting from the mass balances at the following stages:

$$
\begin{aligned}
D: &\quad -(1+\chi_I^k)\cdot c_D^k + c_{I,1_I}^k = 0 && (7.20)\\
1_I: &\quad (\gamma_I^k - 1)\cdot c_D^k - \gamma_I^k \cdot c_{I,1_I}^k + c_E^k = 0 && (7.21)\\
N_I: &\quad c_D^k - \eta_I^k \cdot c_{I,N_I}^k + (\eta_I^k - 1)\cdot c_E^k = 0 && (7.22)\\
E: &\quad \chi_I^k \cdot c_{I,N_I}^k - (1+\chi_{II}^k+\chi_E^k)\cdot c_E^k + c_{II,1_{II}}^k = 0 && (7.23)\\
1_{II}: &\quad (\gamma_{II}^k - 1)\cdot c_E^k - \gamma_{II}^k \cdot c_{II,1_{II}}^k + c_{II,N_{II}}^k = 0 && (7.24)\\
N_{II-1}: &\quad c_E^k - \eta_{II}^k \cdot c_{II,N_{II-1}}^k + (\eta_{II}^k - 1)\cdot c_{II,N_{II}}^k = 0 && (7.25)\\
N_{II}: &\quad \beta^k \cdot \chi_{II}^k \cdot c_{II,N_{II-1}}^k - \beta^k \cdot (1+\chi_{II}^k)\cdot c_{II,N_{II}}^k + c_F^k = 0 && (7.26)\\
F: &\quad \beta^k \cdot \chi_{II}^k \cdot c_{II,N_{II}}^k - (1+\chi_{III}^k)\cdot c_F^k + c_{III,1_{III}}^k = -\chi_F^k \cdot c_{Feed}^k && (7.27)\\
1_{III}: &\quad (\gamma_{III}^k - 1)\cdot c_F^k - \gamma_{III}^k \cdot c_{III,1_{III}}^k + c_R^k = 0 && (7.28)\\
N_{III}: &\quad c_F^k - \eta_{III}^k \cdot c_{III,N_{III}}^k + (\eta_{III}^k - 1)\cdot c_R^k = 0 && (7.29)\\
R: &\quad \chi_{III}^k \cdot c_{III,N_{III}}^k - (1+\chi_R^k)\cdot c_R^k = 0 && (7.30)
\end{aligned}
$$

A summary of the linear algebraic systems is given by Equation (7.31):

$$M \cdot c = b \tag{7.31}$$

where unknown concentrations are expressed in the following vector c:

$$c = \begin{bmatrix} c_D^k \\ c_{I,1_I}^k \\ c_{I,N_I}^k \\ c_E^k \\ c_{II,1_{II}}^k \\ c_{II,N_{II-1}}^k \\ c_{II,N_{II}}^k \\ c_F^k \\ c_{III,1_{III}}^k \\ c_{III,N_{III}}^k \\ c_R^k \end{bmatrix}$$

The right-hand side vector, b, is equal to:

$$b = \begin{bmatrix} 0 \\ 0 \\ 0 \\ 0 \\ 0 \\ 0 \\ 0 \\ -\chi_F^k \cdot c_{Feed}^k \\ 0 \\ 0 \\ 0 \end{bmatrix}$$

Finally, the matrix of the coefficients, M, of the linear system is:

$$M = \begin{bmatrix} -(1+\chi_I^k) & 1 & 0 & 0 & 0 & 0 & 0 & 0 & 0 & 0 & 0 \\ (\gamma_I^k - 1) & -\gamma_I^k & 0 & 1 & 0 & 0 & 0 & 0 & 0 & 0 & 0 \\ 1 & 0 & -\eta_I^k & (\eta_I^k - 1) & 0 & 0 & 0 & 0 & 0 & 0 & 0 \\ 0 & 0 & \chi_I^k & -(1+\chi_{II}^k+\chi_E^k) & 1 & 0 & 0 & 0 & 0 & 0 & 0 \\ 0 & 0 & 0 & (\gamma_{II}^k - 1) & -\gamma_{II}^k & 0 & 1 & 0 & 0 & 0 & 0 \\ 0 & 0 & 0 & 1 & 0 & -\eta_{II}^k & (\eta_{II}^k - 1) & 0 & 0 & 0 & 0 \\ 0 & 0 & 0 & 0 & 0 & \beta^k \cdot \chi_{II}^k & -\beta^k \cdot (1+\chi_{II}^k) & 1 & 0 & 0 & 0 \\ 0 & 0 & 0 & 0 & 0 & 0 & \beta^k \cdot \chi_{II}^k & -(1+\chi_{III}^k) & 1 & 0 & 0 \\ 0 & 0 & 0 & 0 & 0 & 0 & 0 & (\gamma_{III}^k - 1) & -\gamma_{III}^k & 0 & 1 \\ 0 & 0 & 0 & 0 & 0 & 0 & 0 & 1 & 0 & -\eta_{III}^k & (\eta_{III}^k - 1) \\ 0 & 0 & 0 & 0 & 0 & 0 & 0 & 0 & 0 & \chi_{III}^k & -(1+\chi_R^k) \end{bmatrix}$$

The pH-profile is considered implicitly by adjusting H_{ii}^k. Thus, the linear algebraic system in Equation (7.31) can be easily solved by standard linear equation solvers using MATLAB.

7.2 Region of feasible operating parameters

The necessary conditions on the flow rate ratios to achieve complete separation under linear conditions were studied by Mazzotti et al. [91]. In the case of the standard classical isocratic closed-loop 4-zone SMB the corresponding inequalities that must be fulfilled in the frame of the equilibrium theory were given in Section 3.4.3.

An extension for an open-loop 3-zone pH-gradient SMB process must consider that the lower and upper boundaries of the m_i values depend on pH values of the mobile phase as well as the adsorption equilibrium constants. In Section 7.1.1, it was shown that for the application of a stepwise pH-gradient holds $pH_F > pH_{I-II} > pH_{III} > pH_D$. This fact yields two distinct adsorption equilibrium coefficients corresponding to the two distinct internal pH levels in zone I-II (formed by zones I and II) and zone III (formed by zone III).

For an open-loop 3-zone pH-gradient SMB configuration, the fulfilment yields:

$$H_{III}^{k_1}(pH_{III}) < m_{III} < H_{III}^{k_2}(pH_{III}) \tag{7.32}$$

$$H_{I-II}^{k_1}(pH_{I-II}) < m_{II} < H_{I-II}^{k_2}(pH_{I-II}) \tag{7.33}$$

$$H_{I-II}^{k_2}(pH_{I-II}) < m_I \tag{7.34}$$

with $H_i^{k_2}(pH_i) > H_i^{k_1}(pH_i)$, assuming that the more retained component is k_2 and the less retained component is k_1.

Replacing $pH_D = pH_{I-II}$ and $pH_R = pH_{III}$, the inequalities become:

$$H_R^{k_1}(pH_R) < m_{III} < H_R^{k_2}(pH_R) \tag{7.35}$$

$$H_D^{k_1}(pH_D) < m_{II} < H_D^{k_2}(pH_D) \tag{7.36}$$

$$H_D^{k_2}(pH_D) < m_I \tag{7.37}$$

The specification of a concrete pH at the raffinate stream, pH_R, leads to a particular adsorption equilibrium constant of the components in the zone III. Thus, a region of feasible operating parameters can be derived by scanning of all possible pH_R values in the range between pH_D and pH_F, accordingly with the spanning of all suitable values of m_{II} and m_{III} using Equation (7.6) that fulfills the inequalities of Equation (7.35) and Equation (7.37).

As mentioned in Section 6.3, the adsorption equilibrium constants depend in a non-linear manner on the mobile phase composition. This dependency has a significant impact on the size and shape of regions of operating conditions. Different strategies can be applied for designing stepwise gradient SMB process in order to improve the specific productivities or minimize the specific buffer consumption as discussed by Antos and Seidel-Morgenstern [8].

It is worth noting that Equation (7.35), Equation (7.37), and Equation (7.38) define a region in the three dimensional space spanned by the three internal flow rate ratios, m_I, m_{II}, and m_{III}. A shortcut to fully define a concrete operating point consists in the specification of the internal flow rate ratio in zone I, m_I, by transforming the inequality into an equality introducing a safety factor, β, larger than 1:

$$m_I = \beta \cdot H_D^{k_2}(pH_D) \tag{7.38}$$

In the frame of the equilibrium theory the points belonging to this region achieve complete separation of the components, k_1 and k_2, i.e. pure k_1 at the raffinate port and pure k_2 at the extract port. It is also rather clear that the boundaries of the complete separation region depend only on the external pH values pH_D and pH_F and of course on the retention behaviour of the components, which in this case is described by the dependence of the adsorption equilibrium constants, H^k, on the pH using Equation (6.11).

7.3 Parametric study

In Section 7.2, the region to achieve complete separation was derived for the binary mixture of components, k_1 and k_2. The cell culture supernatant described in Section 6.1 is considered as a pseudo-binary mixture made up of the IMP and ABF fraction as illustrated in Figure 6.1. The single-chain antibody fragment is contained in the ABF fraction in a very low concentration.

Two characteristic adsorption equilibrium constants H^{IMP} and H^{ABF} given in Equation (6.11) and Table 6.3 provide the initial basis to design a continuous pseudo-binary separation process bringing the corresponding fractions to the raffinate port, IMP fraction, and to the extract port, ABF fraction, of a potential SMB process.

A parametric study was conducted to theoretically evaluate possible regions of operating parameters for IMP and ABF under the influence of the number of equilibrium stages, the purity constraints at the outgoing streams and the concentration of the impurities. Detailed simulations of the process were performed using an equilibrium stage model code programmed in MATLAB.

The regions of feasible operating parameters were determined by screening all values possible for the pH, pH_{III}, i.e. between the pH at the feed, pH_F, and the pH at the desorbent, pH_D. Each pH_{III} value generated the corresponding adsorption equilibrium constants for the components in zone III. In addition, every single scanned m_{II}, m_{III}-pair must fulfill the constraints in Equation (7.35), Equation (7.37), and Equation (7.38). The m_{II}, m_{III}-pairs fulfilling the boundary constraints specify a system of linear of equations representing mass balances of each component. The concentrations of each component at the beginning and end of each zone of the TMB unit can be found solving the system of linear equations in Equation (7.31). Only the $m_{II}, mIII$-pairs fulfilling the constraints were used to depict the region of operating parameters by simulation [28].

For the simulations the following parameters were kept constant (if nothing else is indicated): number of equilibrium stages per zone 20, purity constraints for both components $> 99\%$, column length 2.5 cm, column diameter 0.7 cm, column configuration 1/1/1, external feed flow rate 1.28 mL/min, $pH_F = 6.5$, $pH_D = 4.0$, number of steps for the outer and inner calculation loops were equal to 200 and safety factor was set to 1.10.

7.3.1 Influence of the number of equilibrium stages

The influence of the number of equilibrium stages on the shape and size of the separation region is illustrated in Figure 7.3. As expected the region of feasible operating parameters is becoming larger when the number of equilibrium stages increases. The results of the simulations are in agreement with these expectations.

The difference between having 20 and 50 equilibrium stages per zone or 60 and 150 for the whole SMB unit can be observed in Figure 7.3. In all cases is possible to achieve purities above 99%.

The shape of the regions of feasible operating parameters in the m_{II},m_{III}-plane illustrated in Figure 7.3 under linear conditions takes for the case of an open-loop 3-zone pH-gradient SMB the shape of distorted acute triangle with base on the diagonal $m_{II} = m_{III}$. Basically, the shape remains the same but not the size. Different sizes were obtained according to the number of equilibrium stages considered in the simulation.

The simulations for the SMB process with 40 and 50 equilibrium stages showed that the change in size was not as significant as it was between 20 and 30, or 30 and 40 equilibrium stages indicating that a simulation with 50 stages is closer to the ideal case with infinite efficiency or infinite number of equilibrium stages.

Van Deemter describes in Equation (3.16) the relation between efficiency, i.e. the height equivalent to a theoretical plate or number of equilibrium stages, and the linear velocity or flow rate [34]. Assuming the same number of equilibrium stages per zone is not completely accurate since the internal volumetric flow rates in each zone are different. It is known from experience that SMB separations have a lower sensitivity against a decreasing number of equilibrium stages in comparison to batch separations, which can occur due to changes in column homogeneity during operation [67].

The number of equilibrium stages characterizes the efficiency of the columns conforming a zone of the SMB unit as explained in Section 3.2.1. A large number of equilibrium stages means more efficiency. A conservative theoretical design can be

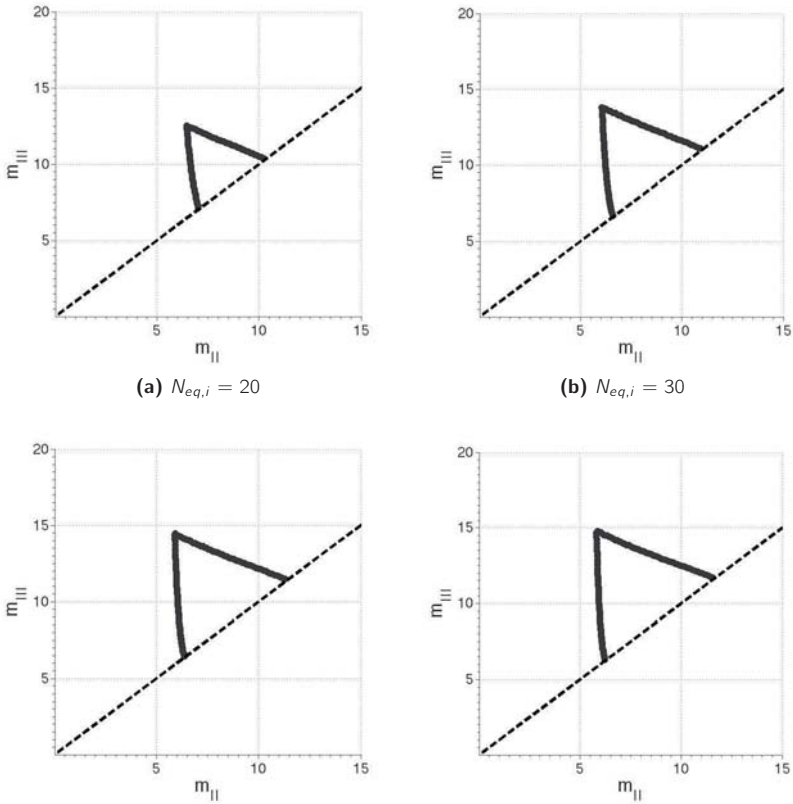

(a) $N_{eq,i} = 20$ **(b)** $N_{eq,i} = 30$

(c) $N_{eq,i} = 40$ **(d)** $N_{eq,i} = 50$

Figure 7.3: Influence of the number of equilibrium stages per zone i, $N_{eq,i}$, on the region of feasible operating parameters: (a) $N_{eq,i} = 20$; (b) $N_{eq,i} = 30$; (c) $N_{eq,i} = 40$; and, (d) $N_{eq,i} = 50$

done considering that the each zone of the SMB unit has very low efficiency equal to the least efficient zone with largest internal flow rate. In this way, an additional safety factor can be introduced in the design.

7.3.2 Influence of the purity constraints

The influence of the purity constraints on the shape and size of the separation region is illustrate in Figure 7.4 . As expected the region of feasible operating parameters is becoming larger when the purity constraint decreases. The simulations showed a good agreement with the theory.

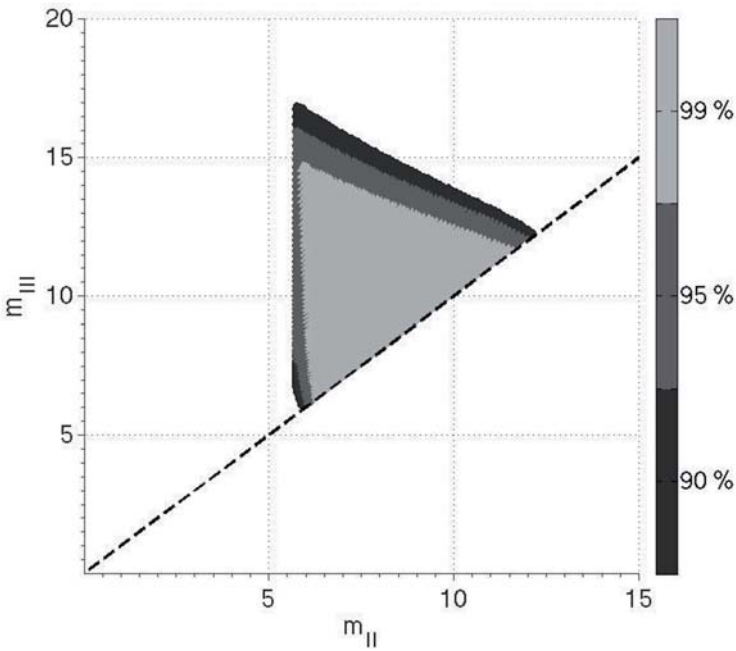

Figure 7.4: Influence of the purity constraints, *PUR*, on the region of feasible operating parameters at different purity requirements: PUR > 99 %, PUR > 95 %, and PUR > 90 %

The region of possible operating conditions for the separation of IMP and ABF fractions is significantly smaller when the purity constraints for both fractions are above 99 %. Additionally, the maximal productivity under this purity requirements is small but could be gradually increased if the purity requirements decreases. The equilibrium stage model performed such predictions in a short computational time.

From the theoretical point of view, it is possible to increase the productivity of the process going far away from the diagonal and still have purities of 95 % or even 90 % at the extract and raffinate port.

7.3.3 Influence of the concentration of the impurites

In this work, the concentration of the antibody fragment in the feed, c_{Feed}^{scFv}, is the most important parameter for improving the productivity of an open-loop 3-zone pH-gradient SMB process. This parameter was not studied in this parametric study because it is only possible to dilute the cell culture supernatant. An enriched supernatant can only be obtained by optimization of the upstream process.

However, the effect of the concentration of impurities (IMP) in the feed on the separation performance was theoretically investigated using the equilibrium stage model. The protein impurities are present in large and unknown amount in comparison to the target product. The effect of the concentration of impurities in the feed on the shape and location of the region of feasible operating parameters was analyzed and discussed in the literature [90].

An operating point, $m_{II} = 6.5$, $m_{III} = 13.5$, within the region of feasible operating parameters in Figure 7.3 (d), was chosen and by simulation the internal concentration profiles for both components were evaluated. The results of the simulation for different levels of impurities concentration at the feed are shown in Figure 7.5.

It is worth noting that large concentrations of impurities decreased the final purity of the ABF fraction containing the single-chain antibody fragment at the same operating point. This effect can be observed in Figure 7.5 by the movement of the concentration front of the impurities towards the extract port when the concentration of IMP fraction increases. For instance, a concentration of the impurities 25 times higher than the feed concentration of the single-chain antibody fragment reduces the purity of the ABF fraction to 90%. The effect is even more dramatic with a 50-fold concentration of impurities as illustrated in Figure 7.5.

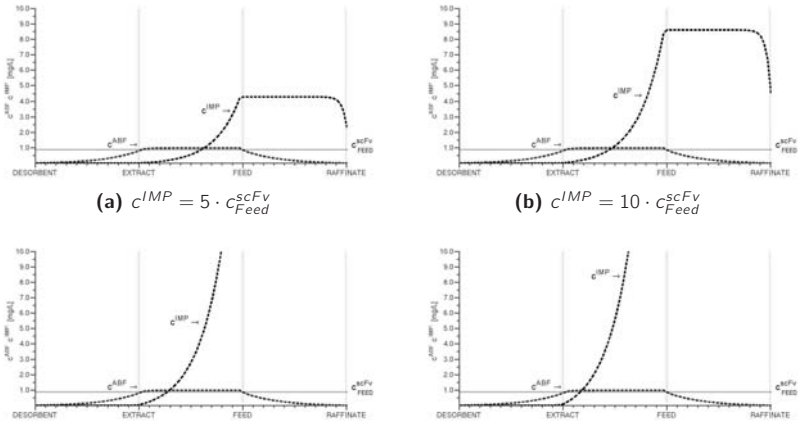

(a) $c^{IMP} = 5 \cdot c^{scFv}_{Feed}$ **(b)** $c^{IMP} = 10 \cdot c^{scFv}_{Feed}$

(c) $c^{IMP} = 25 \cdot c^{scFv}_{Feed}$ **(d)** $c^{IMP} = 50 \cdot c^{scFv}_{Feed}$

Figure 7.5: Influence of the concentration of impurities (IMP) on the internal concentration profile: (a) $c^{IMP} = 5 \cdot c^{scFv}_{Feed}$, (b) $c^{IMP} = 10 \cdot c^{scFv}_{Feed}$, (c) $c^{IMP} = 25 \cdot c^{scFv}_{Feed}$, and (d) $c^{IMP} = 50 \cdot c^{scFv}_{Feed}$

The shape and size of the region of feasible operating parameters was significantly affected by the feed concentration ratio of components involved in the pseudo-binary separation (ABF and IMP) as depicted in Figure 7.6 (a). The location of the region of feasible operating parameters was displaced to the right when the concentration of impurities is 25 times larger than the concentration of the antibody fragment in the cell culture supernatant. Furthermore, the size of the new region of feasible operating parameters covered a larger region of operating conditions in the m_{II},m_{III}-plane.

A new operating point was chosen $m_{II} = 7.5$, $m_{III} = 16.9$, inside the larger region but outside the smaller region of operating parameters, to illustrate the separation performance taking into account that the concentration of impurities entering the SMB unit is 25 times higher than the concentration of the antibody fragment (see Figure 7.6 (a)). The new operating point succeeded in moving the IMP concentration front towards the raffinate port and restored the conditions to achieve a good separation performance between ABF and IMP as illustrated by the internal concentration profiles shown in Figure 7.6 (b).

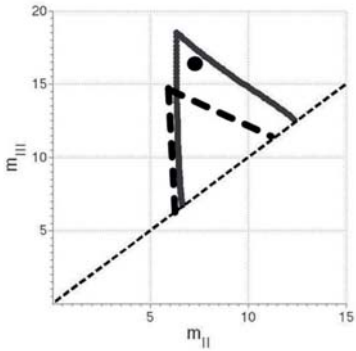

(a) Region of feasible operating parameters

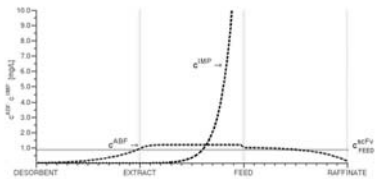

(b) Internal concentration profile

Figure 7.6: Effect of a 25-fold concentrated IMP fraction on: (a) the region of feasible operating parameters, and (b) the internal concentration profile

7.4 Concluding remarks

During the last decade, intensive research on applications of SMB chromatography in bioseparations brought a broad process understanding of the theoretical foundations and practical issues of continuous counter-current multi-column gradient elution chromatography.

Among these, a theoretical design for a closed-loop 4-zone two-step gradient SMB under linear conditions was described by Beltscheva et al. [12]. A modification was applied in this work as a design tool to predict regions of feasible operating conditions for a continuous chromatographic purification of a single-chain antibody fragments using an open-loop 3-zone pH-gradient SMB.

The use of the TMB model was appropiate to identify the region of feasible

operating parameters in the m_{II},m_{III}-plane [112, 122]. The valuable information obtained can be translated into the internal and external volumetric flow rates and the switching time of the equivalent SMB unit when the volumetric feed flow rate is given [67, 91]. The strategy can be easily extended to any solvent, salt or other pH-gradient elution regime typically found in gradient elution chromatography for protein purification. Many conditions can be evaluated theoretically in advance reducing the experimental validation to a certain promising operating conditions.

This design approach might be useful for optimization of SMB chromatography where the influence of certain parameters such as column length, column configuration, flow rates, feed concentration, and switching times can be studied in detailed. In this case, the model can be used for calculating the SMB using the steady state of an equivalent TMB unit with different numbers of equilibrium stages, whether the number of stages in each zone is identical or not.

By simulation, the influence of the number of equilibrium stages and purity constraints on the region of feasible operating parameters were determined. For validation of the equilibrium stage model, different purity constraints were used assuming low number of equilibrium stages and columns, and the SMB system operating in steady state.

The shape and location not only of the internal concentration profile of the IMP fraction but of the region of operating parameters in a m_{II}, m_{III}-plane were affected by the feed concentration of components involved in this pseudo-binary separation.

The equilibrium stage model is able to predict the trends of the separation in an open-loop 3-zone pH-gradient SMB process when some parameters are changed. Now, these trends need will be experimentally validated using a lab-scale SMB unit in the next chapter.

Chapter 8

Continuous chromatographic purification: Experimental Validation

The scope of this final chapter is the experimental validation of the open-loop 3-zone pH-gradient SMB process described and designed using the equilibrium stage model in the frame of the equilibrium theory for pH-gradient SMB separations under linear conditions [1, 12].

The adsorption equilibrium constants of ABF and IMP fractions were determined as a function of pH in Chapter 6 and used in the equilibrium stage model for the estimation of the region of feasible operating parameters of an open-loop 3-zone pH-gradient SMB in Chapter 7. In this chapter, certain operating conditions were chosen and experimentally validated in a small scale SMB unit. The proof of concept covers the effects of the switching time and the dimensionless flow rate ratio in zone II on the performance of the SMB operation. The results of the experimental runs are presented and discussed below in detail.

At the end of the chapter, the open-loop 3-zone pH-gradient SMB is compared with the stepwise pH-gradient batch process in terms of purity, yield, specific buffer consumption, and specific productivity. The discontinuous single-column separation case was analyzed and evaluated in Chapter 6.

8.1 Implementation of the open-loop 3-zone pH-gradient SMB

An easy method to implement SMB system is the open-loop configuration made of three zones. The stream leaving zone III corresponds to raffinate stream.

The pilot system CSEP® C916 had to be adapted in advance for the requirements of an open-loop 3-zone pH-gradient SMB process. The scheme of the "unfolded" multi-function valve with all the capillary connections necessary for implementing an open-loop 3-zone pH-gradient SMB system with one column per zone is depicted in Figure 8.1:

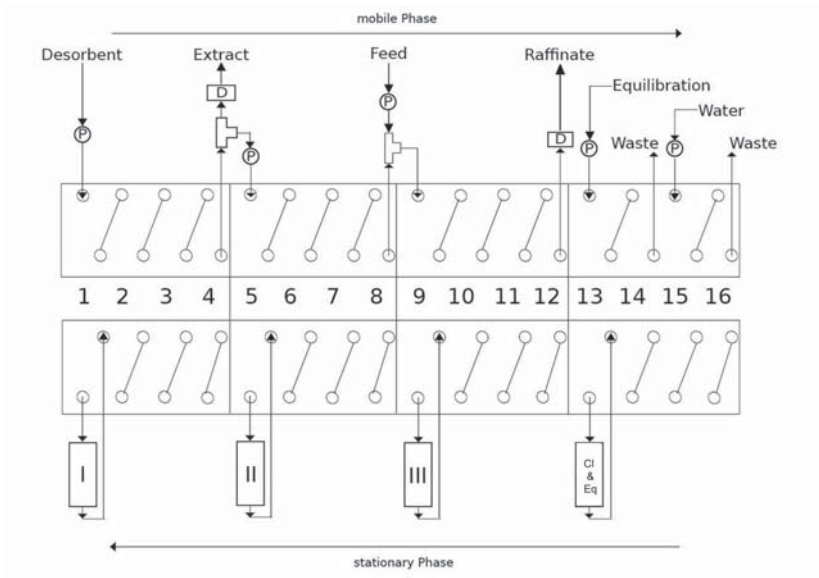

Figure 8.1: Schematic representation of the capillary connections to the CSEP® C916 Simulated Moving Bed unit [129]

In addition to the three zones, the experimental set-up included an extra-zone to perform the necessary cleaning and equilibration of the stationary phase when gradients in SMB units are applied. This zone was responsible for the cleaning and equilibration of the column coming from zone I (high elution strength and low pH)

and going to zone III (low elution strength and high pH).

Cleaning and equilibration zone was located just in the middle of the two distinct conditions and its location can be used effectively for two purposes: in the first half of the zone, the column coming from zone I was cleaned with water and after that, in the second half of the zone, the column was equilibrated to the adsorbing conditions required in zone III where the components were adsorbed. The pH-value of the equilibration buffer might be also a sensitive parameter for the optimization of the separation performance and should have a pH-value close to the pH of zone III to guarantee adsorbing conditions in zone III.

The application of a pH-gradient SMB implies also an adequate and continuous cleaning of the columns involved in the separation like in batch chromatography, where the cleaning step was performed after each cycle [103]. Such an open-loop concept is a simple configuration to overcome cross-contamination caused due to the recycling of unregenerated mobile phase containing undesired impurities. Cross-contamination could be critical when the target product is the last eluting and very diluted component present in a multi-component mixture where several unknown and low-value components with diverse adsorption-desorption behavior are present in large concentrations. This is a very common case in the chromatographic purification of biomolecules.

The desorbent inlet stream was equal to the internal flow rate in zone I and it is set by the desorbent pump. The extract stream was equal to the difference between the $\dot{V}_I$ and $\dot{V}_{II}$ and it was set by the pump for zone II. The mobile phase leaving zone II met the feed which was pumped directly into the system and at this point, the pH-gradient was created. The target component, ABF fraction, adsorbed in the zone III was transported towards the extract outlet port where was eluted. The protein impurities lumped together in the IMP fraction were less adsorbed on the stationary phase and therefore dragged out by the mobile phase at the raffinate port. For the implementation of the gradient SMB process, at least three columns were necessary for the separation. One extra column was involved for the cleaning and equilibration. Next to the SMB unit, a flow meter and pH meter were installed for online monitoring of the outlet streams.

In order to avoid the crystallization of salts contained in the buffers inside the pumps, the pistons of the pumps were washed continuously during operation with a solution of 20% (v/v) ethanol in water.

Before the operation of the SMB, the pumps were checked for accuracy and the dead volumes of the entire SMB pilot plant and each zone were determined. The error of the pumps were between 1 - 2%, depending on the volumetric flow rate

used. This sort of error is in agreement with the manufacturer's instructions.

8.2 Continuous chromatographic purification of the single-chain antibody fragment

The region of operating parameters was predicted using the equilibrium model with 50 equilibrium stages per zone and assuming that the concentration of protein impurities entering the unit was 25 times higher than the feed concentration of the single-chain antibody fragment. Once the region of operating parameters was defined, six different operating points were chosen for the experimental validation as illustrated in the m_{II}, m_{III}-plane in Figure 8.2 (a) and (b):

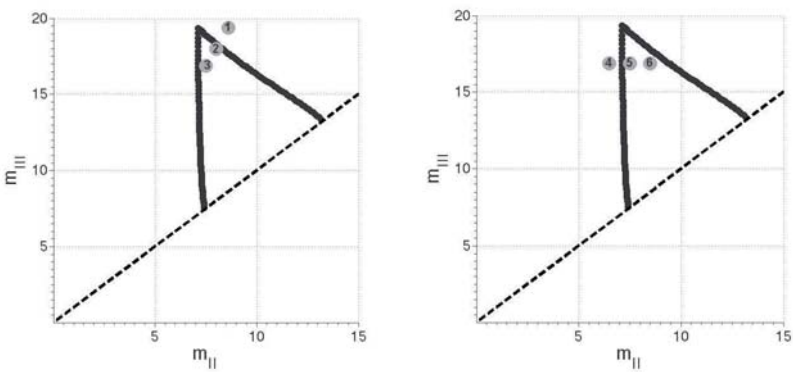

(a) First set of operating points 1, 2, and 3 **(b)** Second set of operating points 4, 5, and 6

Figure 8.2: Region of feasible operating parameters for the open-loop 3-zone pH-gradient SMB process including the position of the experimentally validated operating points: (a) First set of operating points 1, 2, and 3; and, (b) Second set of operating points 4, 5, and 6

The dead volume of the individual zones were equal to 0.50 mL and the dead volume of SMB unit was estimated to be around 1.50 mL. The effects of the non-negligible extra-column dead volume per zone were estimated using Equation (3.42) for the prediction of the region of feasible operating parameters. The presence of extra-column dead volumes shifted the region of feasible operating parameters

upwards along the diagonal in the operating plane spanned by m_{II} and m_{III}. This shifting upwards occurs due to the effect of the extra-column dead volume on increasing the residence time within the SMB unit with respect to the retention time in the column alone [93]. The region of feasible operating parameters where the extra-column dead volumes were ignored is not shown here.

The selected operating points were located either inside or outside the region of operating parameters in order to check the validity of the predicted separation region and were grouped in two sets:

1. The first set corresponds to the operating points 1, 2, and 3. The set was obtained by changing the switching time while the internal and external flow rates were kept constant.

2. The second set corresponds to the operating points 4, 5, and 6. The set was obtained by varying the internal dimensionless flow rate ratio in zone II, m_{II}, while the internal dimensionless flow rate ratios in zone III, m_{III}, and I, m_I, were kept constant.

After the determination of the separation region, the safety factor, β, was selected and internal dimensionless flow rate ratio in zone I, m_I, was estimated according to Equation (7.38). The internal and external flow rates, and the switching time were defined by m_I (i.e. safety factor) and choosing a m_{II}, m_{III} pair located in the m_{II}, m_{III}-plane.

The following conditions were realized: the volumetric flow rate of the feed stream, $\dot{V}_F$, was set equal to 1.28 mL/min. The pH of the buffer solution used at the desorbent, pH_D, was 4.0. The pH of the feed entering the SMB unit, pH_F, was 6.5 and corresponds to the cell culture supernatant diluted in a buffer solution with a pH value around 7.0. Column dimensions are 2.5 cm x 0.7 cm i.d. The column configuration was 1/1/1. The volumetric flow rates of the cleaning and equilibration steps were both kept constant and equal to 3.0 mL/min.

Chromatograms corresponding to the extract and raffinate outlet stream for the individual operating points were recorded. Samples from the extract, raffinate, and cleaning outlet streams were collected over an entire switching period (between two switches). Therefore, the concentration of each sample represents the average concentration over the switching time as considered in Equation (3.49). The amount of collected sample depended on the volumetric flow rates of the outlet streams and switching time (i.e. operating point).

The parameters of the six operating points used for the experimental validation are summarized in Table 8.1:

Table 8.1: Parameters of the six operating points for the experimental validation of the open-loop 3-zone pH-gradient SMB

Parameters	Unit	1	2	3	4	5	6
β	[-]	1.30	1.15	1.09	1.35	1.35	1.35
m_I	[-]	18.5	17.2	16.2	19.0	19.0	19.0
m_{II}	[-]	8.6	8.0	7.5	*6.5*	*7.5*	*8.5*
m_{III}	[-]	19.4	18.0	16.9	16.9	16.9	16.9
$\dot{V}_S$	[mL/min]	0.12	0.13	0.14	0.12	0.14	0.15
$\dot{V}_I = \dot{V}_D$	[mL/min]	2.12	2.12	2.12	2.40	2.65	2.97
$\dot{V}_{II}$	[mL/min]	1.09	1.09	1.09	0.86	1.09	1.37
$\dot{V}_{III} = \dot{V}_R$	[mL/min]	2.30	2.30	2.30	2.14	2.37	2.65
$\dot{V}_F$	[mL/min]	1.28	1.28	1.28	1.28	1.28	1.28
$\dot{V}_E$	[mL/min]	1.03	1.03	1.03	1.54	1.56	1.60
$\dot{V}_{Cle} = \dot{V}_{Equ}$	[mL/min]	3.00	3.00	3.00	3.00	3.00	3.00
t_{switch}	[min]	*5.40*	*5.04*	*4.70*	5.20	4.70	4.20

Experimental evidence for the successful realization of pseudo-binary separation of ABF and IMP was carried out using offline SDS-PAGE and ELISA analytical assays as explained in Section 5.2.2. The concentration of single-chain antibody fragment detected by ELISA corresponds only to active antibody fragment. Thus, the evaluation of the performance parameters was carried out regarding only the single-chain antibody fragment. This is very convenient because the antibody fragment is also the target product.

8.2.1 Effect of the switching time

For the first set of operating points, 1, 2, and 3, the external and internal flow rates were kept constant and the switching time was varied between 5.40 min to 4.70 min. In doing so, the safety factor must be modified for keeping the internal volumetric flow rate in zone I, $\dot{V}_I$, constant (see Table 8.1). In this case, there was one operating point outside of the predicted separation region, 1, and there were two operating points inside the predicted separation region, 2 and 3.

The chromatogram of the operating point 1 shows at the extract port the typical start-up dynamic of a SMB process. At the beginning of the second cycle, a clear

peak was detected in the extract as illustrated in Figure 8.3 (a). The UV-signal slowly builds up over the cycles until the so-called periodic steady state was reached at cycle 5.

The UV-signal of the extract within a switch period consists of a sharp peak at the beginning and a small and broad peak at the end as shown in Figure 8.3 (a). This observation was in agreement with the discontinuous single-column stepwise pH-gradient process, where the elution of the ABF fraction consisted also of two peaks as illustrated in Figure 6.1. The UV-signal of the raffinate remained invariable for the whole first and second set of experiments due to the large amount of protein impurities present and eluting at this port and it will not be shown anymore.

SDS-PAGE analysis of operating point 1 is illustrated in Figure 8.3 (b), which shows the different proteins found within a switching period at the feed mixture and samples collected from the outlet ports (extract, raffinate, cleaning) at the 8th cycle when the periodic steady state was reached. In the feed, extract and raffinate lanes on the SDS-PAGE gel, the single-chain antibody fragment band was recognized around 27 kDa. The extract lane shows the purified ABF fraction containing the single-chain antibody fragment accompanied by the variable domains, and two other protein impurities of larger size than 27 kDa.

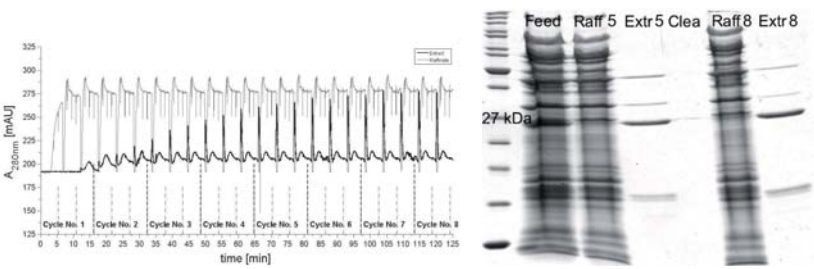

(a) SMB Chromatogram **(b)** SDS-PAGE analysis

Figure 8.3: Operating point 1. Switching time: 5.40 min. Desorbent buffer: 20 mM sodium phosphate, 0.5 M NaCl, pH 4.0. Feed (pH 6.5): clarified cell culture supernatant diluted in 20 mM sodium phosphate, 0.5 M NaCl. Equilibration buffer: 20 mM sodium phosphate, 0.5 M NaCl, pH 5.3. (a) SMB chromatogram; and, (b) SDS-PAGE analysis

In Figure 8.4 (b), the SDS-PAGE analysis of operating point 2 shows that in the raffinate port almost no traces of antibody fragment were detected, which means that the antibody fragment was recovered in great extent at the extract port and

even more concentrated and less contaminated than in operating point 1, this might also explain why in the UV-signal of the extract stream the first peak was becoming broader when changing from operating point 1 to 2 as can be observed in Figure 8.4 (a). A new cyclic steady state was reached very fast when the switching time was reduced from 5.40 min to 5.04 min and remained stable for all subsequent cycles.

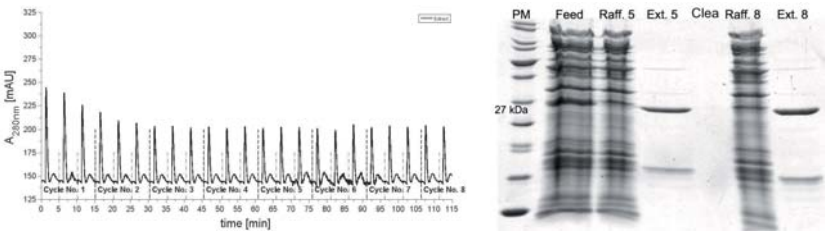

(a) SMB Chromatogram **(b)** SDS-PAGE analysis

Figure 8.4: Operating point 2. Switching time: 5.04 min. Desorbent buffer: 20 mM sodium phosphate, 0.5 M NaCl, pH 4.0. Feed (pH 6.5): clarified cell culture supernatant diluted in 20 mM sodium phosphate, 0.5 M NaCl. Equilibration buffer: 20 mM sodium phosphate, 0.5 M NaCl, pH 5.3. (a) SMB chromatogram; and, (b) SDS-PAGE analysis

In operating point 3, the switching time was further reduced from 5.04 min to 4.70 min. The chromatogram in Figure 8.5 (a) shows an even broader first peak in the UV-signal of extract than the ones found in operating points 1 and 2.

In Figure 8.5 (b), the SDS-PAGE analysis of operating point 3 shows a significant increase of the concentration of the single-chain antibody fragment in the extract consistent with the broad first peak found in the UV-signal of the extract stream. Additionally, even less impurities were detected at the extract accompanying the highly enriched target component compared with operating points 1 and 2. The high enrichment of the antibody fragment at the extract port resulted from the low volumetric flow rate at the desorbent (i.e. low safety factor) obtaining a less diluted target product at extract.

The UV-signal of the raffinate, despite the changes in the switching time continued invariable for the first set of operating points, 1, 2, and 3. Conversely, the UV-signal of the extract changed significantly from operating point 1 to 3. The first peak became broader when the switching time was reduced from 5.40 min to 4.70 min. This observation was consistent with the increased final concentration and yield found at operating point 3.

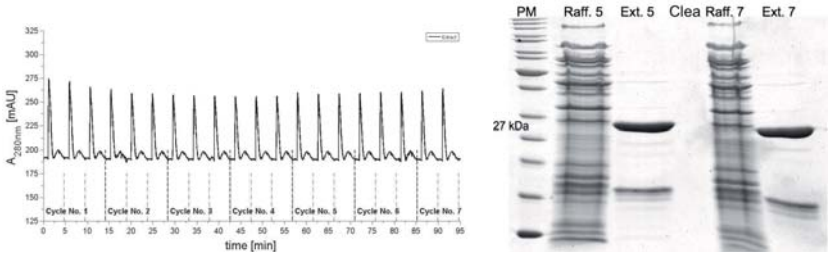

(a) SMB Chromatogram **(b)** SDS-PAGE analysis

Figure 8.5: Operating point 3. Switching time: 4.70 min. Desorbent buffer: 20 mM sodium phosphate, 0.5 M NaCl, pH 4.0. Feed (pH 6.5): clarified cell culture supernatant diluted in 20 mM sodium phosphate, 0.5 M NaCl. Equilibration buffer: 20 mM sodium phosphate, 0.5 M NaCl, pH 5.3. (a) SMB chromatogram; and, (b) SDS-PAGE analysis.

The concentration of the single-chain antibody fragment in the extract increased with increasing number of cycles until the cyclic steady state was reached. This was checked by SDS-PAGE gels of different switching cycles, where thicker bands were found at later cycles which means also an increase of the concentration of the target product.

No evidence of the single-chain antibody fragment or other protein impurities were found at the cleaning outlet streams of operating points 2, and 3 (see Figure 8.4 (b) and Figure 8.5 (b)), indicating the occurrence of a successful purification of ABF fraction from the IMP fraction without any losses in the cleaning and equilibration zone.

Table 8.2 summarizes the evaluation of the performance parameters for the continuous chromatographic purification obtained from the different pooled samples corresponding to the extract outlet stream for operating points 1, 2, and 3:

The estimated performance parameters refer to the switching period and only to the single-chain antibody fragment found at the extract samples. The final concentration of the active antibody fragment increases from operating point 1 to 3 from 0.3 to 1.0 mg/L. At operating point 3, the single-chain antibody fragment was enriched, since the concentration of 1.0 mg/L was higher than the concentration of the antibody fragment in the feed (0.88 mg/L). The lowest safety factor chosen at operating point 3 was translated into a low flow rate at the extract responsible for the enrichment of the target product at the extract port.

Table 8.2: Evaluation of the performance parameters for operating points 1, 2, and 3 according to Section 3.5

Parameter	Unit	1	2	3
$\bar{c}^{scFv}_{Extract}$	[mg/L]	0.3	0.6	1.0
$PUR^{scFv}_{Extract}$	[%]	57.0	60.0	66.0
$Y^{scFv}_{Extract}$	[%]	27.4	54.9	91.4
SDC^{scFv}_{SMB}	[L_{MP}/mg]	30.4	15.2	9.1
$PRD^{scFv}_{Extract}$	[mg/day·L_{SP}]	172.9	345.9	576.5

The purity determined by densitometry increased from operating point 1 to 3 from 57 to 66 %. Analogously, the yield increased significantly from operating point 1 to 3 from 27 to 91 %, which means that reducing for these conditions the switching time increases the recovery of the target product.

At operating points 1 and 2 the antibody fragment moved towards the raffinate port, where it was eluted in high dilution. Thus, the yield of these points was lower than in operating point 3.

The specific desorbent consumption includes the consumption of all buffers employed to purify 1 mg of single-chain antibody fragment. It was equal to 30.4 L_{MP}/mg for operating point 1 and was reduced to only 9.1 L_{MP}/mg for operating point 3. The specific productivity gain of operating point 3 was up to three times higher than the one of operating point 1.

Summarizing, the operating point 3 outperfomed by far operating points, 1 and 2, in terms of final concentration, purity, yield, specific buffer consumption and specific productivity and confirmed the validity of the region of feasible operating parameters.

8.2.2 Effect of the m_{II}-value

For the second set of operating points, 4, 5, and 6, the internal dimensionless flow rates ratios in zone I, m_I, and III, m_{III}, were kept constant and the internal dimensionless flow rate ratio in zone II, m_{II}, was varied from 6.50 to 8.50. In doing so, all external flow rates had to be modified for keeping the internal flow rates in zone I, m_I, and III, m_{III}, constant (see Table 8.1). In this case, there was one operating point outside of the separation region 4, and there were two operating points inside the separation region 5, and 6.

In this set of experiments, a constant safety factor of 1.35 was used for operating points 4, 5, and 6. This was also the largest possible safety factor. Higher safety factors will cause higher external and internal flow rates and higher pressure drops which are not allowed for the low pressure columns used in this work (Maximum pressure drop is 3 bar). Furthermore, it was not possible to concentrate the target product above the feed level and the purities were around 50 % or even lower due to the high safety factor responsible for dilution of the target product at the extract port.

The UV-signal of the extract of operating point 4 was lower than the UV-signals obtained for the first set of experiments due to the high safety factor used in the second set of experiments, which consequently diluted the extract stream (see Figure 8.6 (a)). Again, the UV-signal of the raffinate was invariable and remained at the same level for the second set of experiments and it is not shown here.

In Figure 8.6 (b), the SDS-PAGE analysis of operating point 4 shows a significant amount of protein impurities in the extract together with the diluted single-chain antibody fragment. This was expected for operating point 4, which was chosen outside the region of feasible operating parameters and thus, a deficient separation was achieved.

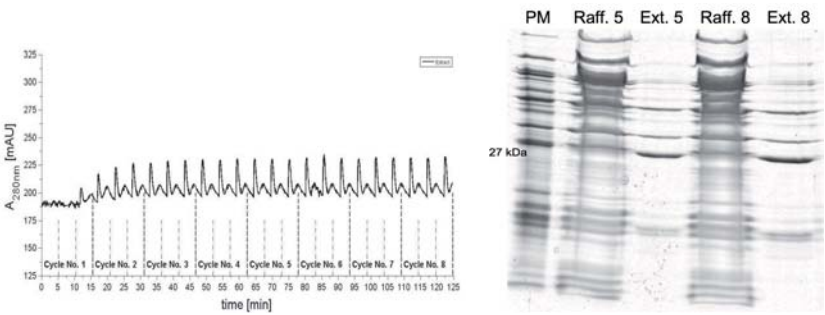

(a) SMB Chromatogram **(b)** SDS-PAGE analysis

Figure 8.6: Operating point 4. Switching time: 5.20 min. Desorbent buffer: 20 mM sodium phosphate, 0.5 M NaCl, pH 4.0. Feed (pH 6.5): clarified cell culture supernatant diluted in 20 mM sodium phosphate, 0.5 M NaCl. Equilibration buffer: 20 mM sodium phosphate, 0.5 M NaCl, pH 5.3. (a) SMB chromatogram; and, (b) SDS-PAGE analysis.

The chromatogram in Figure 8.7 (a) shows a slight increase in the UV-signal of

the extract compared to the chromatogram of operating point 4.

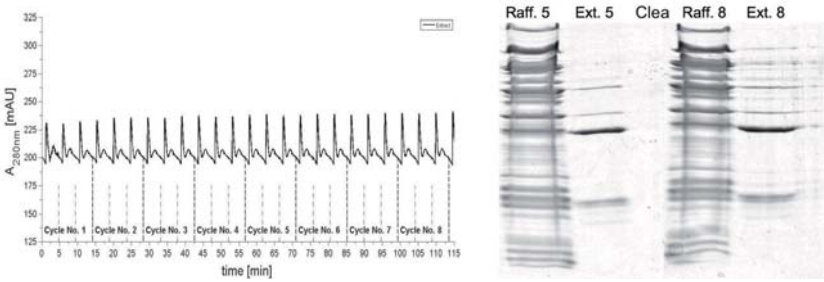

(a) SMB Chromatogram **(b)** SDS-PAGE analysis

Figure 8.7: SMB operating point 5. Switching time: 4.70 min. Desorbent buffer: 20 mM sodium phosphate, 0.5 M NaCl, pH 4.0. Feed (pH 6.5): clarified cell culture supernatant diluted in 20 mM sodium phosphate, 0.5 M NaCl. Equilibration buffer: 20 mM sodium phosphate, 0.5 M NaCl, pH 5.3. (a) SMB chromatogram; and, (b) SDS-PAGE analysis.

Operating point 5 was located in the middle of the region of feasible operating parameters as depicted in Figure 8.2 (b), and thus, a better separation performance than in point 4 was expected. In Figure 8.7 (b), the SDS-PAGE analysis of operating point 5 shows less protein impurities in the extract. Thus, a higher purity of the target product was reached but still several protein impurities larger than 27 kDa were eluted together with the single-chain antibody fragment.

Operating points 3 (see Section 8.2.1) and 5 were located in the upper-middle part of the separation region and represented the same operating point as shown in Figure 8.2 (a) and (b), but using different safety factors. The safety factor for operating point 3 was 1.09 and for operating point 5 was 1.35. Thus, the internal flow rate in zone I, $\dot{V}_I$, and the external flow rate at the extract, $\dot{V}_E$ were also different.

In Figure 8.8 (b), the SDS-PAGE analysis of operating point 6 shows that the final concentration of the antibody fragment were qualitatively very similar for operating points 4, 5, and 6.

At operating point 6, concentration and purity of the antibody fragment were increased but not in a considerable amount. Nevertheless, the purity and yield were better than operating points 4 and 5. The specific buffer consumption of operating point 6 was the lowest among the second set of experiments (see Table 8.3).

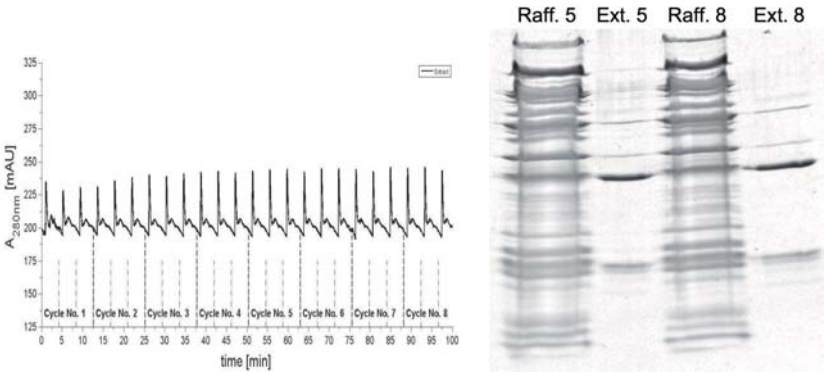

(a) SMB Chromatogram **(b)** SDS-PAGE analysis

Figure 8.8: SMB operating point 6. Switching time: 4.20 min. Desorbent buffer: 20 mM sodium phosphate, 0.5 M NaCl, pH 4.0. Feed (pH 6.5): clarified cell culture supernatant diluted in 20 mM sodium phosphate, 0.5 M NaCl. Equilibration buffer: 20 mM sodium phosphate, 0.5 M NaCl, pH 5.3. (a) SMB chromatogram; and, (b) SDS-PAGE analysis.

As expected, the safety factor had a significant effect on the final concentration of the antibody fragment, specific productivity, and specific buffer consumption due to a higher dilution of the target product at the extract port.

However, higher purity and higher yield were expected of operating point 5 compared to operating point 3. And the result was just the opposite. This could be explained by the low sensitivity of ELISA for antibody fragment concentrations under 0.5 mg/L. A better estimation of the concentration of the single-chain antibody fragment in the extract and raffinate samples was not possible using the available method. In addition to that, the antibody fragment concentrations obtained at the extract port for operating points 4, 5, and 6, were qualitatively and quantitatively close to each other as mentioned above and as illustrated in the SDS-PAGE gels in Figure 8.6 (b), Figure 8.7 (b), and Figure 8.8 (b).

Additionally, in the raffinate samples, the estimation of the concentration of the antibody fragment in the raffinate sample was not possible for the second set of experiments due to a extreme high dilution of the antibody fragment at the raffinate port. Therefore, it can not be demonstrated if the rest of the antibody fragment was moving towards the raffinate port and affecting final yields and purities of operating

points 4, 5, and 6.

It is worth noting that the UV-signal of the extract of the operating point 6 shows almost no difference in comparison to the other points, 4 and 5. This was consistent with the final concentration of the antibody fragment found at this set of experiments.

Table 8.3 summarizes the evaluation of the performance parameters for the continuous chromatographic purification obtained from the different pooled samples corresponding to the extract outlet stream for operating points 4, 5, and 6:

Table 8.3: Evaluation of the performance parameters for operating points 4, 5, and 6 according to Section 3.5

Parameter	Unit	4	5	6
$\bar{c}^{scFv}_{Extract}$	[mg/L]	0.2	0.2	0.3
$PUR^{scFv}_{Extract}$	[%]	42.0	55.0	53.0
$Y^{scFv}_{Extract}$	[%]	27.3	27.7	42.6
SDC^{scFv}_{SMB}	[L_{MP}/mg]	31.4	31.8	21.3
$PRD^{scFv}_{Extract}$	[mg/day·L_{SP}]	172.4	174.6	268.7

The volumetric flow rate of the extract in the second set of experiments was higher than the volumetric flow rate of the feed. This led to a extreme dilution of the ABF fraction at extract port as mentioned above. Since the switching time of operating point 4 was much longer than that for the operating point 5 and 6, such a dilution affected more the final concentration of the target product in the extract. Consequently, the purity and yield at operating point 4 were extremely low.

The specific buffer consumption decreased from operating point 4 to 6 due to the lower switching time and the increased final concentration of the antibody fragment and it was reduced from 31.4 to 21.3 L_{MP}/mg.

The specific productivity was increased from operating point 4 to 6 reaching a maximum specific productivity of 268.7 mg/day·L_{SP} at operating point 6, which means that increasing the value of m_{II} for these conditions increases the productivity.

Although the operating point 6 outperformed operating points 4 and 5 in terms of yield, specific productivity and specific buffer consumption. Operating point 6 was not the best operating point when compared to the results obtained at the first set of experiments.

Again, no evidence of the single-chain antibody fragment or other protein impurities were found at the cleaning outlet streams of operating points 3, 4, and 5, indicating

that no protein are lost or at least qualitatively detected in the lanes corresponding to the cleaning and equilibration zone.

8.2.3 Stability of column behavior

The reproducibility of the commercial and prepacked columns over many cycles was evaluated. All columns, from I to III and the cleaning and equilibration zone, were tested before and after the SMB experiments by a stepwise pH-gradient batch process under the same elution conditions. Each column was used during at least 30 complete SMB cycles.

The corresponding chromatograms were recorded and compared among them. The results are depicted in Figure 8.9.

Before the SMB runs, the chromatograms of all 4 columns were almost identical as illustrated in Figure 8.9 (a) indicating a very similar separation performance and homogeneous packing of all columns. It is worth to mention that the columns used for the experimental validation were commercial and prepacked columns.

After the SMB operation, the chromatograms of all 4 columns were alike as shown in Figure 8.9 (b) meaning that they were operated under similar conditions and during the same number of cycles in different positions of the SMB unit.

The comparison of the separation performance of the four columns showed an evident change in the elution behavior of the last peak of the ABF fraction. The ABF fraction consists of two peaks eluting at the end of the elution train containing the single-chain antibody fragment and the variable domains in different ratios. After the SMB operation, the last peak of the ABF fraction eluted earlier and faster in all columns.

Table 8.4 summarizes the evaluation of the retention times for the peaks considered in Figure 8.9 before and after SMB operation obtained from the four different columns used in the open-loop 3-zone pH-gradient SMB process:

It can be observed that the resolution of the columns after the SMB operation was reduced. The last peak of ABF fraction elutes 2.5 min faster than in the fresh columns. Nevertheless, this represented an apparent benefit because the last part of the antibody fragment was not strong adsorbed as it was assumed. This would mean that the molecules desorbed easily from the stationary phase, and thus, the affinity of the ABF fraction to the stationary phase at some point of the SMB operation was lower than at the beginning of the operation. However, it is out of the scope of these experiments to determine how fast the resolution of the columns

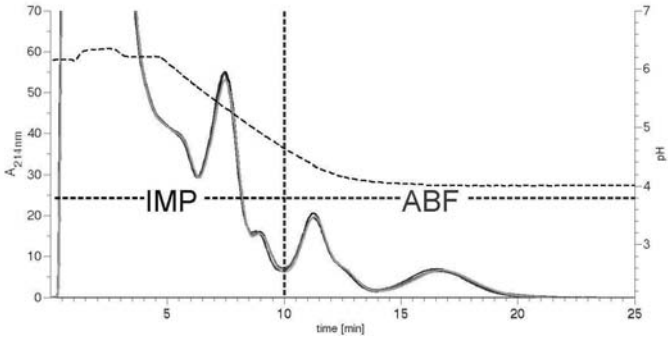

(a) Fresh columns before SMB operation

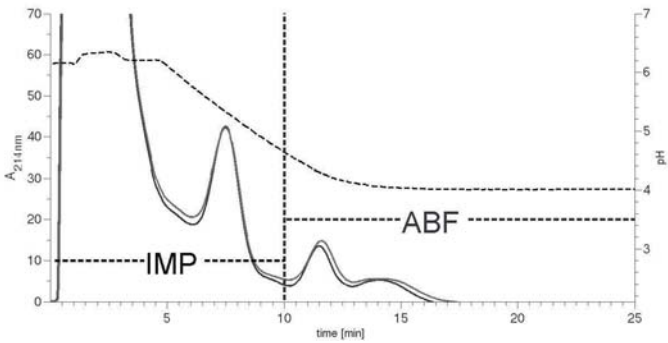

(b) Used columns after SMB operation

Figure 8.9: Reproducibility of the columns: (a) Fresh columns before SMB operation, and, (b) Used columns after SMB operation

changed, or to determine when this change occured.

In the case of the IMP and the first peak of the ABF fraction only a slight difference in retention times was observed (0.3 min).

Table 8.4: Reproducibility of the SMB columns before and after SMB operation according to Figure 8.9

Component	$t^k_{R,before}$ [min]	$t^k_{R,after}$ [min]
IMP	7.3	7.5
ABF, first peak	11.3	11.6
ABF, last peak	16.5	14.0

8.3 Evaluation of performance and comparison with batch process

In this section, a comparison of the discontinuous single-column stepwise pH-gradient and the open-loop 3-zone pH-gradient SMB chromatography based on the evaluation of the performance parameters introduced in Section 3.5 is presented. Similar examples of such a comparison can be found in the literature [125].

The performance of the discontinuous and continuous chromatographic purification processes was quantified by the final concentration of the biologically active single-chain antibody fragment, purity, yield, specific productivity and specific buffer consumption.

Discontinuous single-column stepwise pH-gradient batch elution and continuous pH-gradient SMB chromatography were compared in this work using the same feed concentration.

Figure 8.10 illustrates the evaluation of the purity, yield and productivity at the operating points used for the experimental validation of the open-loop 3-zone pH-gradient SMB process:

Since operating point 3, introduced in Section 8.2.1, showed the best performance among the different operating points used for the experimental validation of the open-loop 3-zone pH-gradient SMB. This operating point was compared against the single-column stepwise pH-gradient batch elution results obtained in Section 6.4.

The single-column batch process was capable of producing a purifed and biologically active single-chain antibody fragment from a relatively large amount of protein impurities. The performance of the discontinuous single-column chromatographic purification process was evaluated considering the overall fraction, where all fractions were lumped together into one fraction as described in Section 6.4. The purity achieved in the batch process was 59% and the yield obtained was 99%. The

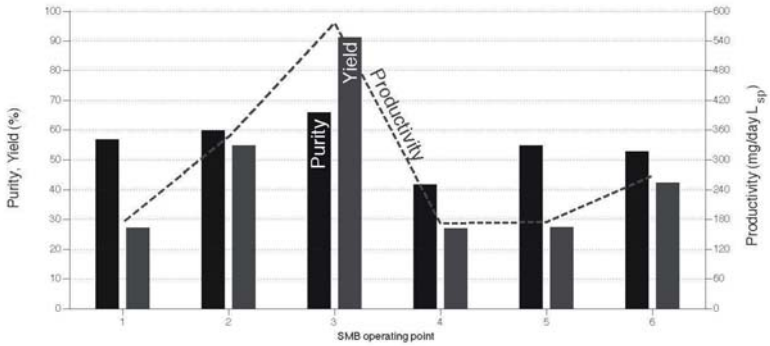

Figure 8.10: Evaluation of the purity, yield and specific productivity at the operating points for the experimental validation of the open-loop 3-zone pH-gradient SMB process

specific buffer consumption was equal to 22 L_{MP}/mg. And the specific productivity of the batch process was 125 mg/day·L_{SP}.

Table 8.5 summarizes the evaluation of the performance parameters for the discontinuous and continuous chromatographic purification obtained from the different pooled samples corresponding only to the ABF fraction containing the single-chain antibody fragment:

Table 8.5: Comparison of the evaluation of the performance parameters for the discontinuous and continuous chromatographic purification according to Section 3.5

Performance Parameter	Unit	Batch	SMB (Point 3)
$\bar{c}^{scFv}$	[mg/L]	0.2	1.0
PUR^{scFv}	[%]	59	66
Y^{scFv}	[%]	99	91
SDC^{scFv}	[L_{MP}/mg]	22	9
PRD^{scFv}	[mg/day·L_{SP}]	125	576

The purity achieved with the SMB process was 66% against 59% in the batch process representing an increment of 7%.

The yield of the SMB process was 91% against 99% in the batch process showing

a recovery lost of 8%. Total recovery in the batch process was expected because the overall fraction contains all the fractions where that antibody fragment was present.

The specific productivity of the SMB process was 576 mg/day·L_{SP} and therefore 4.6 times higher than the specific productivity of the batch process (125 mg/day·L_{SP}). This high productivity resulted from more concentrated target product at the extract port.

Additionally, the specific buffer consumption was significantly lower for the SMB process than in the batch process with a significant reduction of more than 10 L_{MP}/mg.

The low productivity of the single-column batch elution was due to the fact that the batch process was not optimized regarding maximum column load, volumetric flow rates among other parameters. SMB process was not optimized but the best performance was sorted out of the experiments for the comparison. A fair comparison might demand that both batch and SMB processes must be optimized prior to comparison [125].

Figure 8.11 illustrates the evaluation of the purity, yield and productivity of the batch elution and continuous SMB chromatography:

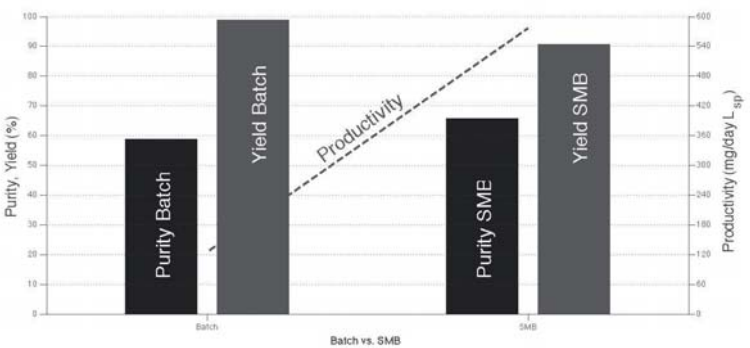

Figure 8.11: Comparison of the batch elution and open-loop 3-zone pH-gradient SMB for the purification of the single-chain antibody fragment regarding the purity, yield and specific productivity

The open-loop 3-zone pH-gradient SMB chromatography outperforms the stepwise pH-gradient elution batch process. Furthermore, it was demonstrated that the

flexibility of the SMB gradient operation was larger than the single-column batch process and the trends from the theory were confirmed [103].

Chapter 9

Concluding remarks and future work

Antibody fragments are considered the new therapeutic drugs in the field of immunotherapy due to their small size, flexibility, and suitability for cheaper expression processes plus the introduction of tags to facilitate the downstream processing [96]. The low-cost bacterial fermentations combined with low-cost affinity-based chromatography such as IMAC, makes the whole antibody fragment production process extremely attractive as an industrial option that can meet market demands enhancing and translating the advantages to the last stage, the price-benefit ratio for the final patient.

With higher titers and shorter fermentation times, bacterial fermentations are driving down the production costs of new biopharmaceutical products. Thus, the development of continuous downstream processes with reproducible quality of the biologically active biopharmaceutical product is an attractive alternative to reduce costs and number of steps on the downstream side and to facilitate the coupling between up- and downstream processes.

An expeditious and more efficient purification of biopharmaceuticals in a robust, continuous, and single chromatographic step might have an important impact in both the volume reduction, and stabilization of the purified protein. From high dilution to high purity is the main objective of downstream processing [76].

The scope of this work can be divided in two sections, in the first section, the discontinuous chromatographic purification of a single-chain antibody fragment was considered and evaluated. In the second section, the continuous chromatographic purification of a single-chain antibody fragment using an open-loop 3-zone pH-gradient SMB was designed and validated. The investigation in this work combined theoretical and experimental aspects of the discontinuous and continuous chromatographic purification of recombinant proteins. Finally, the performance of

both purification processes was evaluated, discussed and compared.

By studying the changes in the pH of the elution buffer, the influence of the pH on the adsorption equilibrium constants was described. This thermodynamic information was essential for the subsequent design of the SMB process. The stepwise pH-gradient batch elution was simulated using the equilibrium-dispersive model. The model was also applied to estimate the dependence of the adsorption equilibrium coefficients on the pH value using an empirical description of the pH profile that considers in an accurate and simple way the batch process under the pH-gradient elution conditions.

The single-column batch experiments showed that the stepwise pH-gradient batch elution was a suitable platform for the development of a pH-gradient SMB process. In the discontinuous single-column process, the elution started immediately after the sample injection using a stepwise pH-gradient analogous to the stepwise pH-gradient generated within the SMB unit where the continuous feeding of components at high pH and elution at low pH was realized.

The design of the open-loop 3-zone pH-gradient SMB was based on mixed fractions or pseudo-components, ABF and IMP. The ABF fraction consisted of the single-chain antibody fragment and the variable domains. The IMP fraction was made up of a large amount of lumped protein impurities eluting before the ABF fraction. The determination of the adsorption isotherms using the pure components was not possible because the pure components were not be available.

A model for the design of the continuous multi-column counter-current chromatographic purification of antibody fragments was presented. The model is based on the equilibrium stage model and could be extended to a broad range of different gradient conditions using salt or solvent gradients. The model provides a steady-state picture of internal concentration profiles in the SMB unit. A theoretical parametric study for linear adsorption equilibria and gradient conditions, exploiting the analogy between TMB and SMB processes, was applied to compare the regions of feasible operating parameters under the influence of some variables such as number of equilibrium stages, the purity and the concentration of impurities in the feed mixture. A region of suitable operating parameters for the lab-scale SMB unit was identified considering also the non-negligible extra-column dead volume.

The effect of the safety factor on the SMB results was also investigated. By reducing the safety factor from 1.35 to 1.10, the purity of the biologically active scFv was increased in more than 10% and the final antibody fragment concentration was 5 times higher. Additionally, the yield gain was 61% (from 30% to 91%) due to the lower safety factor and the specific productivity gain was almost threefold.

Since the internal volumetric flow rate in zone II was always the smallest flow rate present in the SMB unit for each experimental operating point, the assumption of equal number of equilibrium stages per zone for the prediction of the region of suitable operating parameters included an extra safety margin. Thus, a smaller separation region using a less efficient zone II was predicted by the model. But in reality, zone II has more equilibrium stages than zone I and III.

The stability of the columns before and after the SMB operation showed that the separation performance of the columns do not remain constant in time but slight changes occured during SMB operation. If the SMB system is running permanently, there might be a decrease in the separation efficiency of the columns.

IMAC stationary phases are unstable in caustic solutions [96]. Another disadvantage of IMAC columns is metal leaching and subsequently the contamination of the target product. Leaking occurs below pH 4.0. This represents the lowest pH limit of IMAC stationary phases when pH-gradients are applied.

The use of water for cleaning in the extra-zone was implemented to remove the low pH aqueous buffer from the stationary phase after leaving zone I where a high elution strenght was established promoting the complete elution of the most retained fraction, ABF. It was demonstrated by the SDS-PAGE analysis of samples collected from the cleaning step that the use of water was appropiate and sufficient for the cleaning of the columns before their subsequent use in other zones of the SMB unit. In the cleaning and equilibration zone the adsorbing conditions required in zone III were restored in the column coming from zone I where eluting conditions were predominant.

The use of only 3 columns for the separation section and 1 column for the regeneration section at the experimental validation is the roughest discretization of the open-loop 3-zone pH-gradient SMB process. Nevertheless, a continuous chromatographic single-step purification of single-chain antibody fragments was feasible and it was demonstrated to be successful.

Long-term operation results might not be in complete agreement with preliminary validations. Variations during operation due to aging of the stationary phase and normal variations in the external and internal volumetric flow rates might be expected. An exhaustive evaluation of the continuous operation of the SMB unit during several days and even weeks could give more information about the reproducibility of the columns and the efficiency of the continuous cleaning with water and the stability of the stationary phase during longer periods of operation.

A even more strict validation is still needed prior to scaling-up. In addition to that, many alternatives should be evaluated to make SMB fully compatible with

existing equipment and purification strategies. This work should contribute to demonstrate the feasibility of the use of gradient SMB for the purification of high-value biomolecules but still some additional work must be done to incorporate such processes into the current downstream processing schemes.

Perhaps, the most important result of this work was the proof-of-principle. The investigation into the purification of antibody fragments led to several recommendations to help to improve, develop and optimize continuous chromatographic processes. Recommendations fell into two categories: changes in the design such as more detailed modeling and changes in the configuration such as scaling-up the columns or increasing the number of columns per zone.

It is of great interest to maximize the productivity as much as possible. This will imply that the minimum amount of stationary phase will be used to purify a certain volume of sample [91]. More rigid adsorbents could eventually be able to handle larger flow rates shortening the cycle times and reducing specific buffer consumption. This could be a relevant issue considering the costs of high-quality water, salts, resources for buffer preparation and the final size of the tanks for buffer storage and disposal.

The open-loop 3-zone pH-gradient IMAC-SMB described in this work could offer a continuous single-step chromatographic purification of antibody fragments due to the high selectivity of IMAC to histidine-tagged proteins. This novel application of the open-loop 3-zone pH-gradient IMAC-SMB process also increased the specific productivity of single-chain antibody fragments by 4 compared with a similar IMAC-Batch process. Besides outperforming the batch process, the IMAC-SMB system offers some advantages over batch systems such as a more effective and robust operation because of the countercurrent movement and the continuous regime.

Last but not least, this thesis opens up new fields of application for the SMB technology as a promising technique and supports at the same time its orientation to real separation problems. This thesis also contributes to the current trends in protein purification research expanding the applications of gradient SMB chromatography as a tool in downstream processing of biomolecules.

Bibliography

[1] S. Abel, M. Mazzotti and M. Morbidelli. "Solvent gradient operation of simulated moving beds I. Linear isotherms". In: *Journal of chromatography A* 944 (2002), pp. 23–39.

[2] *Affinity Chromatography: Principles and Methods*. GE Healthcare Bio-Sciences AB, 2007.

[3] S. Ahuja. *Handbook of Bioseparations*. Academic Press, 2000.

[4] D. C. Andersen and L. Krummen. "Recombinant protein expression for therapeutic applications". In: *Current Opinion in Biotechnology* 13 (2002), pp. 117–123.

[5] D. C. Andersen and D. E. Reilly. "Production technologies for monoclonal antibodies and their fragments". In: *Current Opinion in Biotechnology* 15 (2004), pp. 456–462.

[6] J. Andersson and B. Mattiasson. "Simulated moving bed technology with a simplified approach for protein purification - Separation of lactoperoxidase and lactoferrin from whey protein concentrate". In: *Journal of chromatography A* 1107 (2006), pp. 88–95.

[7] D. Antos and A. Seidel-Morgenstern. "Application of gradients in the simulated moving bed process". In: *Chemical Engineering Science* 56 (2001), 6667?6682.

[8] D. Antos and A. Seidel-Morgenstern. "Two-step solvent gradients in simulated moving bed chromatography: Numerical study for linear equilibria". In: *Journal of chromatography A* 944 (2002), pp. 77–91.

[9] F. H. Arnold. "Metal-affinity separations: A new dimension in protein processing". In: *Nature biotechnology* 9 (1991), pp. 151–156.

[10] L. Aumann and M. Morbidelli. "A continuous multicolumn countercurrent solvent gradient purification (MCSGP) Process". In: *Biotechnology and Bioengineering* 98 (2007), pp. 1043–1055.

[11] B. V. Ayyar et al. "Affinity chromatography as a tool for antibody purification". In: *Methods* 56 (2012), pp. 116–129.

[12] D. Beltscheva, P. Hugo and A. Seidel-Morgenstern. "Linear two-step gradient counter-current chromatography - Analysis based on a recursive solution of an equilibrium stage model". In: *Journal of chromatography A* 989 (2003), pp. 31–45.

[13] M. Better and A. H. Horwitz. "Expression of engineered antibodies and antibody fragments in microorganisms". In: *Methods in Enzymology* 178 (1989), pp. 476–496.

[14] R. E. Bird et al. "Single-chain antigen-binding proteins". In: *Science* 242 (1988), pp. 423–426.

[15] O. H. Brekke and I. Sandlie. "Therapeutic antibodies for human diseases at the dawn of the twenty-first century". In: *Nature Reviews Drug Discovery* 2 (2003), pp. 52–62.

[16] H. M. Brereton et al. "Single chain antibody fragments for ocular use produced at high levels in a commercial wheat variety". In: *Journal of Biotechnology* 129 (2007), pp. 539–546.

[17] D. B. Broughton. "Production-scale adsorptive separations by simulated moving-bed technology". In: *Separation Science and Technology* 19 (1984), pp. 723–736.

[18] D. B. Broughton and C. G. Gerhold. "Continuous sorption process employing fixed beds of sorbent and moving inlets and outlets". In: *US Patent 2,985,589* (1961).

[19] K. Buhlert, M. Lehr and A. Jungbauer. "Construction and development of a new single-column simulated moving bed system on the laboratory scale". In: *Journal of chromatography A* 1216 (2009), pp. 8778–8786.

[20] G. Carta and A. Jungbauer. *Protein Chromatography: Process Development and Scale Up*. John Wiley and Sons, Inc., 2010.

[21] J. L. Casey et al. "Purification of bacterially expressed single chain Fv antibodies for clinical applications using metal chelate chromatography". In: *Journal of Immunological Methods* 179 (1995), pp. 105–116.

[22] H. E. Chadd and S. M. Chamow. "Therapeutic antibody expression technology". In: *Current opinion in Biotechnology* 12 (2001), pp. 188–194.

[23] G. Chaga. "Twenty-five years of immobilized metal ion affinity chromatography: past, present and future". In: *Journal of Biochemical and Biophysical Methods* 49 (2001), pp. 313–334.

[24] F. Charton and R. Nicoud. "Complete Design of a Simulated Moving-Bed". In: *Journal of chromatography A* 702 (1995), pp. 97–112.

[25] *Cimzia website*. http://www.cimzia.com. [Online accessed 14-December-2012].

[26] R. H. Clemmitt and H. A. Chase. "Facilitated downstream processing of a histidine-tagged protein from unclarified E. coli homogenates using immobilized metal affinity expanded-bed adsorption". In: *Biotechnology and Bioengineering* 67 (2000), pp. 206–216.

[27] L. C. Craig. "Identification of Small Amounts of Organic Compounds by Distribution Studies. II. Separation By Counter-current Distribution". In: *Journal of Biological Chemistry* 155 (1944), pp. 519–534.

[28] C. A. Martinez Cristancho et al. "Discontinuous and continuous purification of single-chain antibody fragments using immobilized metal ion affinity chromatography". In: *Journal of Biotechnology* 163 (2013), pp. 233–242.

[29] J. R. Crowther. *Methods in Molecular Biology. The ELISA Guidebook. Vol. 516*. Humana Press, 2009.

[30] P. V. Danckwerts. "Continuous flow systems. Distribution of residence times". In: *Chemical Engineering Science* 2 (1953), pp. 1–13.

[31] F. David. "Holistic bioprocess engineering of antibody fragment secreting Bacillus megaterium". PhD thesis. Technische Universität Braunschweig, 2012.

[32] F. David et al. "Antibody production in Bacillus megaterium: strategies and physiological implications of scaling from microtiter plates to industrial bioreactors". In: *Biotechnology Journal* 6 (2011), pp. 1516–1531.

[33] F. David et al. "Optimization of antibody fragment production in *Bacillus Megaterium*: The role of metal ions on protein secretion". In: *Journal of Biotechnology* 150 (2010), pp. 115–124.

[34] J. J. van Deemter, F. J. Zuiderweg and A. Klinkenberg. "Longitudinal diffusion and resistance to mass transfer as causes of nonideality in chromatography". In: *Chemical Engineering Science* 5 (1956), pp. 271–289.

[35] C. Dennison. *A Guide to Protein Isolation*. Kluwer Academic Publishers, 2002.

[36] M. Desai. *Downstream Processing of Proteins: Methods and Protocols*. Humana Press Inc., 2000.

[37] M. P. Deutscher. *Methods in Enzymology. Volume 182. Guide to Protein Purification*. Academic Press, Inc, 1990.

[38] R. Ditz. "Separation technologies 2030 - Are 100 years of chromatography enough?" In: *Chemie Ingenieur Technik* 84 (2012), pp. 875–879.

[39] L. Essen and A. Skerra. "Single-Step Purification of a Bacterially Expressed Antibody Fragment-variable Fragment by Immobilized Metal Affinity-Chromatography in the presence of Betaine". In: *Journal of chromatography A* 657 (1993), pp. 55–61.

[40] M. Z. El Fallah and G. Guiochon. "Gradient Elution Chromatography at Very High Column Loading: Effect of the Deviation from the Langmuir Model on the Band Profile of a Single Component". In: *Analytical Chemistry* 63 (1991), pp. 2244–2252.

[41] S. Farid. "Economic drivers and trade-offs in antibody purification processes". In: *Biopharma International* 1 (2009), pp. 38–42.

[42] A. Felinger. *Data analysis and signal processing in chromatography*. Elsevier Science B.V., 1998.

[43] E. Francotte. "Contribution of preparative chromatographic resolution to the investigation of chiral phenomena". In: *Journal of Chromatography A* 666 (1994), pp. 565–601.

[44] D. D. Frey. "Asymptotic Relations for Preparative Gradient Elution Chromatography of Biomolecules". In: *Biotechnology and Bioengineering* 35 (1990), pp. 1055–1061.

[45] F. M. Freyre, J. E. Vázquez and M. Ayala et al. "Very high expression of an anti-carcinoembryonic antigen single-chain Fv antibody fragment in the yeast Pichia pastoris". In: *Journal of Biotechnology* 76 (2000), pp. 157–163.

[46] V. Gaberc-Porekar and V. Menart. "Perspectives of immobilized-metal affinity chromatography". In: *Journal of Biochemical and Biophysical Methods* 49 (2001), pp. 335–360.

[47] V. Gaberc-Porekar and V. Menart. "Potential for using histidine tags in purification of proteins at large scale". In: *Chemical engineering and technology* 28 (2005), pp. 1306–1314.

[48] R. H. Garrett and C. M. Grisham. *Biochemistry*. Brooks/Cole, 2010.

[49] *Gel Filtration: Principles and Methods*. GE Healthcare Bio-Sciences AB, 2007.

[50] U. Gottschalk. "Downstream processing of monoclonal antibodies: From high dilution to high purity". In: *Biopharm international* 18 (2005), pp. 42–58.

[51] N. Gottschlich and V. Kasche. "Purification of monoclonal antibodies by simulated moving-bed chromatography". In: *Journal of Chromatography A* 765 (1997), pp. 201–206.

[52] H. Graf, J. N. Rabaud and J. M. Egly. "Screening of various mammalian cell culture media to establish a downstream purification scheme". In: *Journal of Immunological Methods* 139 (1991), pp. 135–144.

[53] T. Gu. *Mathematical Modeling and Scale-up of Liquid Chromatography*. Springer Verlag, 1995.

[54] L. Gueorguieva et al. "Discontinuous and continuous separation of the monomeric and dimeric forms of human bone morphogenetic protein-2 from renaturation batches". In: *Journal of Chromatography A* 1135 (2006), pp. 142–150.

[55] L. Gueorguieva et al. "Recombinant protein purification using gradient-assisted simulated moving bed hydrophobic interaction chromatography. Part II: Process design and experimental validation". In: *Journal of Chromatography A* 1218 (2011), pp. 6402–6411.

[56] G. Guiochon and B. Lin. *Modeling for Preparative Chromatography*. Academic Press, 2003.

[57] G. Guiochon et al. *Fundamentals of Preparative and Nonlinear Chromatography*. Elsevier Science, 2006.

[58] E. Hochuli et al. "Genetic approach to facilitate purification of recombinant proteins with a novel metal chelate adsorbent". In: *Nature Biotechnology* 6 (1988), pp. 1321–1325.

[59] J. Houwing et al. "Effect of salt gradients on the separation of dilute mixtures of proteins by ion-exchange in simulated moving beds". In: *Journal of chromatography A* 952 (2002), pp. 85–98.

[60] J. Hubbuch. "Isolation and purification of biotechnological products". In: *Journal of non-equilibrium thermodynamics* 32 (2007), pp. 99–127.

[61] P. J. Hudson and C. Souriau. "Engineered antibodies". In: *Nature medicine* 9 (2003), pp. 129–134.

[62] D. P. Humphreys and D. J. Glover. "Therapeutic antibody production technologies: Molecules, applications, expression and purification". In: *Current Opinion in Drug Discovery and Development* 4 (2001), pp. 172–185.

[63] B. Hunt et al. "Economic analysis of immunoadsorption systems". In: *Biochemical Engineering Journal* 9 (2001), pp. 135–145.

[64] *Hydrophobic Interaction Chromatography: Principles and Methods*. GE Healthcare Bio-Sciences AB, 2007.

[65] *Image Processing and Analysis in Java*. http://rsb.info.nih.gov/ij/index.html. [Online accessed 14-December-2012].

[66] *Ion Exchange Chromatography and Chromatofocusing: Principles and Methods*. GE Healthcare Bio-Sciences AB, 2007.

[67] M. Johannsen. "Modeling of Simulated Moving-bed Chromatography". In: *Modeling of Process Intensification*. Ed. by F. J. Keil. Wiley-VCH Verlag GmbH & Co. KGaA, Weinheim, 2007. Chap. 9.

[68] E. Jordan et al. "Production of recombinant antibody fragments in Bacillus Megaterium". In: *Microbial Cell Factories* 6 (2007), 1:11.

[69] A. Jungbauer. "Preparative chromatography of biomolecules". In: *Journal of Chromatography* 639 (1993), pp. 3–16.

[70] D. Karlsson. "Aspects of the design of preparative chromatography for purification of antibodies". PhD thesis. Lund University, 2004.

[71] D. Karlsson et al. "Methodologies for model calibration to assist the design of a preparative ion-exchange step for antibody purification". In: *Journal of Chromatography A* 1033 (2004), pp. 71–82.

[72] A. Kenney and S. Fowell. *Methods in Molecular Biology. Volume 11. Practical Protein Chromatography*. The Humana Press, Inc, 1992.

[73] L. C. Kessler. "Enhancing the potential of Simulated Moving Bed Chromatography". PhD thesis. Otto-von-Guericke Universitaet Magdeburg, 2009.

[74] L. C. Kessler and A. Seidel-Morgenstern. "Theoretical study of multicomponent continuous countercurrent chromatography based on connected 4-zone units". In: *Journal of Chromatography A* 1126 (2006), pp. 323–337.

[75] L. C. Kessler et al. "Step gradients in 3-zone simulated moving bed chromatography application to the purification of antibodies and bone morphogenetic protein-2". In: *Journal of Chromatography A* 1176 (2007), pp. 69–78.

[76] J. Knaeblein. *Modern Biopharmaceuticals*. WILEY-VCH Verlag GmbH and Co. KGaA, 2005.

[77] S. Knecht et al. "Oligohis-tags: mechanisms of binding to Ni^{2+}-NTA surfaces". In: *Journal of Molecular Recognition* 22 (2009), pp. 270–279.

[78] M. Kraettli et al. "Closed loop control of the multi-column solvent gradient purification process". In: *Journal of Chromatography A* 1218 (2011), pp. 9028–9036.

[79] A. Kremser. "Theoretical analysis of absorption process". In: *National Petroleum News* 22 (1930), p. 42.

[80] *La Merie Business Intelligence. TOP 20 Biologics 2009*. http://licprobpl.u-bourgogne.fr/annales_LPro/Chimie_Pharmaceutique/top_20_biologics_2009_rd_pipeline_news.pdf. [Online accessed 14-December-2012].

[81] U.K. Laemmli. "Cleavage of Structural Proteins during the Assembly of the Head of Bacteriophage T4". In: *Nature* 227 (1970), pp. 680–685.

[82] J. Laroche-Traineau, G. Clofent-Sanchez and X. Santarelli. "Three-step purification of bacterially expressed human single-chain Fv antibodies for clinical applications". In: *Journal of Chromatography B* 737 (2000), pp. 107–117.

[83] J. M. Liddell. "Production Strategies for Antibody Fragment Therapeutics". In: *Biopharm International* (2009), pp. 36–42.

[84] M. E. Lienqueo et al. "Mathematical Modeling of Protein Chromatograms". In: *Chemical Engineering and Technology* 34 (2011), pp. 1–13.

[85] D. Low, R. O'Leary and N. S. Pujar. "Future of antibody purification". In: *Journal of Chromatography B* 848 (2007), pp. 48–63.

[86] *Lucentis Historical sales*. http://www.gene.com/gene/about/ir/historical/product-sales/lucentis.html. [Online accessed 14-December-2012].

[87] *Lucentis (Ranibizumab) website*. http://www.lucentis.de. [Online accessed 14-December-2012].

[88] A. J. P. Martin and R. L. M. Synge. "A new form of chromatogram employing two liquid phases". In: *Biochemical Journal* 35 (1941), pp. 1358–1368.

[89] J. Maynard and G. Georgiou. "Antibody Engineering". In: *Annual Review of Biomedical Engineering* 2 (2000), pp. 339–376.

[90] M. Mazzotti. "Equilibrium theory based design of simulated moving bed processes for a generalized Langmuir isotherm". In: *Journal of Chromatography A* 1126 (2006), pp. 311–322.

[91] M. Mazzotti, G. Storti and M. Morbidelli. "Optimal operation of simulated moving bed units for nonlinear chromatographic separations". In: *Journal of Chromatography A* 769 (1997), pp. 3–24.

[92] S. Miethe et al. "Production of single chain fragment variable (scFv) antibodies in *Escherichia coli* using the LEX™ bioreactor". In: *Journal of Biotechnology* 163 (2013), pp. 105–111.

[93] C. Migliorini, M. Mazzotti and M. Morbidelli. "Simulated moving-bed units with extra-column dead volume". In: *AIChE Journal* 45 (1999), pp. 1411–1421.

[94] A. Moosmann et al. "Purification of a PEGylated single chain Fv". In: *Journal of Chromatography A* 1236 (2012), pp. 90–96.

[95] T. Müller-Späth, L. Aumann and M. Morbidelli. "Role of Cleaning-in-Place in the Purification of mAb supernatantas using continuous cation exchange chromatography". In: *Separation Science and Technology* 44 (2009), pp. 1–26.

[96] T. Müller-Späth and M. Morbidelli. "Continuous chromatography for the purification of monoclonal antibodies". In: *Process Scale Purification of Antibodies*. Ed. by U. Gottschalk. John Wiley and Sons, Inc., 2009. Chap. 11.

[97] T. Müller-Späth et al. "Chromatographic separation of three monoclonal antibody variants using multicolumn countercurrent solvent gradient purification (MCSGP)". In: *Biotechnology and Bioengineering* 100 (2008), pp. 1166–1177.

[98] T. Müller-Späth et al. "Two step capture and purification of IgG2 using multicolumn countercurrent solvent gradient purification (MCSGP)". In: *Biotechnology and Bioengineering* 107 (2010), pp. 974–984.

[99] A. D. Naik et al. "Process for purification of monoclonal antibody expressed in transgenic Lemma plant extrac using dextran-coated charcoal and hexamer peptide affinity resin". In: *Journal of Chromatography A* 1260 (2012), pp. 61–66.

[100] A. L. Nelson, E. Dhimolea and J. M. Reichert. "Development trends for human monoclonal antibody therapeutics". In: *Nature Reviews Drug Discovery* 9 (2010), pp. 767–774.

[101] M. Ottens et al. "Multi-component fractionation in SMB chromatography for the purification of active fractions from protein hydrolysates". In: *Food and Bioproducts Processing* 84 (2006), pp. 59–71.

[102] S. Palani et al. "Recombinant protein purification using gradient-assisted simulated moving bed hydrophobic interaction chromatography. Part I: Selection of chromatographic system and estimation of adsorption isotherms". In: *Journal of Chromatography A* 1218 (2011), pp. 6396–6401.

[103] G. Paredes. "Optimal design and operation of the preparative chromatography of bioproducts". PhD thesis. Swiss Federal Institute of Technology Zurich, ETH Zurich, 2006.

[104] H. C. Parmar. "Biopharmaceuticals market overview". In: *Pharmaceutical Technology Europe* 18 (2006), pp. 20–27.

[105] D. D. Perrin and B. Dempsey. *Buffers for pH and Metal Ion Control*. Chapman and Hall, 1974.

[106] J. Porath. "Immobilized Metal-Ion Affinity-Chromatography". In: *Protein expression and purification* 3 (1992), pp. 263–281.

[107] J. Porath et al. "Metal Chelate Affinity Chromatography, a new approach to protein fractionation". In: *Nature* 258 (1975), pp. 598–599.

[108] A. Rajendran, G. Paredes and M. Mazzotti. "Simulated moving bed chromatography for the separation of enantiomers". In: *Journal of chromatography* 1216 (2009), pp. 709–738.

[109] *Reopro website*. www.reopro.com. [Online accessed 14-December-2012].

[110] A. C. A. Roque, C. R. Lowe and M. A. Taipa. "Antibodies and genetically engineered related molecules: production and purification". In: *Biotechnology Progress* 20 (2004), pp. 639–654.

[111] D. M. Ruthven. *Principles of Adsorption and Adsorption Processes*. Wiley, 1984.

[112] D. M. Ruthven and C. B. Ching. "Countercurrent and simulated countercurrent adsorption separation processes". In: *Chemical Engineering Science* 44 (1989), pp. 1011–1038.

[113] D. Sahoo, J. Andersson and B. Mattiasson. "Immobilized metal affinity chromatography in open-loop simulated moving bed technology: Purification of a heat stable histidine tagged beta-glucosidase". In: *Journal of chromatography B* 877.16-17 (2009), pp. 1651–1656.

[114] W. E. Schiesser and G. W. Griffiths. *A Compendium of Partial Differential Equation Models: Method of Lines Analysis with Matlab*. Cambridge University Press, 2009.

[115] T. Schirrmann et al. "Production systems for recombinant antibodies". In: *Frontiers in Bioscience* 13 (2008), pp. 4576–4594.

[116] F. R. Schmidt. "Recombinant expression systems in the pharmaceutical industry". In: *Applied Microbiology and Biotechnology* 65 (2004), pp. 363–372.

[117] H. Schmidt-Traub and A. Seidel-Morgenstern. *Preparative Chromatography*. Wiley-VCH, 2012.

[118] M. Scott and N. Clarke. "Next generation antibody therapeutics: antibody fragments, dual-targeting strategies,and beyond". In: *European Pharmaceutical Review* (2009).

[119] A. Seidel-Morgenstern. "Experimental determination of single solute and competitive adsorption isotherms". In: *Journal of Chromatography A* 1037 (2004), pp. 255–272.

[120] A. Seidel-Morgenstern. *Mathematische Modellierung der präparativen Flüssigchromatographie*. Deutscher Universitaets Verlag Wiesbaden, 1995.

[121] A. Skerra, I. Pfitzinger and A. Pluckthun. "The functional expression of antibody Fv fragments in E. Coli- Improved vectors and a generally applicable purification technique". In: *Bio/technology* 9.3 (1991), pp. 273–278.

[122] G. Storti et al. "Robust design of binary countercurrent adsorption separation processes". In: *AIChE Journal* 39 (1993), pp. 471–492.

[123] G. Strang. *Computational Science and Engineering*. Wellesley-Cambridge Press, 2007.

[124] G. Strang. *Introduction to Linear Algebra*. Wellesley-Cambridge Press, 2009.

[125] J. Strube et al. "Comparison of batch elution and continuous simulated moving bed chromatography". In: *Organic Process Research and Development* 2 (1998), pp. 305–319.

[126] E. Sulkowski. "Purification of proteins by IMAC". In: *Trends in Biotechnology* 3 (1985), pp. 4–13.

[127] *Thermo Scientific Pierce Protein Purification Technical Handbook*. Thermo Fisher Scientific Inc., 2010.

[128] D. Todorova-Balvay et al. "Immobilized metal-ion affinity chromatography of human antibodies and their proteolytic fragments". In: *Journal of chromatography B* 808.1 (2004), pp. 57–62.

[129] *User manual CSEP® C9812 and C916 Simulated Moving Bed Units*. Wissenschaftliche Geraetebau Dr. Ing. Herbert Knauer GmbH, 2007.

[130] S. Vançan, E. Miranda and S. Bueno. "IMAC of human IgG: studies with IDA-immobilized copper, nickel, zinc, and cobalt ions and different buffer systems". In: *Process biochemistry* 37.6 (2002), pp. 573–579.

[131] A. Varma and M. Morbidelli. *Mathematical methods in chemical engineering*. Oxford University Press, 1996.

[132] P. S. Vary. "Prime time for Bacillus megaterium". In: *Microbiology* 140 (1994), pp. 1001–1013.

[133] S. Vunnum and S. Cramer. "IMAC: Nonlinear Elution Chromatography of Proteins". In: *Biotechnology and Bioengineering* 54 (1997), pp. 373–390.

[134] S. Vunnum, V. Natarajan and S. Cramer. "Immobilized metal affinity chromatography self-sharpening of protein-modulator interfaces in frontal chromatography". In: *Journal of Chromatography A* 818 (1998), pp. 31–41.

[135] S. Vunnum et al. "Immobilized metal affinity chromatography: modeling of nonlinear multicomponent equilibrium". In: *Chemical Engineering Science* 50 (1995), pp. 1785–1803.

[136] N. E. Weisser and J. C. Hall. "Applications of single-chain variable fragment antibodies in therapeutics and diagnostics". In: *Biotechnology Advances* 27 (2009), pp. 502–520.

[137] J. J. Winzerling, P. Berna and J. Porath. "How to use immobilized metal ion affinity chromatography". In: *Methods* 4 (1992), pp. 4–13.

[138] G. Xindu and W. Lili. "Liquid chromatography of recombinant proteins and protein drugs". In: *Journal of Chromatography B* 866 (2008), pp. 133–153.

[139] S. Yamamoto, M. Nomura and Y. Sano. "Preparative chromatography of proteins: Design calculation procedure for gradient and stepwise elution". In: *Journal of Chromatography* 512 (1990), pp. 89–100.

[140] S. Yamamoto, M. Nomura and Y. Sano. "Stepwise elution chromatography as a method for both purification and concentration of proteins". In: *Chemical Engineering Science* 47 (1992), pp. 185–188.

[141] S. Yamamoto, T. Suehisa and Y. Sano. "Preparative separation of proteins by gradient- and stepwise-elution chromatography: zone-sharpening effect". In: *Chemical Engineering Communications* 119 (1993), pp. 221–230.

[142] J. Yan, J. Ko and Y. Qi. "Generation and characterization of a novel single-chain antibody fragment specific against human fibrin clots from phage display antibody library". In: *Thrombosis research* 114 (2004), pp. 205–211.

[143] G. Zhong and G. Guiochon. "Simulated moving bed chromatography. Effects of axial dispersion and mass transfer under linear conditions". In: *Chemical Engineering Science* 52 (1997), pp. 3117–3132.

Appendix A

Sodium dodecyl sulphate-polyacrylamide gel electrophoresis

This appendix includes the details for realizing the sodium dodecyl sulphate-polyacrylamide gel electrophoresis (SDS-PAGE) explained in Section 5.2.2. The method is divided in many steps such as the gel casting, sample preparation, gel running, and staining and destaining of the electrophoretic gel.

Gel casting

In this work, a two-layer polyacrylamide gel consisting of a lower separating gel and an upper stacking gel was used. Concentration of the proteins takes place in the stacking gel. And separation of the proteins in the so-called separation gel. This occurs due to the pore-size of the matrices (the former is a 4% acrylamide gel while the latter a 12 %). In this case, proteins with a molecular size from 10-200 KDa can be separated and identified later in the separating gel.

The procedure of gel casting is:

1. The gel casting form is assembled by putting together the two glass plates and the rubber spacer. The spacers must be aligned and clamped properly.
2. Separating gel solution is prepare as indicated by Table A.1. Do not add TEMED or ammonium persulfate until the separating gel is ready to be poured.
3. 4.8 mL are poured quickly into the gel casting form.

4. Bubbles must be removed completely with 2-propanol.
5. Separating gel polimerizes completely in 90 minutes.
6. 2-propanol is removed carefully and completely.
7. Stacking gel is prepared as described in Table A.3.
8. 2.2 mL are poured quickly into your gel casting form until the top is reached.
9. The comb is carefully placed an appropriate comb into the stacking gel. Stacking gel polymerizes in 60 minutes.
10. The gels can be stored with the combs in place tightly wrapped in wet paper inside a sealable bag at 4°C for 2 to 3 weeks. Keep the gels moist.

The composition of gels, as well as the recipe to make four gels, are included below (4 Gels = 24 ml). In Table A.1 are listed the reagents for the casting of the separating gel.

Table A.1: Reagents for the 12% acrylamide separating gel

Reagents	Unit	4 Gels
Milli Q Water	[mL]	9.2
Acrylamide 30%	[mL]	8.8
1.5 M Tris-HCl pH 8.8	[mL]	6.0
10% APS	[μL]	20.0
TEMED	[μL]	40.0

In Table A.2 are listed the reagents for the preparation of the 1.5 M Tris-HCl, pH 8.8 solution. The pH is adjusted with HCl 37%. After that, volume is made up to 100 mL water.

Table A.2: Reagents for the 1.5 M Tris-HCl, pH 8.8 solution

Reagents	Unit	Amount
Milli Q Water	[mL]	Up to 100
SDS 10%	[mL]	4
Tris	[g]	18.15

In Table A.3 are listed the ingredients for the casting of the stacking gel.

Table A.3: Reagents for the 4% acrylamide stacking gel

Reagents	Unit	Amount
Milli Q Water	[mL]	6.50
Acrylamide 30%	[mL]	1.00
0.5M Tris-HCl pH 6.8	[mL]	2.50
10% APS	[μL]	20
TEMED	[μL]	50

In Table A.4 are listed the reagents for the preparation of the 0.5 M Tris-HCl, pH 6.8 solution. Again, the pH is adjusted with HCl 37%. After that, volume is made up to 50 mL water.

Table A.4: Reagents for the 0.50 M Tris-HCl, pH 6.8 solution

Reagents	Unit	Amount
Milli Q Water	[mL]	Up to 50
SDS 10%	[mL]	2
Tris	[g]	3

Sample Preparation

The procedure for the sample preparation is:

1. 48 μL of sample are mixed with 16 μL of Laemmli buffer in the plastic recipients labeled according to the collected samples.
2. Recipients are put into the thermomixer during 10 minutes at 99°C with 750 rpm.

In Table A.5 are listed the reagents for the preparation of the Laemmli buffer.

Table A.5: Reagents for Laemmli buffer

Reagents	Unit	Amount
Milli Q Water	[mL]	0.4
0.5 M Tris-HCl pH 6.8	[mL]	2.0
Glycerol	[mL]	1.6
SDS 10%	[mL]	3.2
Bromophenol Blue	[mg]	1.0
β-mercaptoethanol	[mL]	0.8

Running the gels

The procedure for running the gels is:

1. The comb is removed from the gels and the gels are rinsed with the running buffer 1x poured into the gel caster.
2. 20 μL of the prepared samples are pipetted into the wells.
3. Constant current is applied (50 mA) until the dye front reaches the bottom of the separating gel (aprox. 60 minutes).

In Table A.6 are listed the reagents for the preparation of 1 liter of 5-fold concentrated running buffer. Running buffer is diluted 5 times before use.

Table A.6: Reagents for the running buffer, 5x

Reagents	Unit	Amount
Milli Q Water	[mL]	908
Tris	[g]	15.1
Glycine	[g]	72.0
SDS	[g]	5.0

Staining the gels

The procedure for staining the gels is:

1. Gels are carefully removed and put into glass recipients.
2. Staining solution is poured into the glass recipient until the gel is covered completely.
3. Gels are stained overnight at 40 rpm on the shaker plate.

In Table A.7 are listed the reagents for the staining solution.

Table A.7: Reagents for the staining solution

Reagents	Unit	Amount
Milli Q Water	[mL]	600
Ethanol	[mL]	300
Acetic Acid	[mL]	100
Coomassie	[mg]	50

Destaining the gels

The procedure for destaining the gels is:

1. Staining solution is removed and destaining solution is poured into the glass recipient until the gel is covered completely.
2. Destaining process is finished when the gels are transparent and the bands on the gel can be seen clearly.

In Table A.8 are listed the reagents for the destaining solution.

Table A.8: Reagents for the destaining solution

Reagents	Unit	Amount
Milli Q Water	[mL]	600
Ethanol	[mL]	300
Acetic Acid	[mL]	100

Appendix B

Enzyme-linked immunosorbent assay

The following protocol describes the enzyme-linked immunosorbent assay (ELISA) for the quantification of the single-chain antibody fragment concentration explained in Section 5.2.2.

1. First, the adsorption of antigen on the microtiter plate is carried out. The antigen (in this case lysozyme) diluted in the coating buffer (a neutral phosphate buffered saline (PBS) around pH 7.4) is immobilized onto the 96-well microtiter plate (100 μL per well). The concentration of lysozyme is 10 μg/mL. Incubation takes place overnight at 4°C.

2. After incubation, any excess and non-bound antigen is washed away with PBST (PBS + 0.1 % (v/v) Tween 20).

3. Coated wells are blocked with 320 μL of blocking agent (2% M-PBST) per well followed by incubation for 90 minutes at room temperature.

4. Again after incubation, coated wells are washed three times with PBST (PBS + 0.1 % (v/v) Tween 20).

5. The samples containing the single-chain antibody fragment are serially diluted in the coating buffer (2% M-PBST). Afterwards, 100 μL of diluted samples are added per well and incubated for 90 minutes at room temperature. After incubation, repeat the washing step.

6. 100 μL of his-mAb mouse anti-penta is added per well and incubated for 90 minutes at room temperature. The antibody solution is made with 1 μg of the mAb mouse anti-penta his in 10 mL of 2% M-PBST, that means a dilution equal to 1:10000. After incubation, repeat the washing step.

7. 100 μL of polyclonal goat anti-mouse-IgG Fab, conjugated with horse radish peroxidase (HRP) is added per well and incubated for 90 minutes at room temperature. The antibody solution is made with 1 μL of the mAb mouse anti-penta his in 10 mL of 2% M-PBST, that means a dilution equal to 1:10000. After incubation, repeat the washing step.

8. 100 μL of substrate solution (TMB solution) is added per well and incubated at room temperature until blue color appears. Then the reaction should be stopped by addition of 100 μL of 1 N H_2SO_4 and blue color turns to yellow.

9. Absorbances at 450 mn and scattered light at 620 nm are measured using a microtiter plate spectrophotometer. The absorbance at 620 nm must be substracted.

Buffer solutions

In Table B.1 are listed the reagents for the preparation of the PBS buffer, 20x (20-fold concentrated).

Table B.1: Reagents for the PBS buffer

Reagents	Unit	Amount
Milli Q Water	[mL]	Up to 1000 mL
NaCl	[g]	170
Na_2HPO_4	[g]	21.40
NaH_2PO_4 x H_2O	[g]	6.10

Dilute to 1x (1-fold) for the working solution (100 mL PBS Buffer and 1900 mL water). If necessary, the pH can be adjusted with $NaOH$.

In Table B.2 are listed the reagents for the preparation of the PBST buffer.

Table B.2: Reagents for the PBST Buffer

Reagents	Unit	Amount
PBS 1x	[mL]	Up to 1000 mL
Tween 20	[mL]	0.5

In Table B.3 are listed the reagents for the preparation of the M-PBST buffer.

Table B.3: Reagents for the M-PBST Buffer

Reagents	Unit	Amount
PBS 1x	[mL]	Up to 100 mL
Milk Powder	[g]	2.0
Tween 20	[μL]	100.0

Table B.4: Reagents for the TMB-A Solution

Reagents	Unit	Amount
Kalium Citrate	[g]	9.73
Citric Acid	[g]	10.0 in 100 ml water
Milli Q Water	[mL]	Up to 1000 mL

In Table B.4 are listed the reagents for the preparation of the TMB-A solution.

In Table B.5 are listed the reagents for the preparation of the TMB-B solution.

Table B.5: Reagents for the TMB-B Solution

Reagents	Unit	Amount
Tetramethylbenzidin	[mg]	240
Acetone	[mL]	10.0
Ethanol	[mL]	90.0
H_2O_2 30 % (v/v)	[μL]	907.0

The TMB solution is prepared by mixing 476 μL of TMB-B with 9.50 mL of TMB-A.